

Root depth: a trait to increase water use and yield of wheat

Alan David Severini

A thesis submitted for the degree of

Doctor of Philosophy of

The Australian National University

November 2015



**Australian
National
University**

Dedication

To Maru, Mario, Andrés, Marco and Joana,

who gave me the inspiration and strength needed

to overcome any obstacle.

Declaration

This thesis is an account of research undertaken between October 2011 and November 2015 in the division of Plant Industry, Commonwealth Scientific and Industrial Research Organization (CSIRO), and the Research School of Biology, Australian National University, under the supervision of Dr Michelle Watt, Dr Richard Richards, Dr John Passioura and Professor John Evans.

The data presented in Figure 3.3 was adapted from a report presented by Dr Warren Bond, Land & Water, CSIRO. Figure 6.1 was redrawn from Chenu *et al.* (2013 fig. 5), and Figure 6.2 was adapted from Dardanelli *et al.* (1997).

Except where otherwise indicated, this thesis is my own original work.

Alan David Severini

Acknowledgements

Thanks to my supervisors, Michelle Watt, John Evans, John Passioura, and Richard Richards for their supervision and guidance during these four years of PhD. Thanks to Anton Wasson, who wasn't within my PhD committee but behaved as a supervisor, from whom I learned a considerable amount of science.

I'd also like to thank Gilbert, for excellent field assistance, practical ideas (always smarter than mine), and most of all, his friendship. Mick provided courageous field assistance facing any duty, like camping on site and measuring soil water with a neutron probe once per hour during the whole night!

Everyone in our 'root team' made me feel that it was possible to do serious science while having fun: Ritika, Vincent, Aki, Geetha, Harriet, Cathrine, Sarah, Kathy.

I am thankful to David Deery, José Jiménez-Berni, Wayne Thompson and Paul Hutchinson, for help with all the work installing and getting data from gypsum blocks, the infrared thermometers and other fancy devices, as well as sharing stimulating discussions.

I am very grateful for all the amazing scientists at CSIRO Plant Industry, from whom I learned a lot, sharing innumerable talks in the tea room, in the halls, or in the field.

My whole PhD field experiments would not been possible without the tremendous help from the excellent team at Ginninderra Experiment Station: Phil Dunbar, Byron Corcoran, Bernie Michelson, James Byrne, Tom McLachlan, and Matt Lynch.

I am very happy of having met such friends as Leone Jansen and Peter Hairsine, for their wise company, and giving me a free, wonderful Toyota Corolla 1989, that lasted for the duration of the whole PhD and is still going!

Warren Bond gave me a lot of help with the neutron probe calibration data and scientific teachings—like the Ockham's razor.

I thank also INTA, for letting me come to Australia to do the PhD and keeping my position.

And surviving a PhD in Australia wouldn't be possible without the support from all my close friends from Argentina, who always supported me in the distance.

I am greatly indebted with Australians and Australia, for letting me live and enjoy such a beautiful country, which is indeed my second home.

And I deeply appreciate Katherine, for all her love and support when they were most needed.

Abstract

Crops with deeper roots could potentially capture more soil resources and as a consequence yield more. However, as sampling roots by soil coring is challenging, there are few examples of genetic diversity determined under field conditions. Canopy temperature, an indicator of transpiration, could be used instead of direct coring to screen for wheat varieties with increased access to deep water and hence deep roots in the field. In this thesis we aimed (i) to seek genetic diversity in rooting depth, root length density and relate these traits to yield in a wide range of triticale and wheat germplasm, and (ii) to test the usefulness of continuously-monitored canopy temperature and soil water status for phenotyping two commercial wheat varieties that differ in rooting depth. In the first set of field experiments, rooting depth, root length density and yield were measured in 34 wheat and 2 triticale varieties. Roots were sampled by soil-coring with a tractor-mounted hydraulic press and were later counted by the 'core break' method. Root length density was predicted from root count density. In the second set of experiments, canopy temperature was measured with fixed infra-red thermometers, and soil water suction was determined with gypsum blocks buried at 20 cm intervals, from 20 to 160 cm depth. A crop water-stress index (CWSI) was calculated to normalise for the effects of vapour pressure deficit over canopy temperature. Soil water retention curves fitted to the soil of the site were used to convert soil water suction into soil water content. Shoot biomass and grain yield were estimated from 0.7 m² samples per plot in all experiments. In the experiments seeking genetic variability, we found that triticale produced deeper roots than commercial spring-wheat ($p < 0.10$), and shorter varieties produced deeper roots than taller varieties ($p < 0.10$). Moreover, rooting depth was related to shoot biomass ($R^2 = 0.66$, $p < 0.001$) and grain yield ($R^2 = 0.56$, $p < 0.001$) across experiments and genotypes but not between

genotypes within the same experiment. In the experiments analysing canopy temperature and water-use continuously, differences in deep-root length were not statistically significant between the two varieties. The variety Gregory had greater root length at depths beneath 1 m, was cooler, used more water and that water was withdrawn from deeper soil layers than the other variety, Derrimut. Using CWSI gave better predictions of soil water status than canopy temperature *per se*. By taking up more water during grain filling, Gregory produced more yield at a rate of 54 kg ha⁻¹ mm⁻¹. CWSI did not correlate with day-to-day changes in water use. We conclude that (i) there is genetic diversity in rooting depth within triticales and wheat germplasm; (ii) by enabling the calculation of a CWSI, continuously measured canopy temperature allows phenotyping of root systems with superior deep water access.

Contents

Contents.....	xi
List of Figures	xv
List of Tables.....	xxiii
Chapter 1 Introduction: review of the potential of root depth to increase crop yield	25
1.1 Introduction	25
1.1.1 The framework of water-limited grain yield	26
1.1.2 How can deeper root systems improve water-limited yield?	33
1.1.3 Improvement of root depth through management and genotype selection 40	
1.2 Thesis aims	44
1.3 Thesis outline.....	44
Chapter 2 Field experiments used for wheat phenotyping.....	47
2.1 Introduction	47
2.2 Growing conditions: soils and weather	48
2.3 Sowing and agronomic management.....	54
2.4 Germplasm sown	57
2.5 Statistical designs	64
2.6 Field measurements	71
2.6.1 Phenology.....	72
2.6.2 Soil coring to sample roots.....	72
2.6.3 Soil washing to separate roots from soil	73
2.6.4 Root scanning to quantify root length density	74
2.6.5 Predicting root length density from root count density.....	76
2.6.6 Estimation of maximum rooting depth.....	79
2.6.7 Root length per soil depth intervals or the whole soil profile	81
2.6.8 Above-ground biomass and grain yield	81

Chapter 3	Using gypsum blocks for phenotyping water use in the field.....	83
3.1	Introduction	83
3.2	Measuring bulk density	85
3.3	Estimating soil water content with neutron probe.....	88
3.4	Converting resistance into suction and correcting for temperature	95
3.5	Field measurement of soil water suction with gypsum blocks.....	101
3.6	Estimating soil water retention curves for the site	104
3.7	Validation against neutron-probe soil water content.....	109
3.8	Conclusions	119
Chapter 4	Searching for genetic diversity in rooting depth and its relationship with crop growth and yield	123
4.1	Introduction	123
4.2	Materials and methods	126
4.3	Results	129
4.3.1	Differences in shoot and root traits between genotypes and environments 129	
4.3.2	Genotypic differences in rooting depth, total root length, biomass and yield 130	
4.3.3	Relationships between rooting depth, total root length, biomass and yield 134	
4.3.4	Plant height, root and shoot growth	138
4.4	Discussion	140
4.5	Conclusions	142
Chapter 5	Relating deep-root length with water use, canopy temperature and grain yield 145	
5.1	Introduction	145
5.2	Materials and methods	148

5.2.1	Growing conditions	148
5.2.2	Measuring canopy temperature	148
5.2.3	Calculating a crop water-stress index.....	150
5.2.4	Calculating water use and the fraction of plant available water	152
5.2.5	Measuring root length density along the soil profile.....	154
5.3	Results	154
5.3.1	Growing conditions	154
5.3.2	Root length density distributions.....	154
5.3.3	Canopy temperature and water use	155
5.3.4	Crop water-stress index.....	161
5.3.5	Crop growth and water use.....	170
5.4	Discussion.....	172
5.4.1	Water use was higher in Gregory than Derrimut, but differences in root length were not demonstrable	173
5.4.2	Canopy temperature was cooler in Gregory than Derrimut	174
5.4.3	CWSI was a better surrogate of plant water-status than CTD	175
5.4.4	Daily changes in CWSI did not correlate with water use	175
5.4.5	Trial size is more important than continuous monitoring for detecting overall differences between genotypes—but continuous monitoring can reveal genotype interactions with time	177
5.4.6	Trial size also remains important for detecting smaller genotype by time interactions overall	178
5.5	Conclusions	179
Chapter 6	General discussion and implications for crop improvement	181
6.1	Overview of the thesis	181
6.2	The benefits of deeper roots to wheat growth and yield	182
6.3	Ways of improving root depth by breeding.....	185
6.4	Phenotyping for deep roots.....	192

6.5	Future research	194
6.5.1	Automation of soil coring	194
6.5.2	Measuring root function without measuring roots	195
6.5.3	Enhanced root vertical distribution, trade-off-free opportunities and root self/non-self recognition	198
6.6	Conclusion.....	199
Appendix A	ASReml-R models.....	201
Appendix B	Validation of gypsum blocks calibration against neutron probe.....	203
References	209

List of Figures

Figure 2.1. Location of the 6 field experiments and their corresponding sites (Creek, Quarantine and Valley).	49
Figure 2.2. Soil chemical characteristics measured during May 2011, just before sowing of experiments 1 and 2. Soil electrical conductivity, soil pH, soil ammonia concentration, and soil nitrate over nitrite concentration as a function of soil depth. Bars are the standard errors of the means. Colours indicate the soil of origin: Creek or Valley.	52
Figure 2.3. Soil physical characteristics measured during May 2013, just before sowing of experiment 4. Soil bulk density and air-filled porosity as a function of soil depth. Air-filled porosity was estimated from bulk density, BD , and water contents per layers at the start of the season, θ ($\text{cm}^3 \text{ cm}^{-3}$), and an average soil particle density, PD (g cm^{-3}) of 2.65. Then air-filled porosity = $1-BDPD-\theta$. The dashed vertical line in the right panel indicates the theoretical limit of air-filled porosity below which most soils produce anoxia to roots (Wesseling <i>et al.</i> 1957). Colours indicate the soil of origin: Creek or Valley. Bars are the standard errors of the means.	53
Figure 2.4. Rainfall and reference evapotranspiration (top) and maximum and minimum monthly-mean temperatures (bottom) for the four years when experiments were conducted and a long term period from 1889 to 2014 for the Ginninderra Region. Boxplots indicate percentiles 0.10, 0.25, 0.50, 0.75, and 0.90, where points represents outliers (i.e. smaller than percentile 0.10 or larger than percentile 0.90). In each panel, numbers on the top-right corner indicate total annual rainfall (red) and total annual evapotranspiration (blue). For the period 1889-2014 rainfall and evapotranspiration are described as mean \pm standard error ($n = 125$ years). Data were obtained from http://www.longpaddock.qld.gov.au/	54
Figure 2.5. Diagrams representing plots in the 6 experiments. Above-ground biomass and yield were sampled in the areas limited by dashed lines, and soil coring to sample roots was done over the same areas after sampling biomass. This was done only at maturity in experiments 1, 5 and 6 (Zadoks 87); at anthesis (Zadoks 65) and maturity in experiment 4; and at stem elongation (Zadoks 31), anthesis and maturity in experiment 3. Plots in experiment 5 and 6 were similar to plots of experiment 4, except that they only had one biomass cut at maturity and one infrared thermometer (rather than two), and they lacked neutron probe access tubes.	56
Figure 2.6. Selection of genotypes at experiment 1 (2011) to be sown in experiment 3 (2012). Rooting depth at maturity for all varieties sampled in experiment 1 (left), and above-ground biomass as a function of the sum of root counts (root tips) along the soil profile, both at maturity as well. Coloured dots are the selected genotypes. Dots are means of 4 replicates and bars are standard errors of those means. Grey dots are the rest of the varieties sown in experiment 1, which were not selected to be sown in experiment 3.	61

-
- Figure 2.7. Selection of genotypes at 'hill plots' experiment (2011) to be sown in experiment 3 (2012). Rooting depth at maturity for the 10% deepest and the 10% shallowest roots in the 'hill plots' experiment (left), and above-ground biomass as a function of the sum of root counts (root tips) along the soil profile, both at maturity as well. Coloured dots are the selected genotypes. Dots are means of 4 replicates and bars are standard errors of those means. Grey dots are the rest of the varieties sown in the 'hill plots' experiment, which were not selected to be sown in experiment 3. 62
- Figure 2.9. Statistical design of experiment 2. The experiment was sown during 2011 in the Valley site (yellow podzolic soil). Colour specified as 'rest' (pale green) identify plots that were not sampled, and from those, 'generic' was a wheat genotype that was used as a buffer. 67
- Figure 2.10. Statistical design of experiment 3. The experiment was sown during 2012 in the Creek site (red podzolic soil). Colour specified as 'lodged' (pale green) identify plots that were not sampled because they were stem-lodged at anthesis. 68
- Figure 2.11. Statistical design of experiment 4. The experiment was sown during 2013 in the Creek site (red podzolic soil). Two commercial wheat varieties, with supposedly different root depth at maturity, were sown in combination with 2 nitrogen fertilization treatments aimed to maximise differences in root growth: 0 and 200 kg N ha⁻¹ applied at the stem elongation stage (Zadoks 31). However, and unfortunately, plots were mistakenly fertilised, and therefore blocks 2 and 4 don't have all the possible treatment combinations—i.e. in block 2, Derrimut fertilised with 200 appears in two plots, and Derrimut without fertilization none. Fortunately, nitrogen had no statistical effect over shoot or root growth, so the nitrogen treatment is later disregarded. 69
- Figure 2.12. Statistical design of experiment 5. The experiment was sown during 2014 in the Creek site (red podzolic soil). Four wheat genotypes were sown, but just 2 are evaluated in this thesis: Derrimut and Gregory, same genotypes as in experiment 4. Two sowing densities were sown, a low density of 100 and a high density of 200 plants m⁻². The design is a split-plot design with 4 replicates in blocks. Experiment 6 was sown during 2014 and had the same experimental design as experiment 5, but it differed in its location: it was sown in the Quarantine site, in a yellow podzolic soil (Figure 2.1). 70
- Figure 2.14. Comparison of stained and non-stained samples with Toluidine blue before scanning. The dashed line is $y = x$ and the full line is the best linear fit. It can be seen that the linear fit and the dashed line fall apart in the case of average root diameter and root volume, but they are almost equal for total root length—therefore, staining the root samples with Toluidine blue does not improve the accuracy of measuring root length. 76
- Figure 2.15. Models used to predict root length density from root count density according to soil depth. The graph shows root length density as a function of root count density as measured in the field. Soil depths are denoted by panels, with titles in cm of soil depth. Blue lines are the non-linear fittings with equation as presented in model (2.1) and parameters and statistics presented in Table 2.7. 78

Figure 3.1. Procedures followed to sample bulk density. For the top 60 cm layers, a hand corer was used, which allowed more cautioned sampling in those layers that are more prone to crumbling (a). We dug with a shovel between sampling layers 20, 40 and 60 cm depth, avoiding compaction of the soil to be sampled (b, c). For soil layers deeper than 60 cm, we cored with the same hydraulic corer as described for sampling roots, where the coring tube was actually wider (6.5 cm diameter) (d). After removal from the soil, soil samples were levelled with a scraper in order to have a precise, known volume (e). 87

Figure 3.2. Soil water content as a function of the neutron count ratio during 2012 and 2013 for depths of 20 cm and deeper than 20 cm. The full line shows the regression line, best fit, for both years. The dashed lines are the equations by Dr Warren Bond, detailed later in Figure 3.3. 89

Figure 3.3. Neutron probe generic equations estimated by Dr Warren Bond. The figure shows soil water content as a function of the neutron count ratio, the ratio between the neutrons measured in the soil and the neutrons that can be counted into a tank full of water. The latter is used as a reference measurement to normalise neutron readings that could otherwise vary between devices. 90

Figure 3.4. Validation of Dr Warren Bond's predictions of soil water content from neutron probe data. The graph shows measured soil water content ($\text{m}^3 \text{m}^{-3}$) as a function of neutron count ratio (unitless) for soil beneath 20 cm at 3 locations in New South Wales: Corowa, Ginninderra and Wagga Wagga. Notice that the parameters of the curve (slope and intercept) are closely similar to those of soil deeper than 20 cm in Figure 3.3 91

Figure 3.5. Soil water content estimated from Dr Warren Bond's equations (Figure 3.3) against soil water content calculated from gravimetric water contents at the start and end of the season of experiments 3 and 4 and the soil bulk density measured at the end of experiment 4. These comparisons serve as validations of neutron probe predictions against direct coring data. R^2 are indicated for the linear regressions between both variables for each soil layer. 94

Figure 3.6. Gypsum block suction (kPa) as a function of the logarithm (base 10) of its electrical resistance (Ω , Ohms). The line shows the equation $0.02 r^{7.756}$, where r is the logarithm base 10 of the resistance in Ohms (Johnston 2000). The inset shows the same data in a regular axis for the electrical resistance. 97

Figure 3.7. Trajectories of water suction readings (up) and the pressure-chamber temperature (down) during the calibrations. Arrows indicate the time when the readings reached a plateau (equilibrium), and hence were recorded. Numbers above those arrows (kPa) indicate the pneumatic pressure inside the chamber by that time. The colour of lines indicates each of the 4 gypsum blocks placed inside the chamber. These sets of 4 suction readings per temperature and per pneumatic pressure recorded at equilibrium are later plotted in Figure 3.9. 99

-
- Figure 3.8. Idem Figure 3.7 but for a water suction of 1500 kPa. The figure was separated from Figure 3.7 to show the longer time needed for equilibrium at a greater suction. 99
- Figure 3.9. Suction given by 4 gypsum blocks as a function of the suction in the pressure plate at three bath temperatures of 5, 15 and 25 °C. The dashed line represents $y = x$. The graph on the right summarises how the slopes of the lines from the graph on the left change as a function of temperature. The latter is the equation that I used to correct suctions by temperature: $y = -0.023 x + 1.472$ 100
- Figure 3.10. Soil water suction, uncorrected or corrected by soil temperature (upper panel), and soil temperature (lower panel) across time for soil at 20 cm depth in experiment 1 during 2011. 101
- Figure 3.11. Installation of gypsum blocks and thermistors. The same hydraulic press mounted to a tractor that was used for soil coring when sampling roots was used for digging holes in the centre of plots for installing gypsum blocks, albeit a thinner metallic core was used (a, b). Gypsum blocks were soaked in water the night before (d), and covered in mud made from the same soil layer where they were supposed to be buried (c). Thermistors were deployed as well so that soil temperature could be recorded. Frame (e) shows the white cable that worked as an extension necessary to reach the desired soil depth, joint to a thermistor (black wire) with a lead sinker at the tip. After reaching the desired soil depth, the hole where either a gypsum block or a thermistor was installed was filled with bentonite to prevent the preferential flow of water along the walls of the hole (f). 103
- Figure 3.12. Example water retention curves for typical soils. Data were generated from default water retention curves present in the software RETC (van Genuchten *et al.* 1991). 105
- Figure 3.13. Water retention curves estimated for the site in experiment 4. The vertical axis is soil water content and the horizontal axis the soil water suction. Samples in the paddock were taken at two extremes of the experimental area: north and south. Soil water contents at suctions greater than zero were measured in a pressure plate apparatus. Soil water content at complete saturation (i.e. suction equal zero) was estimated as 0.93(1-BDPD) as Paydar and Cresswell (1996). 109
- Figure 3.14. Soil water content predicted by the water retention curves (red lines, same curves as in Figure 3.13), and soil water content measured by neutron probe (blue dots), as a function of the soil water suction measured by gypsum blocks. 111
- Figure 3.15. A closer look at Figure 3.14, narrowing the focus within soil suctions from 20 to 60 kPa. The graph shows the disagreement between the water retention curves measured in the pressure plate (red line) and the data measured with neutron probe at suctions less than 50 kPa (blue dots), where points cluster at higher values than what the pressure-plate water retention predicts (20 and 40 cm depth). The blue line shows a surrogate water retention curve that results from fitting the gypsum-neutron probe data

with RETC (van Genuchten *et al.* 1991). The latter is however unrealistic and will be later discarded, as explained in the main text. 113

Figure 3.16. The start of the calibration of gypsum blocks, where 'glistening point' shows the approximate period when the soil surrounding the gypsum blocks was shining because of being saturated with water. The graph suggests that, even when fully saturated, gypsum blocks are blind to suctions under c. 50 kPa. 114

Figure 3.17. Surrogate water retention curves obtained by fitting soil water suction measured by gypsum blocks to soil water content measured by neutron probe in the field. Dots are neutron-probe-measured soil water content (circles are data < 50 kPa, triangles are suction > 50 kPa). Notice that the parameter θ_s was fixed as in equation (3.4). Two possible surrogate water retention curves can be obtained. First, in blue, the lines show water retention curves fitted using all data. Second, in green, the lines show the water retention curves fitted after excluding data < 50 kPa. Reasons for excluding data whose suctions are less than 50 kPa are detailed in the main text and supported by Figure 3.16. 116

Figure 4.1. Root length density distributions across experiments and genotypes. Lines represent root length densities every 10 cm, each of which is a mean of 4 replicates. Experiments are designated as colours, as in the top-left first panel. Genotypes are detailed in the title of each panel. From those, Bogong and Currency are triticales; the rest are wheat varieties. 130

Figure 4.2. (a) Root length, (b) rooting depth, (c) shoot biomass and (d) grain yield for each group of genotypes in experiments 1 and 2. Each bar is the predicted mean, generated by the ASReml model, of the genotype group when combining experiments 1 and 2. Error bars are standard errors for each mean. Above and in the middle of group bars to be compared, p-values indicate significance of their differences; where none is present comparisons are not statistically significant. 132

Figure 4.4. Shoot biomass (left), grain yield (centre) and harvest index (right) as a function of the root length per soil layer (rows) in each of the three experiments. Points are the predicted means, generated by the ASReml model, for each genotype in each experiment. R^2 is the adjusted R-squared and p is the p-value for the straight-line fit relating either shoot biomass or grain yield with root length deeper than 120 cm only at experiment 3. Note the change in scale in the x-axis across depth intervals. 137

Figure 4.5. Predicted genotypic means, modelled from experiments 1 and 2 combined, of rooting depth (a), shoot biomass (b), and grain yield (c) as a function of final canopy height achieved by crops after anthesis. Bars are the standard errors of the predicted means. The 8 genotypes evaluated are those differing in point mutations for the dwarfing genes (Chandler and Harding 2013). Lines represent the best fit with the following statistics: (a) $R^2 = 0.47$, $p < 0.06$; (b) $R^2 = 0.44$, $p < 0.07$; (c) $R^2 = 0.63$, $p < 0.02$ 139

Figure 5.1. Pictures showing the infrared thermometers used to measure canopy temperature hour after hour. On the left, it can be better appreciated that they were positioned in a 45° angle from the vertical line. On the right, it can be seen more about its construction: a PVC tube inside which the electronic components are installed, and a frontal aluminium head with a hole in the middle where the infrared sensor lays. 150

Figure 5.2. Graphical depiction of the concept of crop water-stress index (CWSI) developed by Idso *et al.* (1981) and Idso (1982). The CWSI is a ratio between how far the current CTD of a crop is from the non-water-stressed CTD, and the maximum possible difference in CTD with the non-water-stressed CTD. The current CTD of the crop is exemplified in the graph as a black point. The non-water-stressed CTD (CTD lower limit = CTD_{LL}) is determined by equation (5.2) and is represented by the blue line. The maximum CTD at the current air temperature (CTD upper limit = CTD_{UL}) is the top grey line. The segment representing the distance between CTD and CTD_{LL} is the numerator, and the segment between CTD_{UL} and CTD_{LL} the denominator, of equation (5.1). 152

Figure 5.3. Root length density distributed along soil depth for the varieties Derrimut and Gregory during 2013 (left) and 2014 (centre and right). The complete profile is plotted on top, and a subset, at 100 cm and deeper, is plotted at the bottom for better appreciation of small root length density values. Points are means, and horizontal bars are standard errors, of 8 replicates. For data from 2014, an extra site is shown (right). For that extra site only data of root length density is shown in this thesis, since air temperature and soil water characteristics were not measured, making estimations of canopy temperature deviation and soil water content inaccurate. 155

Figure 5.4. Trajectory of canopy temperature deviation from air temperature (CTD) at solar noon ± 2 hours, during 2013 and 2014 (top); water use per day during 2013 and 2014 (middle); vapour pressure deficit (VPD) at solar noon ± 2 hours; and rainfall per day during 2013 and 2014 (bottom). Rainfall bars are stacked on top of each other when coinciding between years. Anthesis and physiological maturity dates are indicated, respectively, by a vertical, dashed line the 22nd October and another the 12th December. For CTD and water use, points are the means, and bars the standard errors, of 8 replicates. 156

Figure 5.5. Relative water use per soil layer and per day for Derrimut and Gregory during 2013 (top) and 2014 (middle), and rainfall per day (bottom). Water use is relative to the total water use per day, and it is indicated by coloured areas. Numbers inside those areas are their soil depths, in cm. Rainfall bars are stacked on top of each other when coinciding between years. Vertical, dashed lines across panels indicate anthesis (left) and physiological maturity (right) dates as in Figure 5.4. Relative water uses per soil layer are means of 8 replicates. 158

Figure 5.6. Accumulated water use from anthesis to maturity along the soil profile for Derrimut and Gregory during 2013 (left) and 2014 (right). Accumulated water use was determined as the sum of every negative change in volumetric water content ($\text{m}^3 \text{m}^{-3}$) measured by gypsum blocks between two successive days. Points are means, and

horizontal bars are standard errors, of 8 replicates. Asterisks at soil depths 100 and 140 during 2013 indicate statistically significant differences ($p < 0.05$). Other soil depths during 2013 and 2014 did not differ statistically. 160

Figure 5.7. Soil water content along the soil profile, at the start of the season (black line and triangles), and at maturity of each genotype (coloured points and lines) measured by neutron probe during 2013. Points are the means, and horizontal bars the standard errors, of 8 replicates in the case of soil water content at maturity. Initial soil water content is a mean of all plots in the trial, as they did not vary appreciably. 161

Figure 5.8. Canopy temperature deviation around solar noon (CTD) when fitted within the framework of Idso *et al.* (1981) and Idso (1982) during our experiments in 2013 and 2014. Each individual point is the CTD of each of 8 replicates per genotype, either Derrimut (pale red) or Gregory (pale blue). CTD_{UL} and CTD_{LL} represent, respectively, the CTD upper limit and CTD lower limit as explained in Figure 5.2. 162

Figure 5.9. Crop water-stress index (CWSI) calculated from canopy temperature (top), fraction of plant available water (FPAW) (middle), and rainfall per day (bottom) across time during 2013. Vertical, dashed lines across panels indicate anthesis (left) and physiological maturity (right) dates as in Figure 5.4. For CWSI and FPAW, points are the means, and bars the standard errors, of 8 replicates. For CWSI, data are missing between 20th October and 7th November due to malfunction of the infrared thermometers' data loggers. 165

Figure 5.10. Crop water-stress index (CWSI) calculated from canopy temperature (top), fraction of plant available water (FPAW) (middle), and rainfall per day (bottom) across time during 2014. Vertical, dashed lines across panels indicate anthesis (left) and physiological maturity (right) dates as in Figure 5.4. For CWSI and PAW, points are the means, and bars the standard errors, of 8 replicates. 167

Figure 5.11. A figure showing how crop water-stress index (CWSI) is a better predictor of the fraction of plant available water than the canopy temperature deviation from air temperature (CTD) alone. The figure shows either CTD (top row) or CSWI (bottom row) as a function of the fraction of soil available water (soil water held between suctions from 30 to 1500 kPa) during 2013 (left) or 2014 (right). Each data point is the mean of 8 replicates per genotype, for genotypes Derrimut (pale red) or Gregory (pale blue). R^2 are the r-squared values fitted per genotype per year. 168

Figure 5.12. Crop water stress index (CWSI) of Gregory minus Derrimut, as a function of water use of Gregory minus Derrimut during 2013 and 2014. Axes are the values of Gregory minus the values of Derrimut—i.e. $CWSI_{Gregory} - CWSI_{Derrimut}$, and $(water\ use\ Gregory) - (water\ use\ Derrimut)$. For instance, a value in the y-axis of -0.1 could mean that the CWSI of Gregory was 0.3 (less water-stressed) while the CWSI of Derrimut was 0.4 (more water-stressed). Correlation between ordinate and abscissa is nil, but data fall within the quadrant of negative difference in CWSI corresponding to positive difference in water use between Gregory and Derrimut—more water use corresponded with less water stress. 170

Figure 6.1. Simulated water supply-demand ratio for four environment types that typify the most common water balances for wheat across the Australian wheat-belt as a function of thermal time accumulated from anthesis (base temperature = 0 °C). Numbers indicate 4 possible environment types: environment 1: no or light stress; environment 2: post-flowering mild stress; environment 3: stresses that began before flowering but were relieved during grain filling; and environment 4: severe stresses that began during the vegetative period and lasted until maturity. Redrawn from Chenu *et al.* (2013 fig. 5). 191

Figure 6.2. Depiction of the method for determining the maximum water uptake per day per soil layer (kl). On the left, the graph shows the available soil water content at a given time t (θ_t) as a function of time since sowing for three soil depths. The parameters of equations (6.1) and (6.2) are indicated as well. On the right, the kl calculated as in the graph in the left are plotted along soil depth for two sunflower hybrids. Bars are standard errors. It must be noted that the data on the left is peanut and therefore does not relate to the data on the right; it only serves as an example. The figure was redrawn from Dardanelli *et al.* (1997). 197

List of Tables

Table 2.1. The classification of the soils of each experiment site under Australian (Stace <i>et al.</i> 1968; Northcote 1971; Isbell 1993) and American (Soil Survey Staff 1999) classification systems.	50
Table 2.2. Depth, percentages of sand, silt and clay, and field texture of the horizons of both soils evaluated in this study. Data were taken from Sleeman (1979 pp. 17, 21). ...	50
Table 2.3. Agronomic practices for each experiment, including sowing date, sowing density (pl ha^{-1}), fertilizer applied at sowing (kg ha^{-1}), nitrogenous fertilizer applied at the beginning of stem elongation (GS31, (Zadoks <i>et al.</i> 1974)) (kg N ha^{-1}), and harvest date.	57
Table 2.4. Agronomic characteristics of Derrimut and Gregory, the wheat varieties sown in Experiment 4.	59
Table 2.5. List of genotypes, and their characteristics, sown in the three field experiments. Genotypes sown during 2011 were the same in both experiments done during that season.	63
Table 2.6. List of measurements done in the field in each year. Measurements were taken at specific developmental stages (root and shoot samplings), once or twice in the whole season (bulk density, water retention parameters, water content by coring), weekly (water content by neutron moderation) or by continuous logging (water tension with gypsum blocks and canopy temperature). Stages of crop development were stem elongation (SE, growth stage 31, Zadoks <i>et al.</i> , 1974), anthesis (A, growth stage 65) and physiological maturity (M, growth stage 87).	71
Table 2.7. Parameters of the equation $\text{RLD} = a \text{RCD} / (1 + b \text{RCD})$, describing the root length density, RLD (cm cm^{-3}), as a function of the root count density, RCD (cm^{-2}). Each model was fitted separately for each soil layer. Significance levels of each estimate are: 0 '***' 0.001 '**' 0.01 '*' 0.05. SE is the standard error of each estimate. RMSE is the root mean square error and R^2 is the coefficient of determination of each model.	79
Table 4.1. Predicted genotypic means of rooting depth, root length per unit area, shoot biomass and grain yield per experiment. Asterisks (*) or a single dot (.) indicate statistical significance, for genotype, experiment and the interaction between both, as follows: 0 '***' 0.001 '**' 0.01 '*' 0.05 '.' 0.1 'NS' 1. Values within brackets are the least significant difference, calculated as twice the maximum standard error for pairwise comparisons given by the ASReml model.	133
Table 5.1. Means of shoot biomass, grain yield, harvest index, and cumulative water use during grain filling, per year (top 3 rows), per genotype (middle 3 rows), and per year \times genotype combination (bottom 5 rows). P values are specific to the rows above them. n.s. indicate comparisons that were not significant.	171

Chapter 1 Introduction: review of the potential of root depth to increase crop yield

1.1 Introduction

Projections of global food demand for the year 2050 tell us that we must double the amount of food that we produce today. Forecasts of whether we can or cannot achieve this are not encouraging, given that the rates of farm yield improvement for the major grain crops—wheat, soybean, maize, and rice—are smaller than what they should be in order to feed the world by 2050 (Ray *et al.* 2013). The issue is even worse if we consider that this large increase in food production needs to be achieved with reduced water supply, since fresh water demanded from cities and other sinks will compete with fresh water required by irrigation. Therefore, rather than relying on irrigation for grain yield, increasing yield per unit of water supply in rain-fed agriculture seems a more appropriate, sustainable alternative. But climate change is also expected to make rainfall more uncertain in some areas and droughts are expected to be more unpredictable as well as severe (Gornall *et al.* 2010). Under this scenario, it seems that the best alternative is to increase the resilience of agricultural systems to scarce water availability, and *deeper root systems* may offer a solution. Since most of the increase in grain production must come from rain-fed agricultural systems, while considering water as the limiting resource, we can learn some lessons from water-limited wheat production.

1.1.1 The framework of water-limited grain yield

We can understand water-limited grain yield by dividing the analysis between a qualitative framework, where ways in which a crop can face water shortages are categorised, and a quantitative framework, where grain yield is formalised as a function of water capture by crops.

A qualitative framework to understand water-limited yield was proposed by Ludlow and Muchow (1990). Within this framework, a crop facing drought can opt to escape or to resist. It could escape by completing its growing cycle just before the onset of the dry period at the beginning of summer, as is the case in Mediterranean environments.

'Escaping' was indeed one of the biggest innovations in wheat breeding in Australia, where controlling time of flowering so that phenology matched water availability, was one the breeding traits with the highest impact (Richards 1991). Fitting crop development within the period with most benign water availability during the season, so that crops can escape drought, is the primary aim when breeding for water-limited environments.

A crop can, on the other hand, resist a drought by either tolerating or avoiding it.

Tolerating drought is not such a widespread strategy within grain crops, and as such won't be a matter of this thesis; but as a matter of reference, it is related to protoplasmic cell resistance to dehydration (Ludlow and Muchow 1990), so that cells can remain alive. Avoiding drought, on the other hand, refers to *avoid* in the sense of eluding leaf dehydration by keeping leaves supplied with water as needed for transpiration. It involves the regulation of water loss by leaves, and the maintenance of water uptake,

possibly by deeper roots. Some examples of dehydration avoidance involve reductions in water loss by direct evaporation from the soil, which are possible by means of faster leaf area expansion in early stages of the crop—as is the case of increased early vigour in wheat (Rebetzke and Richards 1999; Rebetzke *et al.* 2004)—or by strategic management, such as earlier sowing date (Kirkegaard and Hunt 2010). Another way of controlling water loss is by modification of leaf geometry, as in the case of leaf rolling. Leaves roll when evaporative demand is highest during the middle of the day, thereby reducing their exposed leaf area and consequently transpiration, conserving water (Sirault 2007). As it will be developed onwards, the core matter of this thesis is indeed dehydration avoidance, specifically by means of deeper roots that can extract water from deep soil layers.

The second way of looking at water-limited yield is through a quantitative framework. This framework considers yield to be a function of the most limiting resource, water, and is represented by the following model deduced by Passioura (1977):

$$\text{Grain yield} = \text{Water used} \times \text{Water-use efficiency} \times \text{Harvest index} \quad (1.1)$$

where water used refers here to the accumulated transpiration (mm), water-use efficiency is the amount of above-ground biomass produced per unit transpiration ($\text{kg ha}^{-1} \text{mm}^{-1}$), and harvest index is the ratio of grain biomass to total above-ground biomass (unitless).

The first two terms, water used (WU) and water-use efficiency (WUE), are sometimes ambiguous because the spatial and temporal scales on which they are based are occasionally not defined (Passioura 2007). For instance, WUE could refer to the ratio of

CO₂ assimilation to transpiration within a square centimetre of leaf, which in regard to time would happen almost instantly, or, on a larger scale, it can refer to the ratio of grain yield to the amount of water input into the paddock—either as rain or irrigation, or both—within the duration of a whole crop season. On the other hand, harvest index, a ratio between two quantities that vary in congruence (grain mass to total above-ground plant mass), is invariably correct—e.g. if grain mass is expressed as kg ha⁻¹ so will be biomass.

Now that care has been taken about the various meanings of the terms, especially the most ambiguous term, WUE, I'll refer to them in order of increasing relevance for the statement of this thesis in relation to root depth.

WUE is the term that, in principle, would be less affected by the rooting depth of the crop than the other terms. This is because it depends on both extrinsic environmental factors and intrinsic factors unrelated to root function. From the extrinsic environmental factors, the most influential over WUE is vapour pressure deficit (VPD), a measure of 'how dry' the atmosphere is. This is because the higher the VPD the more water molecules are traded per molecule of CO₂ that is incorporated by photosynthesis. Greater VPD, therefore, reduces WUE (Kemanian *et al.* 2005). From the intrinsic factors, carbon isotope discrimination (CID), the ratio between the less abundant isotope ¹³C and the more common ¹²C in plant tissues relative to the same ratio in the atmosphere, is inversely related to WUE at the leaf level (Condon *et al.* 2002). This relationship enabled phenotyping for more water-use efficient wheat varieties, since measuring CID in plant tissues, a sort of autopsy of the crop, is much easier than measuring cumulative water use throughout the season and biomass at maturity.

However, the problem was not that straightforward. When scaling from leaf to crop, Condon *et al.* (2002) showed that CID did not always predict WUE at this higher-order level of organization. When crops relied on stored soil moisture to grow, the CID was inversely related to WUE, as expected, but when in-season rainfall was present, the relationship was reversed, with CID being directly related to WUE at the crop level. Whichever way WUE affects water-limited yield, it is certainly unrelated to root function. There is one way, though, in which more vigorous root systems could affect WUE at the crop level: by increasing water use early in the season. For winter cereals like wheat, this coincides with a time in the season when VPD is low and therefore dry matter is 'cheap' to produce in relation to its cost in water use (Gomez-Macpherson and Richards 1995). This could be the case for crops like barley (*Hordeum vulgare* L.) or triticale (\times *Triticosecale*) which have greater leaf area expansion rates and apparently greater root depth than wheat early in the season. Under these conditions, if barley and triticale could exploit soil water faster than wheat early in the season by means of a larger root system coupled with a larger leaf area, then they could grow more biomass with a high WUE. Therefore, more vigorous roots early in crop development, either deeper or longer, could slightly increase WUE, but in other circumstances root growth would not affect WUE.

Harvest index (HI) can vary slightly between genotypes and can be affected by stress conditions during the reproductive period, like drought. Changes in HI due to breeding were responsible for the so called 'Green Revolution'. Before this revolution wheat plants used to have heavier, longer stems. By intensive breeding in the field, crossing a wide range of wheat cultivars, Norman Borlaug and colleagues reduced the height of the

plant by introducing *Rht* dwarfing genes, and improved disease resistance. While reducing plant height, they possibly altered the competition for assimilates between stems in favour of grains, increasing HI and yield. If conditions for plant growth are potential (i.e. only limited by incoming radiation and temperature; not water, nutrients or disease), HI only depends on the genotype. On the other hand, under stressful growing conditions HI can be drastically reduced. This reduction is more severe in some stages of crop development than other stages, and so this gives rise to the definition of critical periods for yield determination, when HI is most sensitive to changes in resource availability and therefore stresses.

Knowing about the critical period of yield determination helps one to understand how deeper roots can affect HI of wheat. The critical period for yield determination in many annual grain crops occurs almost always around flowering, when the number of grains that the plant will have is determined (Fischer 1985). Once the critical period has ended, the number of grains is fixed. Because grains have a narrow range of possible sizes that they can grow (Sadras 2007), a ceiling for achievable yield is set. Subsequent benign conditions cannot repair the reductions in grain number. HI and yield both correlate highly with the number of grains per unit area. After the critical period has ended, stresses over plant growth can only reduce yield by reducing the other component of grain yield—grain weight. How could deeper roots affect grain number and grain weight increase and harvest index?

The mechanism by which deeper root systems could increase access to water could happen in two ways. First, they could prevent the occurrence of intermittent stresses around flowering that reduce grain number. Second, during the grain-filling period,

avoiding terminal droughts could ensure that most of the grains set during the critical period are properly filled. The greatest impact of deeper roots seems to be by maintaining the source during grain filling, for there is no evidence that having deeper roots could increase the number of grains, and therefore the sink size and HI. Setting more grains and growing more roots around flowering could be in competition similar to that between stem growth and grain number before the Green Revolution. It is not clear, however, how reducing stem growth by breeding, while increasing HI, affected the growth of roots. Miralles *et al.* (1997) found no differences between wheat cultivars differing in dwarfing genes, but effects of reduced stem growth on root growth are certainly likely to happen and might still not be properly documented. I will show later that reducing stem height could increase not only yield but rooting depth as well, where potentially both interact with each other—i.e. less partitioning of biomass to stems, free assimilates to grow deeper roots, more water use, more yield.

Water used (WU), the amount of water transpired by the plant, is the single most important factor to be affected, in principle, by more vigorous root systems with deep roots. This is because deep roots can explore volumes of soil that would otherwise be unexploited by plants, and thus, they can increase the supply of water to the crop, *avoiding* drought. But the amount of transpiration, or WU, depends on supply and demand. The supply is determined by the capacity of the soil and the root system to provide water to the evaporation sites in the leaves. The demand is determined by the atmospheric vapour pressure, radiation, wind and the total leaf area. Final transpiration will be equal to either the supply or the demand, whichever is smaller (Cowan 1965). To illustrate this point, if on a given sunny, hot day a wheat crop could transpire 3 mm

(i.e. the potential evapotranspiration is 3 mm) but the root system can only provide 2 mm, then transpiration will be 2 mm. On a different day, with cool and cloudy conditions and consequently low VPD, a wheat crop with an extensive root system growing in a wet soil that can provide 4 mm/day but with a low potential evapotranspiration of 1 mm/day, will transpire 1 mm/day. From this view, having deep roots does not guarantee higher WU—it only helps in providing water when it is actually demanded. Deeper root systems can only affect the supply.

Finally, and importantly, the terms in equation (1.1) are not independent between each other, and the interaction is most likely to happen between terms where deep roots can have an effect: water used and harvest index. More precisely, when regarding WU, the amount is only part of the story—the timing of the uptake is important as well. A crop could maximize WU by depleting soil moisture before flowering, and if there is no rainfall thereafter, there will not be enough water for grain filling. Under these circumstances WU will be high but HI will be very low or nil, and so will be yield. This is exemplified by Passioura (1976), who achieved higher grain yields in potted wheat when the same amount of water was administered in equal amounts along the plants' development than when applied all at once at the start of their life cycle. This occurred because photosynthesis was sustained during grain filling and the plant tissues necessary for an adequate remobilization of assimilates to the developing grains also survived (Passioura 1976). Indeed, HI can be interpreted as a function of the fraction of WU after anthesis over WU for the whole cropping season (Sadras and Connor 1991). An example of this concept is expressed in field conditions is the study of Siddique *et al.* (1990), where 10 wheat cultivars representing different years of release were

evaluated. They found that modern cultivars used less water but more of that water was used during the post-anthesis phase than the pre-anthesis phase. These cultivars also yielded more through a higher harvest index. Thus, timing is as important as the amount. Deep roots could increase the danger to crops by exhausting all soil moisture before anthesis.

1.1.2 How can deeper root systems improve water-limited yield?

Having deeper roots can, at the same time, (i) increase the total amount of potential WU as well as (ii) increase the risk of reducing HI so dramatically as to achieve a point where there is no yield. Having the right balance between pre- and post-anthesis water use is a key to maximize yield, and using as much water as possible is a key to maximize biomass. There are therefore two opposite strategies on how a crop might deal with water shortages. A conservative strategy minimizes WU pre-anthesis, increasing the chances of having water left in the soil during grain filling. The opposite strategy is where crops use as much water as possible, in a luxurious way, so that biomass is maximized. The issue is how deep roots may affect these strategies.

1.1.2.1 Deep roots, conservative and luxurious use of water

Being conservative can increase yield by increasing HI and WUE when crops grow primarily on stored soil moisture. This is why, as discussed before, Condon *et al.* (2002) obtained higher yields when increasing WUE through less CID only in years when wheat grew with limited water supply during grain filling. Yield benefits from being conservative as a crop in terms of water use is also supported in a simulation modelling

study by Sinclair *et al.* (2005). When sorghum limited its transpiration rate to a maximum by closing stomata during midday, yields were increased on average by 7%, and even higher yield increases were obtained in the worst (driest) seasons. Regarding roots and conservative use of water, there was a successful breeding programme based on a plant physiological framework developed by Richards and Passioura (1989).

Wheat lines were developed with reduced xylem diameter in the seminal roots. This resulted in a larger resistance to axial flow, so plants withdrew water from the soil at a much slower rate, leaving more water for later during the critical period of yield determination. This increased yield when plants were growing mostly on stored soil moisture. This is one example of conservative behaviour of water use. Are there examples of the opposite, that is, luxurious use of water?

In environments where the soil profile could be replenished by later rainfall, crops usually leave water unused at the bottom layers of their rooting depth (Jordan and Miller 1980). Therefore, a crop with an 'luxurious' strategy that can exploit that unused deep water could be more effective in the use of water. WU could be increased and consequently yield. The advantage of being luxurious as a crop in using water is supported by Blum (2009), who proposed the concept of *efficient use of water*, by which he states that water use and harvest index are the drivers of yield in water-limited conditions, not transpiration efficiency. He suggested that if we call water use and harvest index 'drivers', transpiration efficiency should be called 'a passenger'. He emphasized the value of deep root systems for maintaining transpiration during grain filling. For Blum (2009), being water-use efficient is not the solution for breeding crops that produce more under water-limited conditions, but rather to have crops that are

better 'exploiters' of deep water. The key to increase water-limited yield, for him, was to increase water use. He also argued that the success of Condon *et al.* (2002) in selecting for lower CID related to high WUE and resulting in high yields was because in this region of Australia, NSW, wheat relies on stored water, supporting the deduction of Passioura (1976) of the timing of water use.

A strong argument against Blum (2009), however, is that breeding has not yet improved the amount of total WU but rather the WUE in an evapotranspiration basis, meaning that either transpiration efficiency was increased or direct soil evaporation was reduced. This is shown by Campos *et al.* (2004) for maize in the US and Sadras and Lawson (2013) for wheat in South Australia. Campos *et al.* (2004) found that new maize hybrids used less water but produced more yield, and, interestingly, water use at shallow soil layers was less than in old hybrids, with a slight increase in deep water use (Fig. 3 in Campos *et al.*, 2004). This may be telling us that total water use is a difficult trait to improve and that it wasn't improved yet, but it certainly does not mean that it is impossible to change. Moreover, it could be possible to develop a crop that can at the same time exploit the deeper soil by means of deeper roots, and have a reduced stomatal conductance during critical times of the day, around noon, when fixing CO₂ is relatively expensive in terms of water use. In fact, the analysis of Sinclair *et al.* (2005) is about limiting transpiration rate to a maximum by limiting leaves conductance. Leaves conductance is an independent trait from deep water use, and opens the possibility, provided the traits are independent and can be separated, of breeding for both traits pyramided in the same genotype (Wilson *et al.* 2015). There seems to be no reason against having both traits in the same plant.

1.1.2.2 Objections, and their solutions, to higher production with deeper roots

While it is intuitive to suppose that more root length deep in the soil will increase WU and improve the fate of crops facing droughts, there are many objections. Some objections are related to the fact that growing more roots implies diverting assimilates to them, assimilates that could otherwise be directly used in growing more grain. Others, to the fact that sometimes roots, while present in deep soil with apparently sufficient length-density and time, fail to extract the available water leaving after maturity valuable water deep in the soil.

Investing more biomass in deep roots, because of the law of conservation of matter, means that there would be less assimilates to invest in grains. Therefore, it could be the case that the extra roots do not recover, in terms of grains, the amount of assimilates for growth and maintenance respiration that were initially invested into them. This is aggravated by the fact that roots often respire, per unit dry weight, more than the shoot tissues (Passioura 1983). And investing in deeper roots can also compete with the accumulation of water soluble carbohydrates (Lopes and Reynolds 2010), which often sustain grain growth when conditions of drought prevail during grain filling. Perhaps it could be more advantageous for grain growth just to allocate carbon to grains or to store sugars into stems rather than investing in more root growth.

Another objection for crops with deeper roots is that there are many cases where water-stressed crops fail to extract much of the available water in the subsoil even if sufficient root length was present (Jordan and Miller 1980; Kirkegaard *et al.* 2007). Several

reasons were proposed. One of those reasons is that sometimes roots do not actually distribute evenly in the subsoil, but they rather follow the structure of the soil. For instance, in highly structured soils, roots usually grow along the paths of less resistance, which drives them to clump together inside macro-pores left behind by past roots or worms or planes formed by cracks in the soil (White and Kirkegaard 2010). This soil structure limits the effectiveness of root length density because instead of root length being distributed evenly through the soil, it is confined to macro-pores which are more scarcely distributed in the soil volume. Water uptake under these conditions is not determined by root length density, but rather, by macro-pore distribution. Deery (2008) and Deery *et al.* (2012) explored the possibility of this limitation being caused by the soil or by the rhizosphere itself. Because the parameter that determined soil water flow in the soil, soil water diffusivity, was much larger than they expected, and root distribution was even, they concluded that the limitation was more likely within the rhizosphere. This limitation in the rhizosphere can be caused, as they stated, by shrinkage of the roots as the transpiration rate increased—reducing contact between roots and soil and thereby limiting flow—or the possibility that when transpiration was high the plant itself was increasing the resistance in the roots by means of aquaporins. Control by the plant was suggested through aquaporins (molecular channels across cellular membranes that are responsible for water transport in and out the cells), or control by the root by altering the composition of exudates (Ghezzehei *et al.* 2015). Moreover, a limit to water extraction by roots can be imposed by solute accumulation in the root-soil interface, as suggested by Stirzaker and Passioura (1996).

In spite of these objections to deep roots, there are possible solutions that could justify breeding for them. To address the matter of the waste of carbon when investing in deep roots rather than grains, having deeper roots does not necessarily mean that is necessary to grow more root biomass. In fact, crops may be producing much more root length density in the topsoil than what is actually necessary for water uptake, so why not to shift the allocation of growth from shallow roots to deep roots? According to Deery (2008) the optimum root length density for water uptake is about 0.1 cm cm^{-3} . Root length density at a soil depth of 20 cm is usually 4 cm cm^{-3} . It is worth to introduce here the distinction of the two types of roots that form a grass root system: seminal roots, which originate from the seed embryo, and nodal roots, which originate from subsequent nodes either from seed or stem tissues. Deep root length seems to be more closely related to the growth of seminal roots. In a field study evaluating wheat, barley and triticale, Watt *et al.* (2008) found that most roots present beyond 1 m depth were first- or second-order branches of seminal roots, never nodal roots. In fact, nodal roots have features which make them less suitable for deep water uptake: they emerge later which gives them less time to reach deep soil layers, show less gravitropism, and are more vulnerable to nutrient or water stress (Tennant 1976). However, roots present deep in the soil were neither strictly seminal axes. Based on the number of xylem tracheary vessels, Watt *et al.* (2008) found that these first- or second order roots differed in their inner anatomy to the original seminal root axes. They had indeed less cross-sectional area of xylem trachery vessels (less number and smaller vessels) that make them one to two orders of magnitude less capable of axial water flow when compared to seminal roots. Therefore, it seems that the capture of deep water in the soil relies on branches

from seminal roots, but there is still potential to increase water uptake if seminal root axes, rather than its branches, can reach deep soil layers. Nonetheless, whether deep roots are seminal or nodal, the fact that root length in shallow soil is above the threshold required to maximise water uptake indicates that there is still room to reallocate root growth from shallow to deeper soil layers. Indeed, this shift might have been responsible for the increase in maize yield due to breeding in United States corn belt (Hammer *et al.* 2009).

There may be opportunities for breeding wheat with root growth shifted towards deep soil layers since natural selection, while maximising individual competitiveness, may have rejected a shift of growth to deep roots (Denison 2012, 2015). It happens that natural selection operates much more over individual plants than over plant populations (Denison 2012). Individual plants, in competition with neighbouring plants, can only maximise individual performance by selfishly using resources. Therefore, an overproduction of roots in shallow soil may be a strategy to outcompete neighbouring plants. Moreover, it seems clear that plants can recognise self from non-self roots (Gersani *et al.* 2001; Falik *et al.* 2003), and the response to non-self root encounters is overproduction (Gruntman and Novoplansky 2004). This strategy of outcompeting neighbours in a crop situation is undesirable. This relates to the pivotal research by Donald (1968) and his definition of plant ideotypes, that is, plants with traits that make them better allies when sown in a crop. Ideotypes have in common that while reducing their competitive ability to a minimum the overall collective performance of the crop, with performance defined, for instance, as their capacity to produce grain yield, is higher than common, 'selfish' plants. In relation to the distribution of roots, a wheat

ideotype would have more root growth allocated to deep soil and less in shallow soil layers, and therefore competitiveness between neighbour plants is reduced and that growth surplus can be allocated to other organs, like deep roots (Zhang *et al.* 1999; Lynch 2013). Therefore, there may be opportunities for shifting root growth to deep soil layers while reducing growth in the topsoil.

Another objection to increased investment into deeper roots is the fact that sometimes roots are present but unable to use residual water. Evidence that breeding has improved the WU is still lacking but there are many good reasons that it is worth the challenge. Increasing the availability of water during the critical periods, while maintaining a proper balance of pre- and post-anthesis WU, should increase the stability of yield. Opportunities may also exist to breed crops with steep root angle and higher allocation to deep rather than shallow roots (Lynch, 2013). This will serve as a justification for the next section, where one starts wondering how deep roots could be increased: management and most importantly, as is the focus of my thesis—breeding.

1.1.3 Improvement of root depth through management and genotype selection

As discussed in the previous section, deep roots can increase yield in grain crops, but how do we improve deep roots? Two alternatives seem to be available: by management or by breeding. Management can increase deep-root length by either lengthening the period of root downward growth or by removing soil factors that are detrimental to root growth. An example of root-growth lengthening is sowing earlier. Roots seem to grow mostly during the vegetative period in annual plants. When plants like wheat flower, the

assimilates are partitioned to the developing grains. Organs like leaves even senesce and in doing so remobilize their nitrogen content to satisfy the grains' need for protein. In congruence, roots stop growing—or at least this is commonly believed (Lynch 1995). If sowing earlier can make the period from sowing to flowering longer, and root-growth rates are kept unchanged, then rooting depth and length can be increased (Kirkegaard and Lilley 2007). Sowing earlier was documented by Kirkegaard and Hunt (2010), where they found higher water-use efficiency and more water use than normal sowing times, possibly by the contribution to total water use from deeper roots. Improving the hospitability of soils to detrimental factors, such as acidity and its concomitant aluminium increased concentrations and toxicity (Delhaize *et al.* 2004), can also increase rooting depth and functional root length deep in the soil. Also the introduction of break crops into rotations—in contrast with continuous wheat—has removed some root diseases and improved soil hospitability as well (Kirkegaard and Hunt 2010).

The second alternative, breeding cereals with deeper roots, is the core of this thesis. Relying in breeding rather than management, has the advantage that the improvements can be cheaper and, if the traits are constitutive rather than adaptive, the benefits can be ubiquitous. As an example, an experimental wheat variety developed to expand its leaf area faster so that the soil can be covered quicker also had more vigorous root growth and was better able to cope with soil pathogens (Watt *et al.* 2005). Another breeding aim was to select wheat genotypes with a narrower angle of root growth so that more root length was directed towards deeper soil layers (Manschadi *et al.* 2008). A simulation model predicted that this would increase yield under water-limited conditions (Manschadi *et al.* 2006). Breeding might have been already successful in

improving deep water use in wheat, as new wheat varieties extract more water from deep soil layers than old wheat varieties (Pask and Reynolds 2013).

If breeding is the chosen alternative to improve deep roots, how do we select for genotypes with deeper roots? Several avenues, with different capacities of success, are proposed. First, selection based on measuring roots activity without actually measuring the roots, an alternative that can be illustrated in a quote by the pioneer crop modellers De Wit and Penning de Vries (De Wit and Penning de Vries 1983): "modelling hormone action without modelling the hormones" (Hammer *et al.* 2004). Dardanelli *et al.* (1997) used this technique when growing sunflower in the field. They did not measure root length density but they inferred root presence by quantifying the changes in soil water content by using a model originally proposed by Passioura (1983). They found genotypic differences in the maximum rate of water uptake between two sunflower hybrids, and this example remains one of the few where genotypes differed for the rate of water extraction in field conditions. In another study, Dardanelli *et al.* (2004) applied the same simple model to predict water use by several crop species, such as maize, soybean, sunflower, and peanut, with a high degree of accuracy. A drawback of this technique, however, is that high water extraction could be either due to a more effective deeper root system as to a higher stomatal conductance. Separating conductance from root length is the key to work under this frame work. Another drawback is that to measure the maximum uptake rates the crops have to be kept under conditions where the demand of water from the atmosphere is higher than the achievable supply by the roots. This can only be achieved by preventing input from rainfall, either by sowing in arid environments or by building effective rain-out shelters.

A second alternative is to anticipate rooting depth in the field by previously screening genotypes in the glasshouse. For example, root angle is a trait that can be measured in pots, and can be related to rooting depth of adult plants in the field (Manschadi *et al.* 2008). Root angle may be a stable trait whose selection at young developmental stages of wheat can transcend towards adult stages, like anthesis. Measuring root length at seedling stages, however, may be meaningless for wheat production in the field, for Watt *et al.* (2013) found that root length of juvenile plants growing inside wet paper rolls did not correlate with the root length of adult plants growing in the field. In other words, differences in root length evident during early stages of plant development dilute towards adult stages that are critical for yield determination. Therefore, measuring root angle in young wheat plants is a promising trait but root length is not.

A third selection alternative is to directly sample roots in the field by soil coring. This is time consuming but some automation of the coring process could increase throughput. Digitization of the root sampling images for later analysis could further help to quantify root presence or even root length (Wasson *et al.* 2012, 2014).

A fourth selection alternative is canopy temperature, a trait that can be used as a surrogate of transpiration. Cool canopies during grain filling might indicate access to deep water—hence deeper roots. Reynolds *et al.* (2007) showed that cooler canopies during grain filling left less unused water between 30 and 120 cm soil depth. Lopes and Reynolds (2010) linked drought adaptation to deeper root mass distribution which was detected by cooler canopy temperature. However, caution must be taken when interpreting canopy temperature measurements, as variables such as leaf porosity, plant height, biomass and yield can confound the signal (Rebetzke *et al.* 2012).

This thesis will focus on how to select for wheat crops with deeper roots. First, genetic variability in rooting depth under field conditions was evaluated in a large germplasm collection possessing diversity in stem growth and shoot vigour. Second, canopy temperature was evaluated as a surrogate for transpiration and as a trait to select for deeper roots under field conditions.

1.2 Thesis aims

There are two main aims of this thesis: (i) to identify genetic variability in root depth under field conditions, in relation to biomass and yield of wheat and triticale, and (ii) to see if measuring canopy temperature and soil water content continuously can serve as surrogates of deep root length that is useful for field phenotyping.

1.3 Thesis outline

In Chapter 2 the many methods used to measure roots, biomass, and yield in the field will be detailed.

Gypsum blocks were used to quantify soil water suction (kPa) in the field. The complexities of the methods involved in this calibration to eventually determine volumetric water content ($\text{m}^3 \text{m}^{-3}$) are presented in Chapter 3. Gypsum blocks enabled soil water content to be monitored continuously in 2 wheat varieties.

Rooting depth and root length are explored under field conditions where 34 wheats and 2 triticale varieties were phenotyped. The results of these experiments are presented in

Chapter 4, and the relationships between genetic variability in deep-root length, crop growth, total above-ground biomass and grain yield are analysed.

In Chapter 5, the issue of whether deep-rooted wheats can be selected without digging the ground is addressed. For this purpose, canopy temperature was used as a surrogate for transpiration. Two commercially available high yielding wheat varieties for Australia were investigated. Soil water, as suction (kPa) and as volumetric content ($\text{m}^3 \text{m}^{-3}$), was continuously monitored at different soil depths and changes compared against canopy temperature.

In a final discussion that forms Chapter 6, the major findings of the whole thesis are presented in relation to a unifying hypothesis.

Chapter 2 Field experiments used for wheat phenotyping

2.1 Introduction

In this Chapter I'll explain many of the methods and measurements done in the field. It is a methodological chapter, and thus, unlike the rest of the chapters, no hypothesis is tested.

Most of the experiments were carried out in the field in common growing conditions for wheat farming in New South Wales. A main difference was in the genotypes sown, as we utilised lines recently developed by research in CSIRO in addition to commercially available material. Examples of those developments are the "overgrowth" varieties by Dr Peter Chandler (see Chandler and Harding, 2013), the high initial vigour varieties developed by Dr Greg Rebetzke (Rebetzke *et al.* 2004) and the tillering inhibition isogenic lines by Dr Richard Richards (Duggan *et al.*, 2005). Other agronomic conditions, exclusive to our experiments but unusual to farmers in the region, were the fertilization treatments in experiment 4, where rates of nitrogen applied were too low (none) or excessively high (200 kg ha⁻¹); they were, however, appropriate for our aims of exploring contrasting growing environments for shoots (particularly leaf area) and roots.

In the following sections I'll explain how we performed the experiments in the field during three consecutive seasons from 2011 to 2013, as well as how we measured roots

and soil characteristics in the laboratory when needed. Several devices that quantified soil water suction and content, leaf and soil temperatures, and local weather variables for the experimental site were provided by the High Resolution Plant Phenomics Centre, and will be detailed as well.

All field experiments were done in the Ginninderra Experimental Station, which belongs to CSIRO and is located in the Australian Capital Territory (35.2 S, 149.08 E). The site has a greater annual rainfall than surrounding wheat growing areas in NSW, and thereby crops grew closer to potential conditions—that is, closer to conditions when growth and development are only limited by radiation and temperature.

2.2 Growing conditions: soils and weather

We performed six field experiments in four consecutive growing seasons in 2011, 2012, 2013 and 2014. They were conducted in the Ginninderra Experiment Station in three close locations but belonging to two different soil classes (Figure 2.1). Experiments 1 and 2 were done during 2011, experiment 3 during 2012, experiment 4 during 2013, and experiments 5 and 6 during 2014.

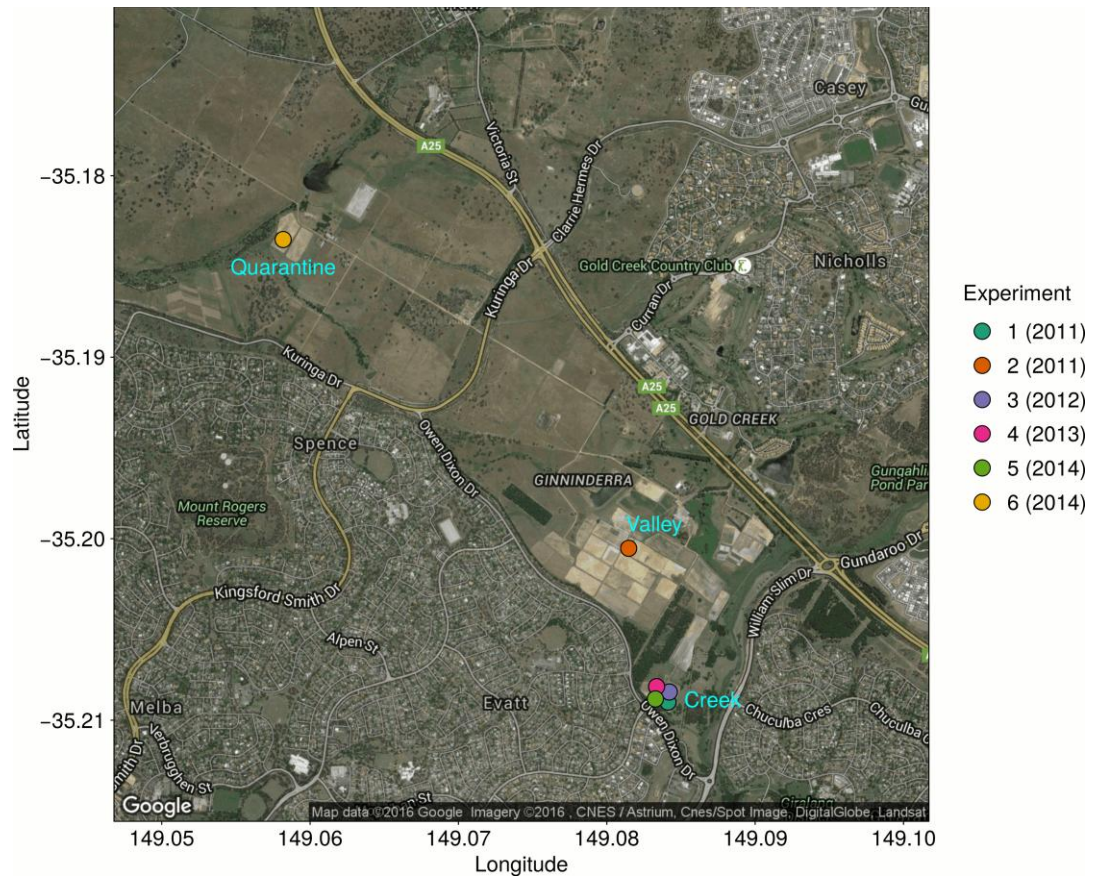


Figure 2.1. Location of the 6 field experiments and their corresponding sites (Creek, Quarantine and Valley).

Experiments 1, 3, 4 and 5 were sown in a Red podzolic soil (Sleeman 1979), on a site that onwards will be called "Creek". Experiments 2 and 6 were sown in a Yellow podzolic soil (Sleeman 1979), in the sites designated as "Valley" and "Quarantine", respectively. The classification of each soil according to Australian (Stace *et al.* 1968; Northcote 1971; Isbell 1993) and American systems (Soil Survey Staff 1999) is listed in Table 2.1. The characteristics of the horizons of each soil are described in Table 2.2. The Red podzolic soil where experiments 1, 3, 4 and 5 were sown, allowed plants to grow better than the Yellow podzolic soil, where experiments 2 and 6 were sown. To

characterize the soil we performed coring until a depth of 2 m; these coring procedures were almost identical to the root coring procedures which will be described later in section 2.6.2, but with a larger diameter coring tube.

Table 2.1. The classification of the soils of each experiment site under Australian (Stace *et al.* 1968; Northcote 1971; Isbell 1993) and American (Soil Survey Staff 1999) classification systems.

Site	Experiments	Stace <i>et al.</i> (1968)	Northcote (1971)	Isbell (1993)	Soil Survey Staff (1999)
Creek	1, 3, 4, 5	Red podzolic soil	Dy3.82	Hydrosol	Oxic Paleustalf
Quarantine and Valley	2, 6	Yellow podzolic soil	Dy3.42	Hydrosol	Udic Paleustalf

Table 2.2. Depth, percentages of sand, silt and clay, and field texture of the horizons of both soils evaluated in this study. Data were taken from Sleeman (1979 pp. 17, 21).

Soil	Horizon	Depth (cm) ^a	Sand (%)	Silt (%)	Clay (%)	Field texture
Red podzolic soil	A1	0-8	68	20	14	Fine sandy loam
	A21	8-16	69	17	13	Fine sandy loam
	A22	16-25	60	19	20	Fine sandy loam
	B1	25-34	29	9	57	Medium clay
	B2	34-52	14	9	70	Medium clay
			52-69	20	12	64
Yellow podzolic soil		69-83	24	14	57	Heavy clay
	A1	0-5	72	18	9	Loamy sand
	A21	5-18	71	21	7	Loamy sand
	A22	18-38	74	11	16	Sandy loam
	B21	38-48	51	16	31	Light clay
			48-78	56	18	25
		78-100	59	18	22	Clay loam

^aSoil depths were registered by Sleeman (1979) until 1 m, but the soil beneath 1 m was homogenous in both profiles and can therefore be described by the last horizon in the table.

Soil chemical (Figure 2.2) and physical properties (Figure 2.3) differed between both Creek and Valley soils. However, physical properties are the most likely candidate to explain the reduction in shoot and root growth in that the Valley soil. A key component of the soil physical properties of a soil is its bulk density, that is, the ratio between the dry weight and the unaltered volume of a soil. Bulk density can be reduced by compaction and that compromises water flow and gas exchange. It can be seen in Figure 2.3 that bulk density was always greater for the soil at the Valley at soil depths beyond 40 cm. The pore space left for gas exchange between the roots and the atmosphere, the air-filled porosity, a function of bulk density, becomes too small, and oxygen supply can be so slow as to limit root growth (Wesseling *et al.* 1957). Anoxia could then be the reason for the impoverished growing conditions for plants, and their roots in particular, in the Valley soil.

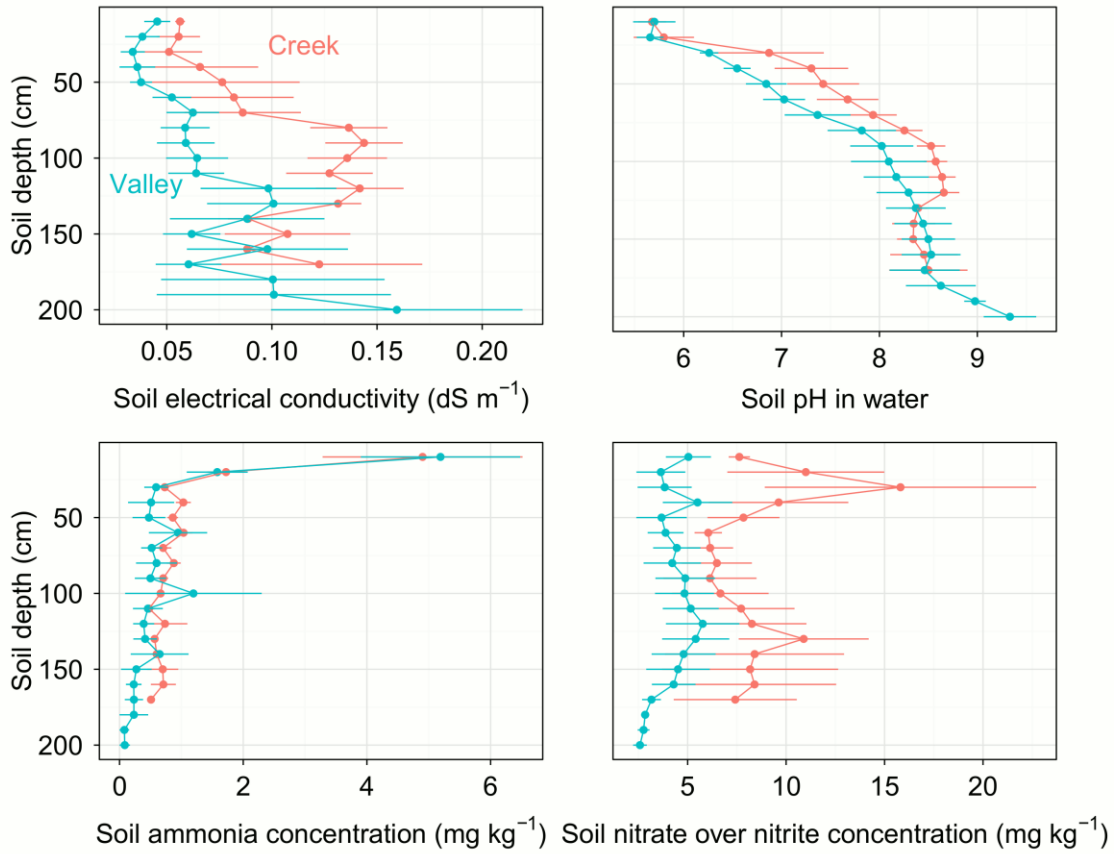


Figure 2.2. Soil chemical characteristics measured during May 2011, just before sowing of experiments 1 and 2. Soil electrical conductivity, soil pH, soil ammonia concentration, and soil nitrate over nitrite concentration as a function of soil depth. Bars are the standard errors of the means. Colours indicate the soil of origin: Creek or Valley.

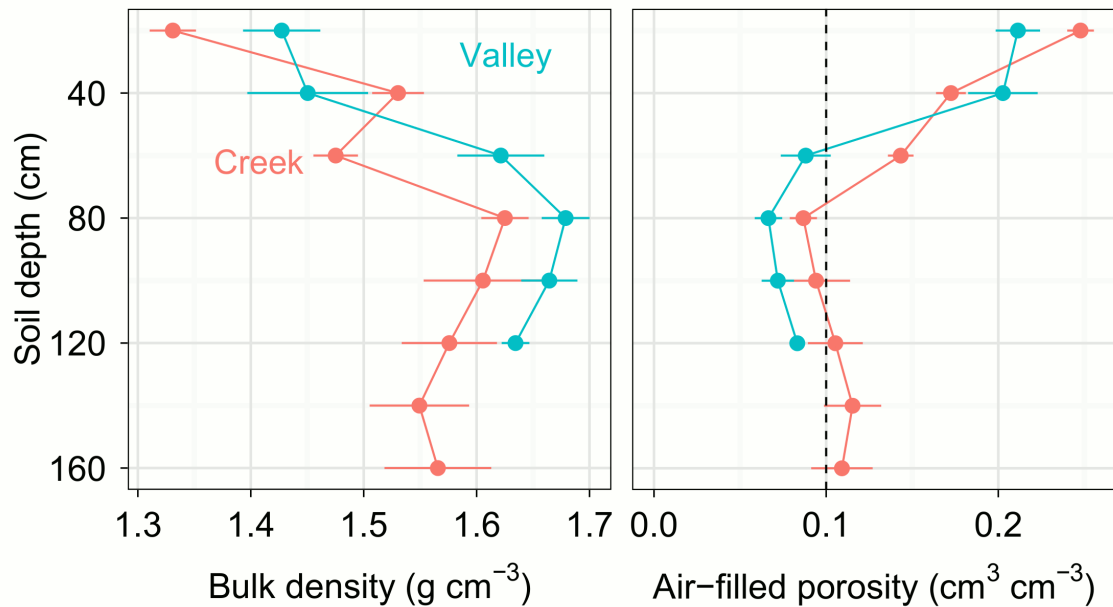


Figure 2.3. Soil physical characteristics measured during May 2013, just before sowing of experiment 4. Soil bulk density and air-filled porosity as a function of soil depth. Air-filled porosity was estimated from bulk density, BD , and water contents per layers at the start of the season, θ ($\text{cm}^3 \text{cm}^{-3}$), and an average soil particle density, PD (g cm^{-3}) of 2.65. Then air-filled porosity = $1 - \frac{BD}{PD} - \theta$. The dashed vertical line in the right panel indicates the theoretical limit of air-filled porosity below which most soils produce anoxia to roots (Wesseling *et al.* 1957). Colours indicate the soil of origin: Creek or Valley. Bars are the standard errors of the means.

The weather conditions, when categorised within the climate classification system of Köppen (1918) (see also Wikipedia, 2014), were those of a temperate class climate, which are characterised by a lack of dry season and a warm summer (designated *Cfb* by Köppen, 1918). Rainfall, reference evapotranspiration as calculated by Penman-Monteith FAO (Zotarelli *et al.* 2010), minimum and maximum air temperatures for the site were obtained from <http://www.longpaddock.qld.gov.au/>. Regarding these data, rainfall varied much more than temperatures (Figure 2.4). In particular, experiment 3, during 2012, might have started with more initial soil-water stored given the high rainfall accumulated during March (Figure 2.4). Season 2012 was probably better in

terms of resource availability for growth than 2011 (and this will be reflected later in Chapter 4).

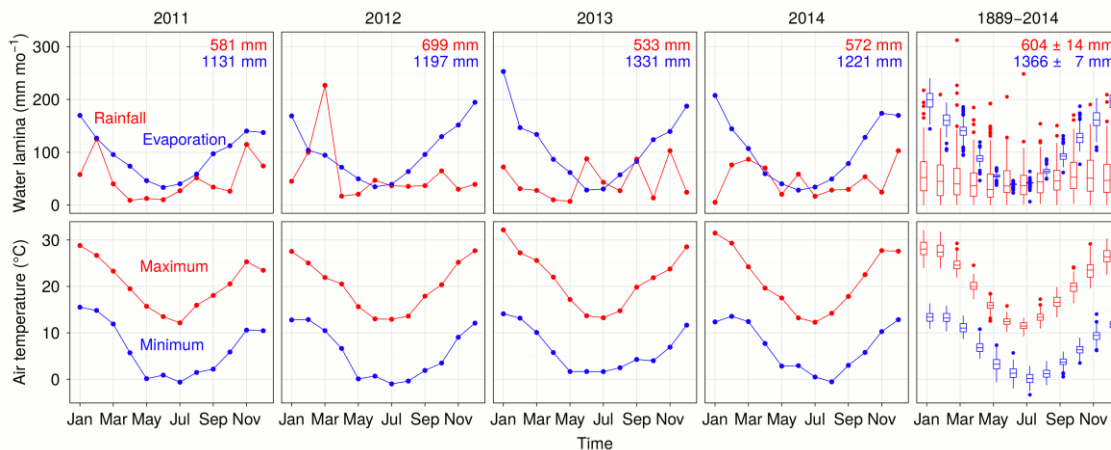


Figure 2.4. Rainfall and reference evapotranspiration (top) and maximum and minimum monthly-mean temperatures (bottom) for the four years when experiments were conducted and a long term period from 1889 to 2014 for the Ginninderra Region. Boxplots indicate percentiles 0.10, 0.25, 0.50, 0.75, and 0.90, where points represents outliers (i.e. smaller than percentile 0.10 or larger than percentile 0.90). In each panel, numbers on the top-right corner indicate total annual rainfall (red) and total annual evapotranspiration (blue). For the period 1889-2014 rainfall and evapotranspiration are described as mean \pm standard error ($n = 125$ years). Data were obtained from <http://www.longpaddock.qld.gov.au/>.

2.3 Sowing and agronomic management

Crops were sown in the field in plots of varied length but constant width (1.8 m, the width of a sowing machine, Figure 2.5). We chose different plot lengths in different seasons as a solution between the total area of paddock available, the required number of measurements for the season, and the number of treatments involved. As a result, plots were 6 m long in experiments 1 and 2, 7 m in experiment 3, and 8 m in experiment 4 and 5 (Figure 2.5). All plots were sown with 10 rows distanced 0.18 m from each other (which is a conventional row spacing for wheat growing in this region). Plots were

fertilized, in all experiments at sowing, with a mix of 15-12-0-12 Croplift 15® (percentages of N, P, S and K, respectively) at a rate of 100 kg ha⁻¹. Additionally, experiment 4 included a fertilization treatment with nitrogen, where, besides the default fertilization with the 15-12-0-12 mix, 0 or 200 kg N ha⁻¹ were added just before the stem elongation growth stage (growth stage 31, Zadoks *et al.*, 1974). Further information about agronomic practices for each experiment are included in . Other abiotic (nutrients) or biotic (weeds, diseases) stresses were avoided by sound management, since we aimed to achieve growing conditions where only radiation, temperature and water limited growth of the crops.

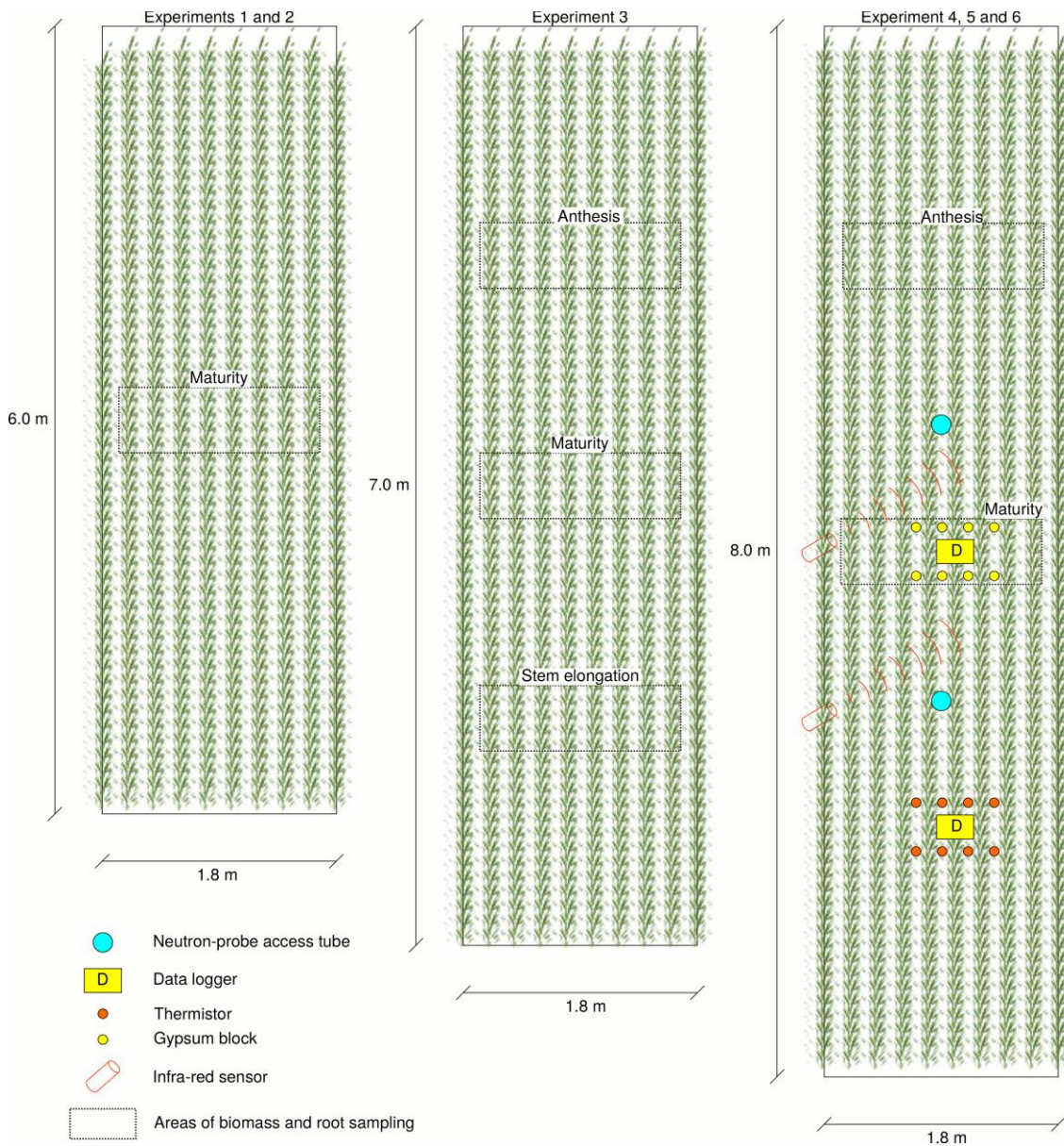


Figure 2.5. Diagrams representing plots in the 6 experiments. Above-ground biomass and yield were sampled in the areas limited by dashed lines, and soil coring to sample roots was done over the same areas after sampling biomass. This was done only at maturity in experiments 1, 5 and 6 (Zadoks 87); at anthesis (Zadoks 65) and maturity in experiment 4; and at stem elongation (Zadoks 31), anthesis and maturity in experiment 3. Plots in experiment 5 and 6 were similar to plots of experiment 4, except that they only had one biomass cut at maturity and one infrared thermometer (rather than two), and they lacked neutron probe access tubes.

Table 2.3. Agronomic practices for each experiment, including sowing date, sowing density (pl ha⁻¹), fertilizer applied at sowing (kg ha⁻¹), nitrogenous fertilizer applied at the beginning of stem elongation (GS31, (Zadoks *et al.* 1974)) (kg N ha⁻¹), and harvest date.

Experiment	Year	Site	Sowing date	Sowing density (pl m ⁻²)	Fertiliser at sowing (kg ha ⁻¹)	N fertiliser at GS31 ^c (kg N ha ⁻¹) ^d	Harvest date
1	2011	Creek	29 th May	150	15-12-0-12 ^b	100	30 th Dec
2	2011	Valley	29 th May	150	15-12-0-12	100	30 th Dec
3	2012	Creek	29 th May	150	15-12-0-12	100	28 th Dec
4	2013	Creek	5 th June	150	15-12-0-12	0, 200 ^e	23 th Dec
5	2014	Creek	2 nd June	100, 200 ^a	15-12-0-12	100	23 th Dec
6	2014	Quarantine	2 nd June	100, 200	15-12-0-12	100	23 th Dec

^aExperiments 5 and 6 included a plant density treatment with levels 100 and 200 pl m⁻² (Figure 2.12).

^bNumbers indicate, in this order, kilograms per hectare of nitrogen, phosphorous, sulphur and potassium. In all cases they were added as a single fertilizer mix (Croplift 15®) at a rate of 100 kg ha⁻¹.

^cGS31 = growth stage 31, beginning of stem elongation (Zadoks *et al.* 1974).

^dIn this case, the fertiliser used was granular urea.

^eExperiment 4 included a nitrogen treatment with levels 0 and 200 kg N ha⁻¹ added at GS31 (Figure 2.11).

2.4 Germplasm sown

Germplasm included a wide variety of wheat (*Triticum aestivum* L.) and triticale (× *Triticosecale*) varieties, either commercially available or experimentally developed (i.e. not available commercially), to explore contrasting patterns of below- and above-ground crop growth (Table 2.5). Patterns of shoot and root growth were thought to change in response to several putative mechanisms that were tested before in laboratory conditions. These mechanisms were (1) "overgrowth" wheat mutants, (2) inhibited tillering, (3) increased early vigour in wheat, (4) and increased early vigour by means of another species, i.e. triticale.

Experiments 1 and 2 included the broadest selection of genotypes, where 34 wheat and 2 triticale varieties were sown. They were selected because they included alternative mechanisms to enhance root growth.

Experiment 3 involved a subset of 12 wheat and triticale varieties from the previous, original 36, but only 8 will be analysed, for the other 4 varieties were lodged by wind at anthesis and their data are suspiciously altered. The remaining 8 varieties were selected after analysis of experiment 1 and 2 data, because they showed to be deep rooted.

Experiment 4 was intended to explore wider ranges of rooting depth and water use by using two contrasting fertilization treatments with nitrogen, and two commercial wheat varieties that, after experiments performed by Dr James Hunt, at CSIRO, shown to have contrasting vertical patterns of water use notwithstanding similar time to flowering and similar grain yield. The fertilization treatments aimed to alter leaf area development and presumably root growth, for it is known of the large effect that nitrogen has over leaf expansion. The varieties were Derrimut, a variety developed for NSW, where wheat usually thrives by using on-season water from rain falls, and Gregory, a wheat variety developed for Queensland, where wheat yield depends more strongly on the use of stored soil water. Their contrasting origin in terms of breeding areas implies that Gregory may be better suited to deep water uptake than Derrimut. James Hunt observed that when comparing both varieties in the field Gregory was able to extract more water deeper than Derrimut, and total water used by the former was greater. Although similar yields and greater water used indicate that Gregory is less water-use-efficient than Derrimut, it is interesting to investigate how the former can capture more water at depth than the latter. Moreover, mechanisms that promote greater water use could be different

from those that confer greater water-use efficiency. In that case, where there is no trade-off, one could breed for varieties that have large water use and optimal water-use efficiency. Further characteristics of these two wheat varieties are shown in Table 2.4

Table 2.4. Agronomic characteristics of Derrimut and Gregory, the wheat varieties sown in Experiment 4.

Variety	Release	Origin	Quality ^c	Maturity type	Morphology	Height (cm)
Derrimut	2007	Nugrain ^a	Australian Hard	Medium early	Semi-dwarf	80
Gregory	2004	EGA ^b	Australian Hard	Medium late	Moderate height	100

^aNugrain Pty Ltd, <http://nuseed.com/au/>

^bGregory was bred by Pacific Seeds (<https://www.pacificseeds.com.au/>) and the Queensland Department of Primary Industries within the Enterprise Grains Australia (EGA) joint venture.

^cThis is the maximum attainable quality grade (<http://wheatquality.com.au/classification/how-it-works/classes/>). The actual grain quality would vary among environments.

Genotypes sown in experiment 3 were selected from experiment 1 and also from a field trial performed by Dr Anton Wasson, from CSIRO as well. Anton's experiment was done during 2011 at the same location as experiment 1 in the current thesis, but instead of being sown in 6-m-long plots, it was sown in "hill plots". "Hill plots" are not groups of equally spaced plants like those sharing a canopy in normal agronomic conditions. Instead, they are sets of ~30 plants growing crowded in an area not bigger than 100 cm². They may not reflect agronomic conditions but they are certainly appropriate for breeding purposes, where hundreds of genotypes are evaluated at one. They are sown by hand by pouring 30 seeds down a 40 mm diameter PVC tube. For selecting genotypes from experiment 1, to be sown in experiment 3, we selected the 8 of the deepest-rooted varieties (Figure 2.6 left), which were as well some of the varieties producing the

highest biomass (Figure 2.6 right). For selecting genotypes from Anton's hill plots, we chose those that fell within the 10% deepest or the 10% shallowest varieties (Figure 2.7 left) and were at the same time having different combinations of root growth and shoot growth (Figure 2.7 right), that is, high root counts and high biomass (CAV4081179); high root counts and low biomass (CAV4081278); low root counts and high biomass (CAV4080667); and low root counts and low biomass (CAV4081444; Figure 2.7 right). Our aim when choosing varieties by root growth in combination with shoot growth was to maximise the chances of finding differences in the allocation of root biomass to deep soil layers—e.g. a variety producing high shoot biomass with low root counts might be allocating more of its root growth to deep soil layers. However, given the standard errors of the means for rooting depth and root counts in Figure 2.6 and Figure 2.7, genotypic differences may not be statistically significant and therefore the alleged differences in root depth and root counts might just be due to environmental factors plus random variation. As seen later in Chapter 4, the ranking of rooting depths and root counts and biomass combinations do not hold from experiment 1 to experiment 3. Four MAGIC varieties were selected but because CAV4081179 was severely lodged at anthesis it was excluded from the analysis (Table 2.5).

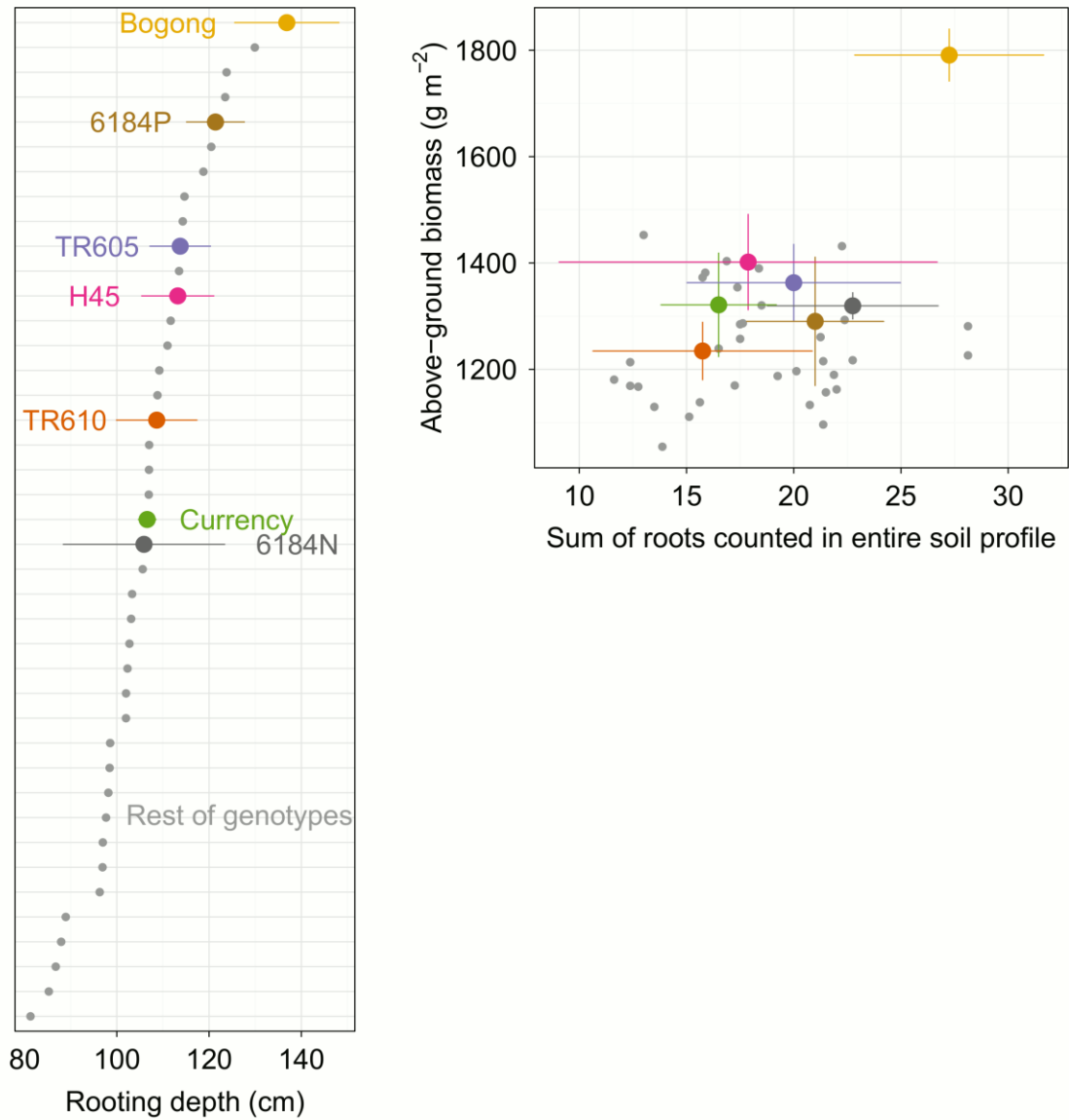


Figure 2.6. Selection of genotypes at experiment 1 (2011) to be sown in experiment 3 (2012). Rooting depth at maturity for all varieties sampled in experiment 1 (left), and above-ground biomass as a function of the sum of root counts (root tips) along the soil profile, both at maturity as well. Coloured dots are the selected genotypes. Dots are means of 4 replicates and bars are standard errors of those means. Grey dots are the rest of the varieties sown in experiment 1, which were not selected to be sown in experiment 3.

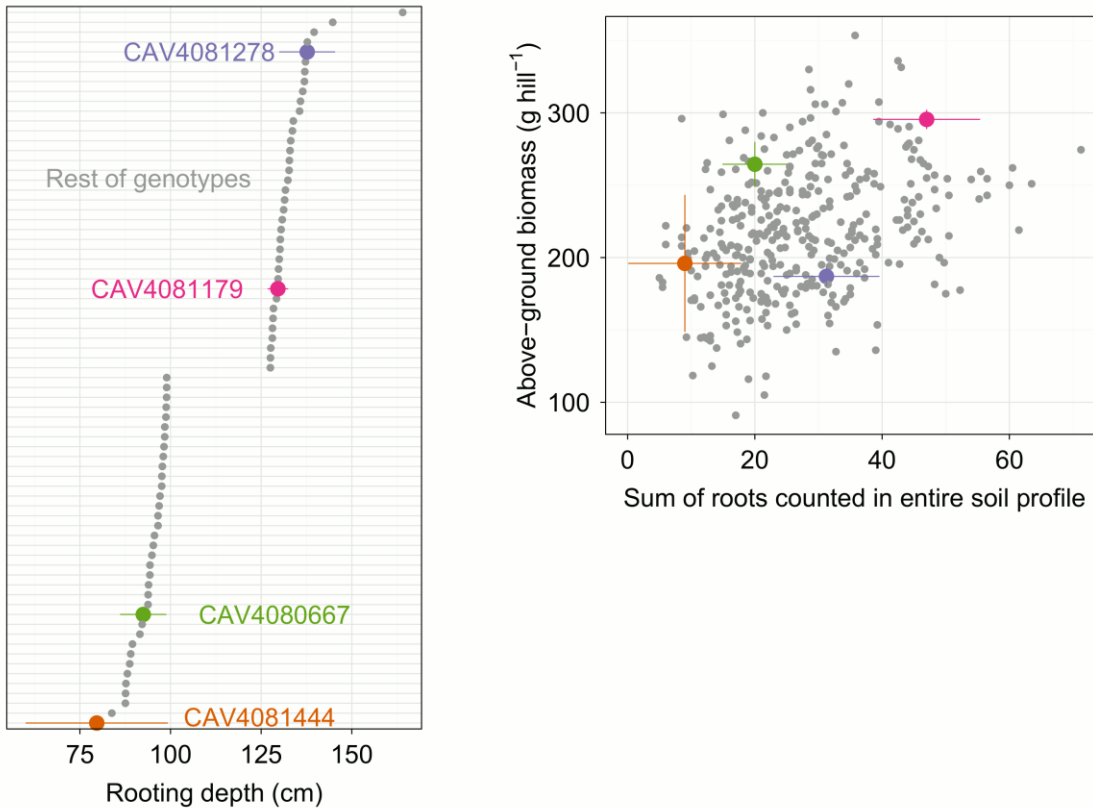


Figure 2.7. Selection of genotypes at 'hill plots' experiment (2011) to be sown in experiment 3 (2012). Rooting depth at maturity for the 10% deepest and the 10% shallowest roots in the 'hill plots' experiment (left), and above-ground biomass as a function of the sum of root counts (root tips) along the soil profile, both at maturity as well. Coloured dots are the selected genotypes. Dots are means of 4 replicates and bars are standard errors of those means. Grey dots are the rest of the varieties sown in the 'hill plots' experiment, which were not selected to be sown in experiment 3.

Table 2.5. List of genotypes, and their characteristics, sown in the three field experiments. Genotypes sown during 2011 were the same in both experiments done during that season.

Group	Genotype	Exp 1 & 2	Exp 3	Exp 4 & 5	Characteristics	
Short (< 80 cm)	TR550	✓			Overgrowth wheat mutants: single point mutants of the Maringa Rht1 and Rht3, BC7 isogenic lines with varying degrees of height recovery (see (Chandler and Harding 2013)).	
Medium (> 80 < 110 cm)	MRht1	✓				
	TR544	✓				
	TR605	✓	✓			
	TR623	✓				
Tall (> 110 cm)	MRht	✓				
	TR606	✓				
	TR610	✓				
Spring	Espada	✓				Commercial, spring wheat, used as a benchmark for root and shoot growth.
	H45	✓				
	Magenta	✓				
	Pastor	✓				
	Westonia	✓				
	Yitpi	✓				
Long spring	Beaufort	✓			Commercial, spring wheat with a longer time to flowering in between spring and winter wheat.	
	Preston	✓				
Winter	Revenue	✓			Winter wheat.	
	Wedgetail	✓				
Tin minus	5447N	✓			Near isogenic wheat pairs with (suffixes P or plus) or without (suffixes N or minus) the <i>tin</i> gene, whose presence inhibits tillering.	
	6184N	✓	✓			
	6266N	✓				
	6460N	✓				
	Kite minus	✓				
Tin plus	5447P	✓				
	6184P	✓	✓			
	6266P	✓				
	6460P	✓				
	Kite plus	✓				
Vigour	3-2-4	✓			Increased early-vigour wheat: faster leaf area expansion and, presumably, more vigorous root growth.	
	7-1-1	✓				
	8-5-3	✓				
	W010104	✓				
	W020204	✓				
	W030503	✓				

MAGIC	CAV4081444		✓		MAGIC wheat, derived from parents Yitpi, Xiaoyan54, Westonia, SB139, Pastor, Chara, Alsen, and Baxter.
	CAV4081278		✓		
	CAV4080667		✓		
Triticale	Bogong	✓	✓		Triticale (\times <i>Triticosecale</i>), which compared to wheat has more vigorous shoot and root growth.
	Currency	✓	✓		
Contrasting commercials	Derrimut			✓	Two commercial spring wheat varieties that contrast in the depth of water use: Gregory, deeper water use, and Derrimut, less-deep water use.
	Gregory			✓	

2.5 Statistical designs

Experiments were always sown in randomized, complete-block designs, in four replicates arranged as blocks—i.e. one replicate per block. In order to remove possible soil or environmental effects over our response variables (e.g. rooting depth, above-ground biomass), the spatial configuration of the experiments was further recorded by positioning each plot within a coordinate system consisting on "columns" and "rows". Recording rows and columns allowed spatial effects to be modelled and eventually removed, with the resulting 'distilled' effects of the genotypes. Models used were fitted in ASReml-R (Butler 2009)(see Appendix A).

Experiment 1 was sown in the Creek soil at the same time as experiment 2 in the Valley soil, during 2011. They share exactly the same genotypes but of course in different spatial configurations given by randomized allocations of the plots (Figure 2.8 and Figure 2.9). Experiment 3 was sown in the Creek soil as well, but the number of genotypes was reduced to 12, 4 of which were lodged at anthesis, yielding a remaining set of 8 genotypes (Figure 2.10). Experiment 4, unlike the previous three, had an extra

treatment that involved nitrogen fertilization of 0 or 200 kg N ha⁻¹ (Figure 2.11). And experiment 5 replicated the same 2 genotypes sown in experiment 4, but in combination with two sowing densities: 100 and 200 plants m⁻² (Figure 2.12).

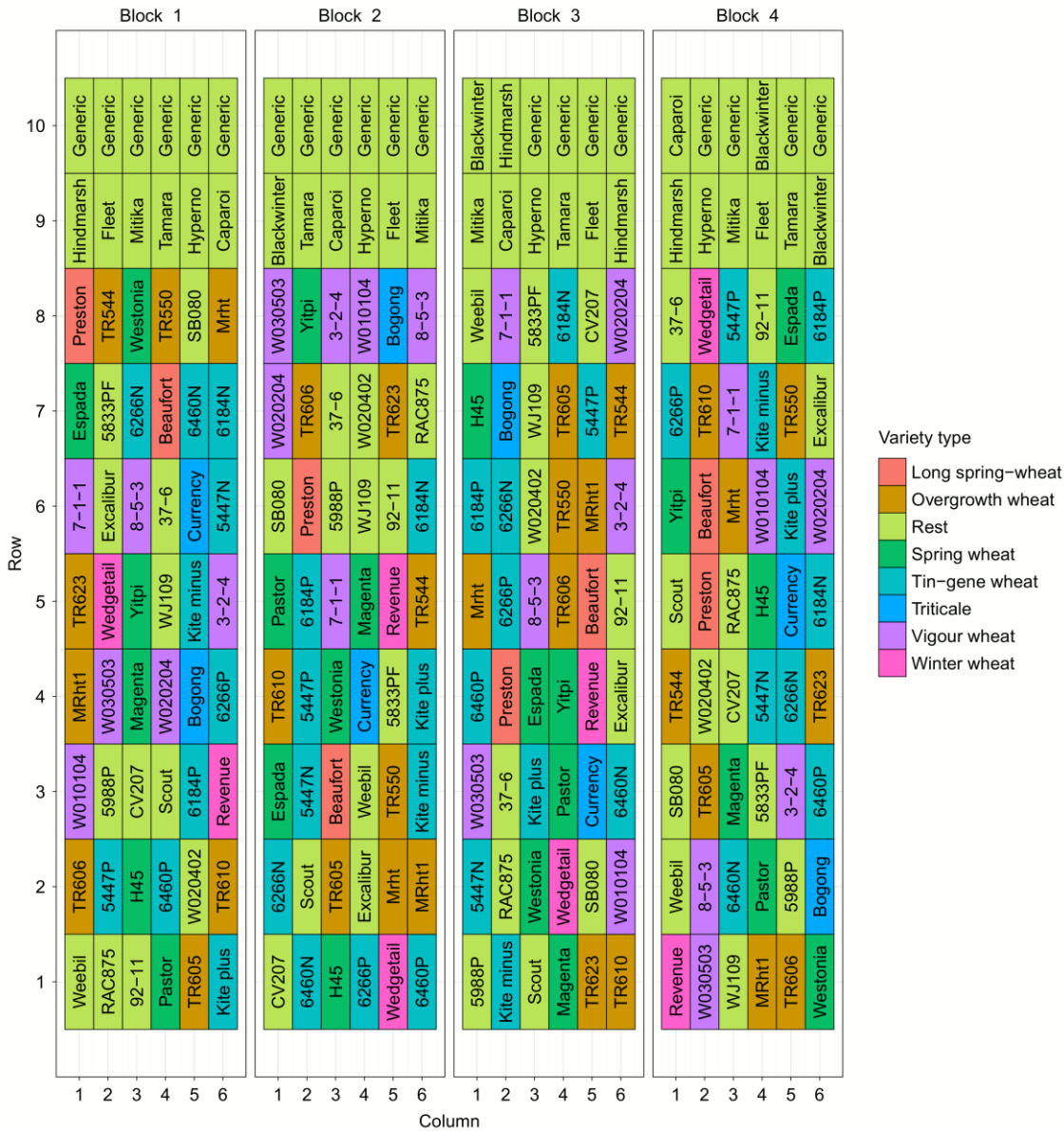


Figure 2.8. Statistical design of experiment 1. The experiment was sown during 2011 in the Creek site (red podzolic soil). Colour specified as 'rest' (pale green) identify plots that were not sampled, and from those, 'generic' was a wheat genotype that was used as a buffer.

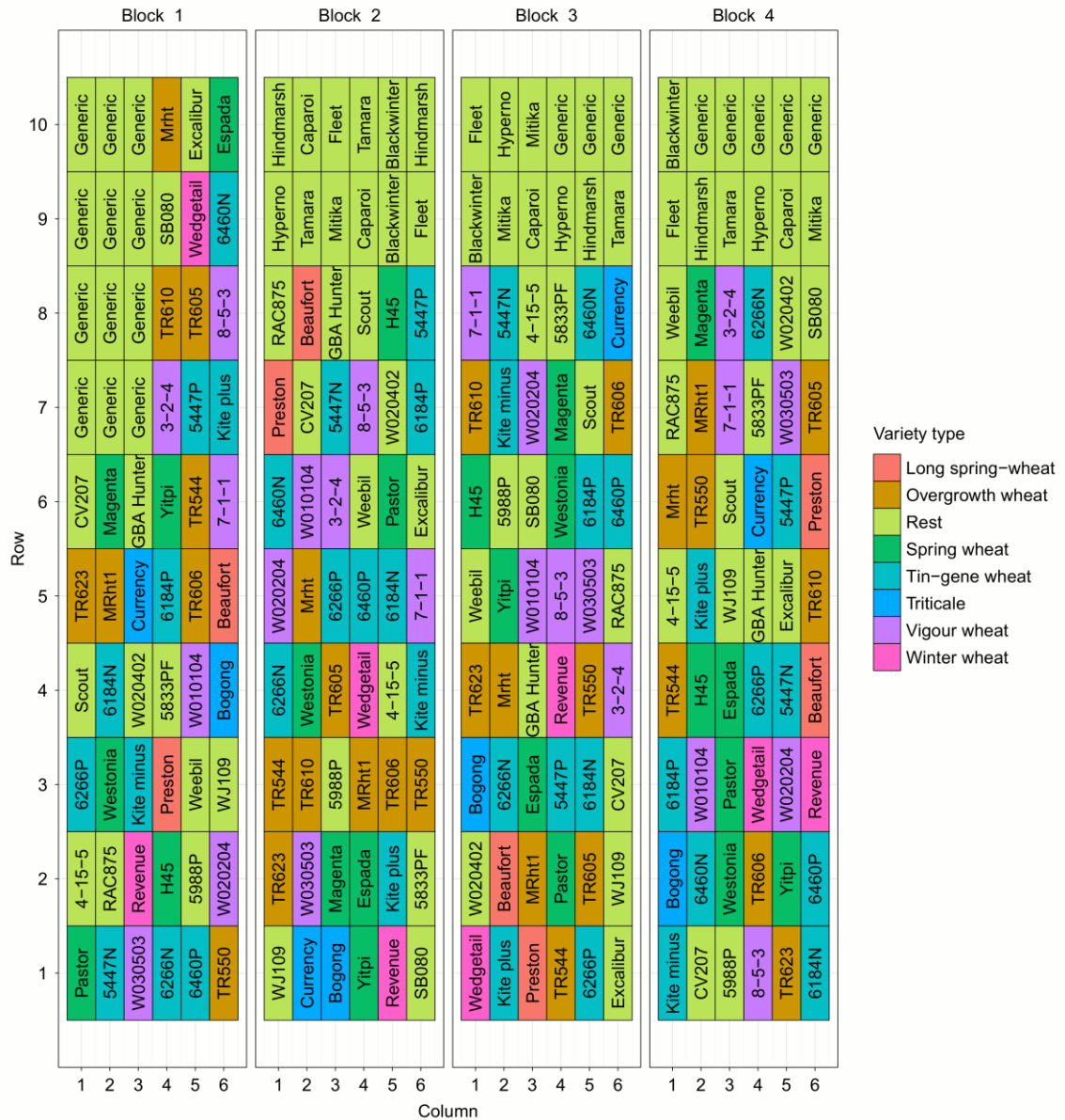


Figure 2.9. Statistical design of experiment 2. The experiment was sown during 2011 in the Valley site (yellow podzolic soil). Colour specified as 'rest' (pale green) identify plots that were not sampled, and from those, 'generic' was a wheat genotype that was used as a buffer.

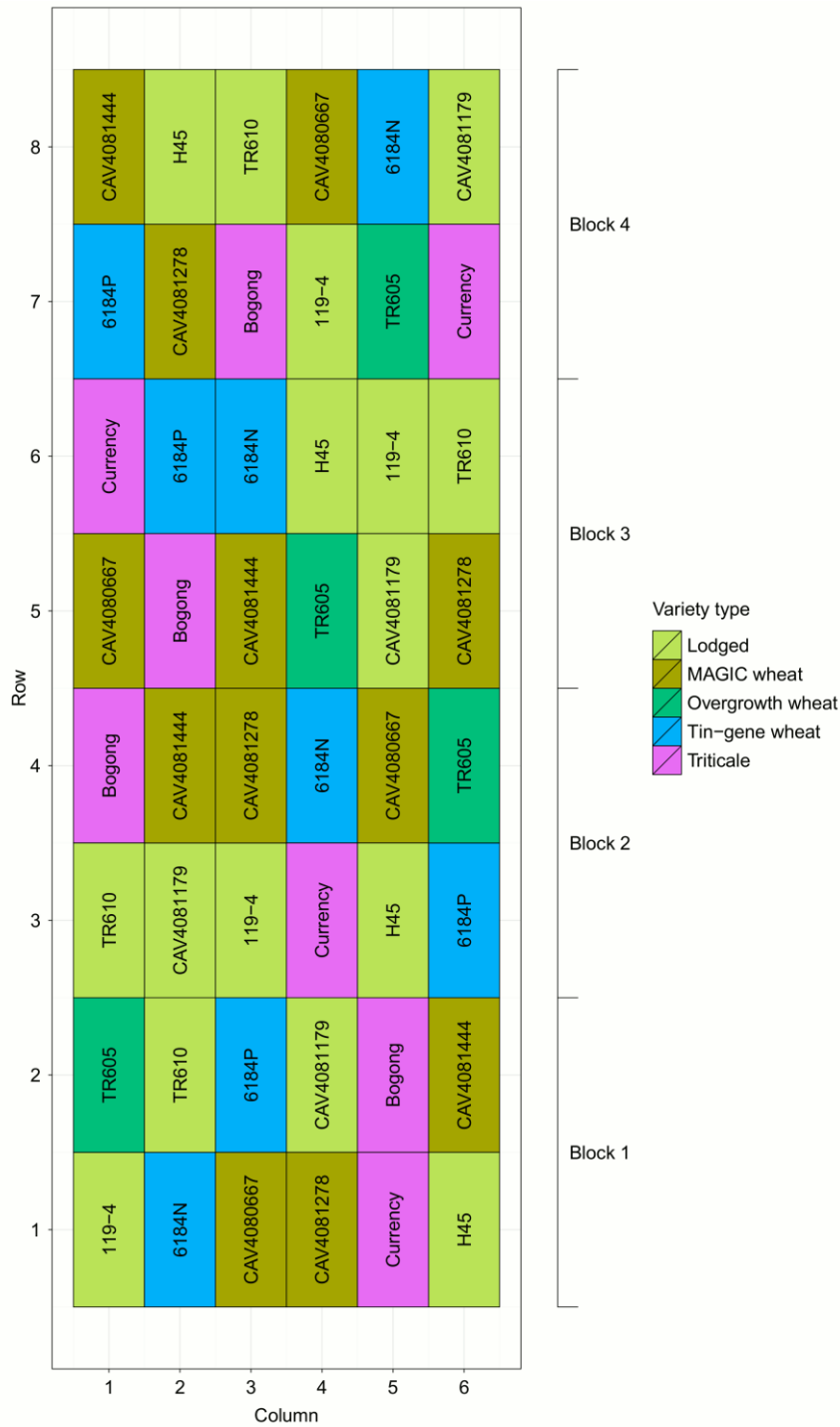


Figure 2.10. Statistical design of experiment 3. The experiment was sown during 2012 in the Creek site (red podzolic soil). Colour specified as 'lodged' (pale green) identify plots that were not sampled because they were stem-lodged at anthesis.

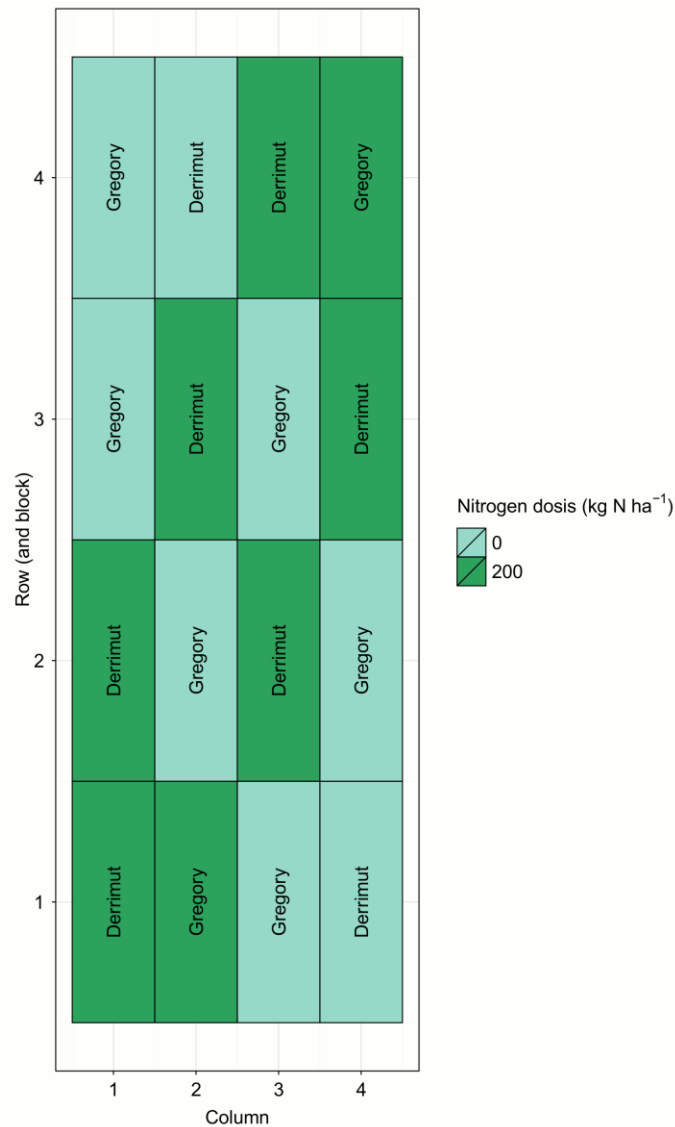


Figure 2.11. Statistical design of experiment 4. The experiment was sown during 2013 in the Creek site (red podzolic soil). Two commercial wheat varieties, with supposedly different root depth at maturity, were sown in combination with 2 nitrogen fertilization treatments aimed to maximise differences in root growth: 0 and 200 kg N ha⁻¹ applied at the stem elongation stage (Zadoks 31). However, and unfortunately, plots were mistakenly fertilised, and therefore blocks 2 and 4 don't have all the possible treatment combinations—i.e. in block 2, Derrimut fertilised with 200 appears in two plots, and Derrimut without fertilization none. Fortunately, nitrogen had no statistical effect over shoot or root growth, so the nitrogen treatment is later disregarded.

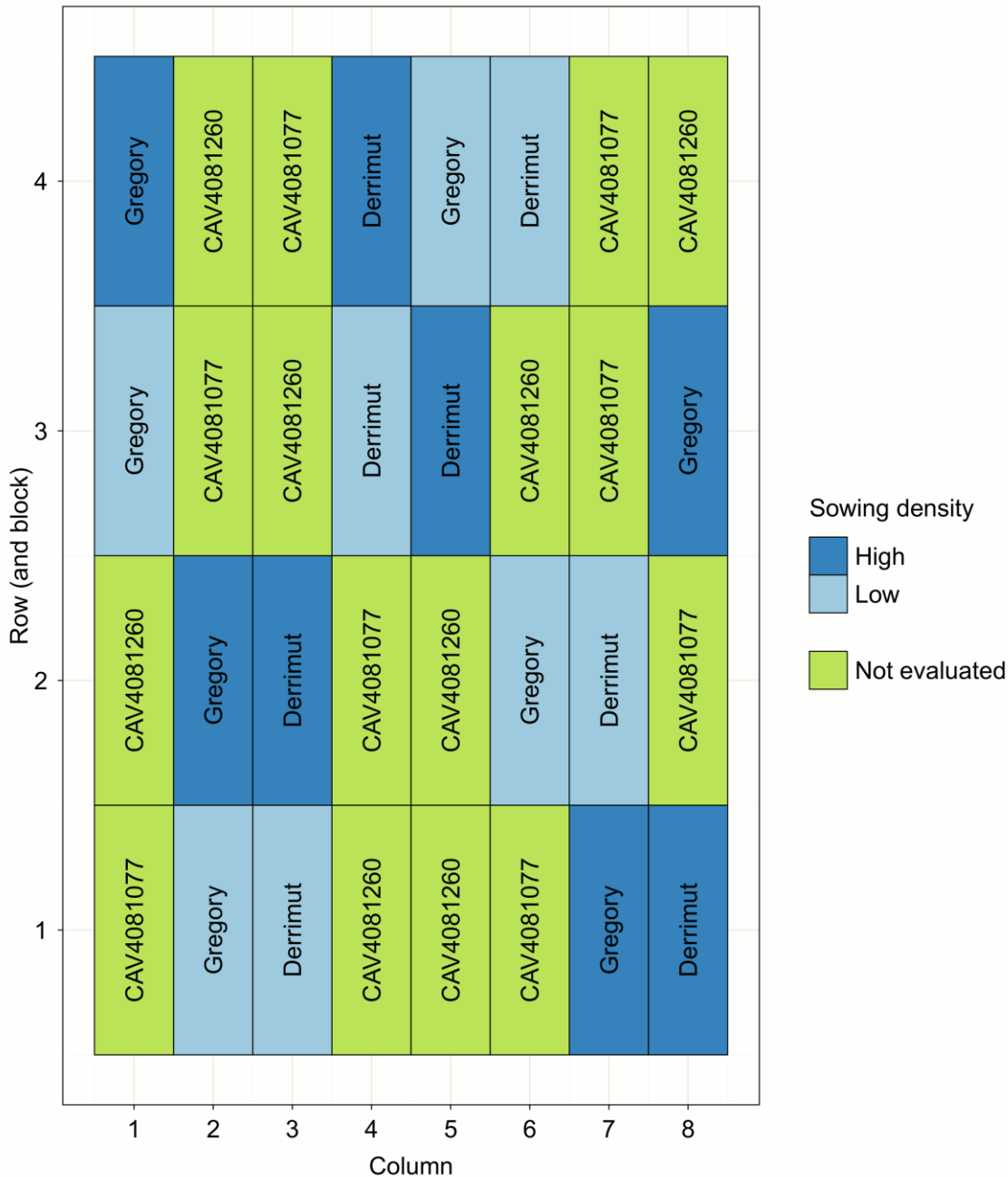


Figure 2.12. Statistical design of experiment 5. The experiment was sown during 2014 in the Creek site (red podzolic soil). Four wheat genotypes were sown, but just 2 are evaluated in this thesis: Derrimut and Gregory, same genotypes as in experiment 4. Two sowing densities were sown, a low density of 100 and a high density of 200 plants m^{-2} . The design is a split-plot design with 4 replicates in blocks. Experiment 6 was sown during 2014 and had the same experimental design as experiment 5, but it differed in its location: it was sown in the Quarantine site, in a yellow podzolic soil (Figure 2.1).

2.6 Field measurements

We performed several field measurements which are described in this section and summarised in Table 2.6. Some measurements were made at discrete times (e.g. stem elongation, anthesis, or physiological maturity), whereas others were made continuously by data logging.

Table 2.6. List of measurements done in the field in each year. Measurements were taken at specific developmental stages (root and shoot samplings), once or twice in the whole season (bulk density, water retention parameters, water content by coring), weekly (water content by neutron moderation) or by continuous logging (water tension with gypsum blocks and canopy temperature). Stages of crop development were stem elongation (SE, growth stage 31, Zadoks *et al.*, 1974), anthesis (A, growth stage 65) and physiological maturity (M, growth stage 87).

Measurement	Exp 1 & 2			Exp 3			Exp 4			Exp 5		
	SE	A	M	SE	A	M	SE	A	M	SE	A	M
Phenology	✓	✓	✓	✓	✓	✓	✓	✓	✓	✓	✓	✓
Root length density from 10 to 180 cm depth (cm cm ⁻³)			✓	✓	✓	✓		✓	✓			✓
Rooting depth (cm)			✓	✓	✓	✓		✓	✓			✓
Shoot biomass (g m ⁻²)			✓	✓	✓	✓		✓	✓			✓
Grain yield (g m ⁻²)			✓			✓			✓			✓
Leaf area index								✓				
Water tension by gypsum blocks (kPa)							✓	✓	✓	✓	✓	✓
Water content by neutron moderation (cm ³ cm ⁻³)				✓	✓	✓	✓	✓	✓			
Water content by coring (g g ⁻¹)							✓		✓			
Soil bulk density (g cm ⁻³)									✓			
Water retention parameters									✓			
Canopy temperature (°C)							✓	✓	✓	✓	✓	✓

2.6.1 Phenology

Phenological stages were recorded regularly between emergence and maturity using the scale of Zadoks *et al.* (1974). Of particular interest were the stages of stem elongation (growth stage 31), anthesis (flowering; growth stage 65) and physiological maturity (growth stage 87). All growing stages were determined in a population basis, i.e. by accounting for phenological events when they occurred in 50% of the individual plants in a plot—though the border rows were excluded because they could have developed faster given the reduced competition compared to the plants inside the plot. Growth stage 31 was defined, according to Zadoks *et al.* (1974), as the start of rapid stem growth, which was quantified visually as the appearance of the second node above the soil surface. This cannot be seen by the naked eye—since the elongating stem is still covered by the leaves sheets—but it can be detected by pressing with two fingers at the base of the pseudo-stem. Growth stage 65 was determined as the date when 50% of the spike area has protruded anthers across its spikelets. Growth stage 87 was determined when peduncles had completed changing colour from green to yellow, when senescence of the phloem vessels in the peduncle implies the end of grain growth.

2.6.2 Soil coring to sample roots

We sampled roots at growth stage 31 only in experiment 3, at growth stage 65 in experiments 3 and 4, and at growth stage 87 in all experiments (Table 2.6), by taking vertical soil cores with a hydraulic corer mounted in the three-point hitch (rear) of a New Holland Tractor.

Soil cores were taken with tubes, 4.25 cm in diameter and 2 m in length, made of a molybdenum-steel alloy. These tubes were pushed into the soil to a depth of 1.8 m. Several of these cores (2 in Exp 1 and 2; 4 in the rest) were taken around the centre of each plot. After pulling back from the soil, tubes were transported and pushed by hand on a cradle over a table and cut at every 10 cm. The resulting 10-cm core cuts were broken once around the middle (in Exp 1, 2 and 3) or twice (in Exp 4), once at one third and again at two thirds of its length. Roots tips appearing in each breakage plane were counted (i.e. two planes in Exp 1, 2, and 3, four planes in Exp 4) according to the core-break technique described by (Drew and Saker 1980). Then the root count density, RCD (cm^{-2}), was determined as a ratio between the average number of root tips per plane and the area of each plane (which was always 14.2 cm^2). Roots from crops in past growing seasons can be mixed up with the actual roots from the crop. We differentiated them by assuming that white roots were from the current crop and brown roots from previous, dead crops (Watt *et al.* 2008).

2.6.3 Soil washing to separate roots from soil

After recording the number of roots, each 10-cm soil-sample was placed into a plastic bag, transported from the field to the lab and stored in a cold room at $5 \text{ }^\circ\text{C}$. These samples were then washed with a hydro-pneumatic soil washer built in the Australian National University following the description made in (Smucker *et al.* 1982). This machine breaks the soil cores by applying pressurized water and air and filtering the resulting dispersed soil and floating roots (Figure 2.13). The filtered roots were later

placed into small plastic containers with 1:1 water-ethanol solution and again inside the cold room at 5 °C, where they were stored for no longer than 2 months.

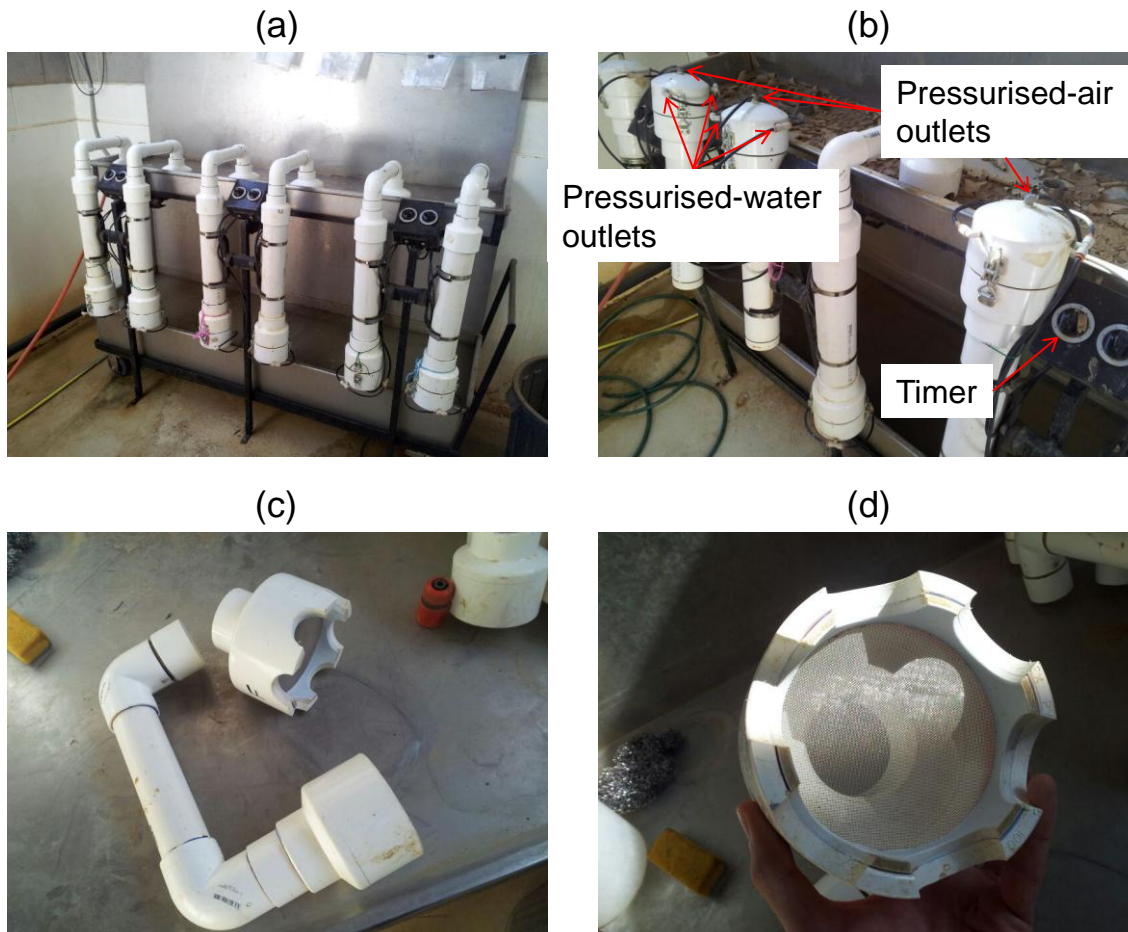


Figure 2.13. Hydro-pneumatic soil washer used to separate roots from soil. The whole device is shown in (a). In (b), the cylinders where the soil samples are deposited are shown, this time upside-down, where one can notice the 3 pressurised-water outlets on the side of each tube's base, and the pressurised-air outlet, 1 on each tube's base. The detachable piece of each washing tube is shown in (c), and the 5-mm-mesh sieve in (d).

2.6.4 Root scanning to quantify root length density

Roots were later scanned and the length of roots per sample was determined. For that, we dispersed the samples in water contained on an acrylic tray (27 cm × 21 cm × 3 cm)

adapted to fit on an A4, Epson 1680 modified-flatbed scanner. At the start of the sampling, during 2011, we used to stain each sample by immersing the filtered roots in a bath of Toluidine blue stain. The process was aimed at increasing the visibility of roots under the scanner. As it was very time consuming so we sought ways of making it faster. We tried scanning roots without staining them and compared the results of stained and no-stain using the same samples. Root diameter and volume differed but root length, our variable of interest, did not—or differences were so small that it was not worth the time lost to stain them (Figure 2.14). Toluidine blue staining is recommended for quantifying root volume and root area. However, for root length, which was our interest, staining was unnecessary.

Later, each sample was scanned at a resolution of 400 dots-per-inch and stored as TIFF image files. We used the software WinRhizo® (Régent Instruments Inc., Québec, Canada) as an image analysis tool to determine the length of roots in each image. I calculated the root length density, RLD (cm [root] cm⁻³ [soil]), of the sample as the ratio between the lengths of roots measured by WinRhizo® and the volume of the sample (which was a constant: 142 cm³).

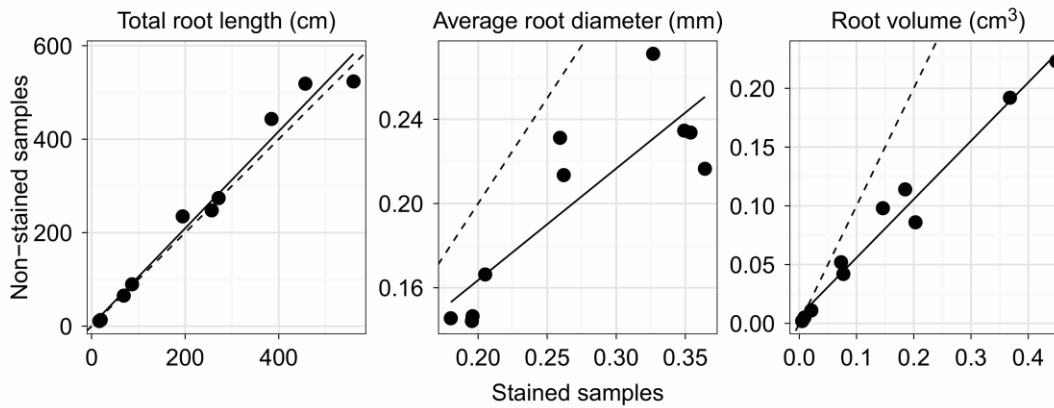


Figure 2.14. Comparison of stained and non-stained samples with Toluidine blue before scanning. The dashed line is $y = x$ and the full line is the best linear fit. It can be seen that the linear fit and the dashed line fall apart in the case of average root diameter and root volume, but they are almost equal for total root length—therefore, staining the root samples with Toluidine blue does not improve the accuracy of measuring root length.

2.6.5 Predicting root length density from root count density

Because *RLD* is a more useful metric than *RCD* (for instance, one can accumulate it per layer of soil or along the entire soil profile, whereas summing counts would not make sense), I estimated *RLD* from *RCD*. To do that I first tried a linear model without intercept (i.e. going through the origin, meaning that zero *RCD* corresponds to zero *RLD*), which fitted the data well at low values of *RCD* but overestimated at high values—we were counting more and more roots but the length of roots was remaining constant. The relationship between *RLD* and *RCD* appeared to be non-linear, reaching a plateau as *RCD* increased (Figure 2.15). To use the simplest model that explained best, I fitted a rational nonlinear model with two dimensionless parameters, a , the initial slope, and b , the curvature:

$$RLD = a \frac{RCD}{1 + b(RCD)} \quad (2.1)$$

I found that these parameters were in turn a function of soil depth, where a in particular decreased as the soil depth increases (Table 2.7). This means that the deeper we sampled roots the less root length there was per root counted in the surface of the soil sample. To estimate RLD from RCD I used the model with the corresponding parameters according to the soil depth (Table 2.7).

For fitting these non-linear regressions, I used the "minpack.lm" R package (Elzhov *et al.* 2013).

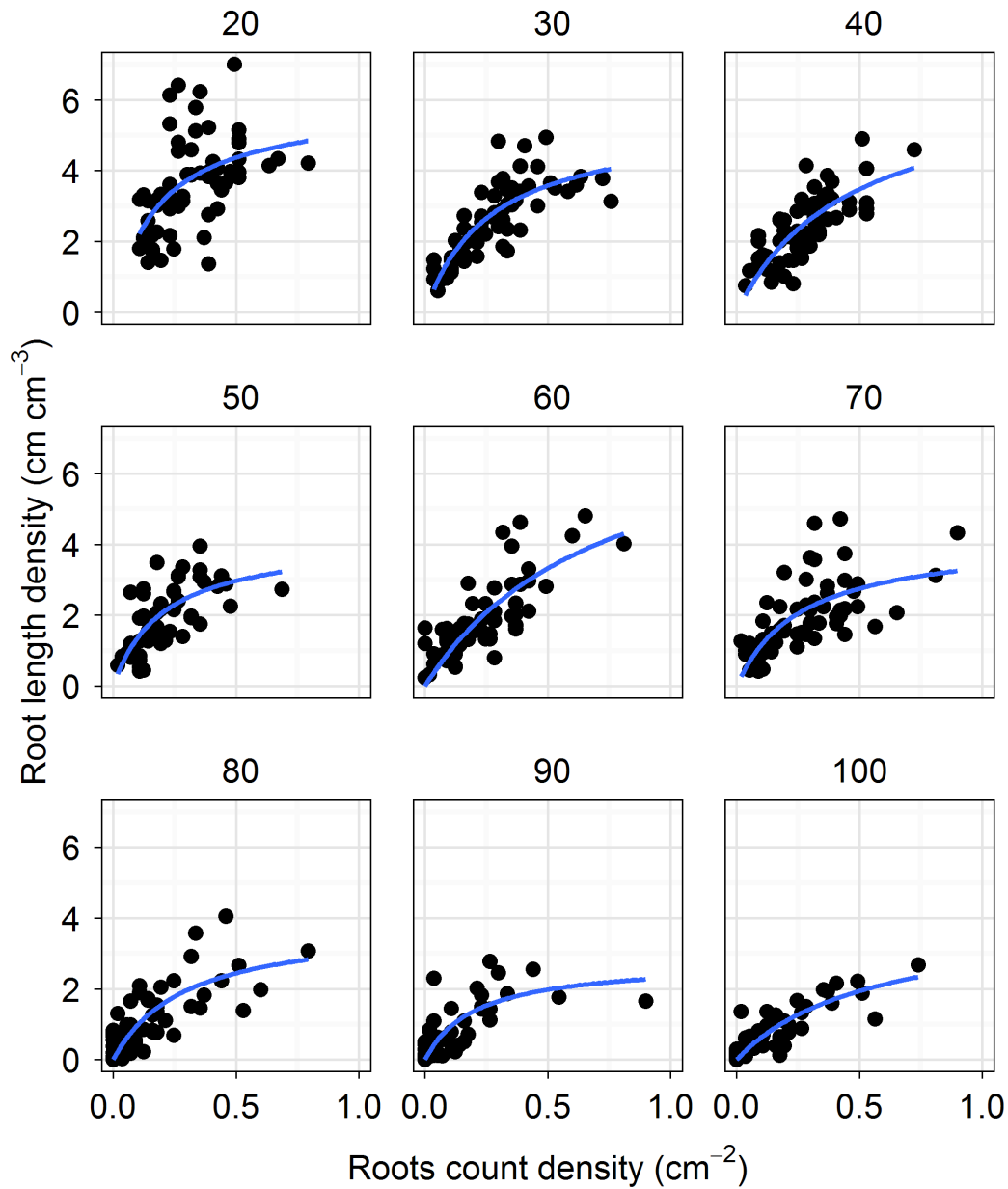


Figure 2.15. Models used to predict root length density from root count density according to soil depth. The graph shows root length density as a function of root count density as measured in the field. Soil depths are denoted by panels, with titles in cm of soil depth. Blue lines are the non-linear fittings with equation as presented in model (2.1) and parameters and statistics presented in Table 2.7.

Table 2.7. Parameters of the equation $RLD = a RCD / (1 + b RCD)$, describing the root length density, RLD (cm cm^{-3}), as a function of the root count density, RCD (cm^{-2}). Each model was fitted separately for each soil layer. Significance levels of each estimate are: 0 '***' 0.001 '**' 0.01 '*' 0.05. SE is the standard error of each estimate. RMSE is the root mean square error and R^2 is the coefficient of determination of each model.

Soil depth (cm)	<i>a</i>		<i>b</i>		RMSE (cm cm^{-3})	R^2
	Estimate	SE	Estimate	SE		
20	33.4 ***	8.2	5.6 **	2.1	1.09	0.30
30	20.6 ***	2.9	3.8 ***	0.9	0.59	0.67
40	14.5 ***	2.2	2.2 **	0.7	0.62	0.57
50	20.4 ***	4.1	4.9 **	1.8	0.65	0.62
60	11.1 ***	1.7	1.3 *	0.6	0.71	0.68
70	16.0 ***	3.5	3.8 *	1.4	0.74	0.50
80	13.3 ***	2.6	3.4 **	1.3	0.57	0.60
90	13.6 ***	3.1	4.9 *	1.9	0.46	0.60
100	7.4 ***	1.1	1.8 *	0.7	0.34	0.75

2.6.6 Estimation of maximum rooting depth

I determined the maximum depth reached by roots in the soil profile, RD (cm), from data of root counts. Because maximum rooting depth is usually defined as the depth of the deepest root that can be found, results can vary greatly due to occasional roots that are encountered growing inside macro-pores (White and Kirkegaard 2010). Soil macro-pores can facilitate single roots growing to great depth. To reduce this uncertainty, I defined maximum rooting depth as the depth where crops accumulated a certain percentage of all their roots, counting from the soil surface down the bottom of the soil profile, RD . I chose 95% as a threshold in similarity with Trachsel *et al.* (2013), though they used the threshold for cumulative root biomass rather than root counts. As roots were sampled each 10 cm, many times the depth where crops accumulated 95% of roots

did not match with the sampling depths (i.e. the spatial resolution). To solve this, I interpolated within soil layers to find the depth of 95% roots. For instance, if one particular core has 90% of its roots accumulated by 110 cm depth and 100% of its roots at 120 cm, the depth of 95% accumulated roots would be 115 cm. I used this 95% depth as the maximum rooting depth.

Consequently, uncorrected rooting depth was usually deeper than 95% rooting depth (Figure 2.16). This was particularly true for rooting depths beyond 100 cm (Figure 2.16), and agrees with the notion that sometimes, by following macro-pores, individual roots can reach depths that are unrepresentative of the whole root system (White and Kirkegaard 2010).

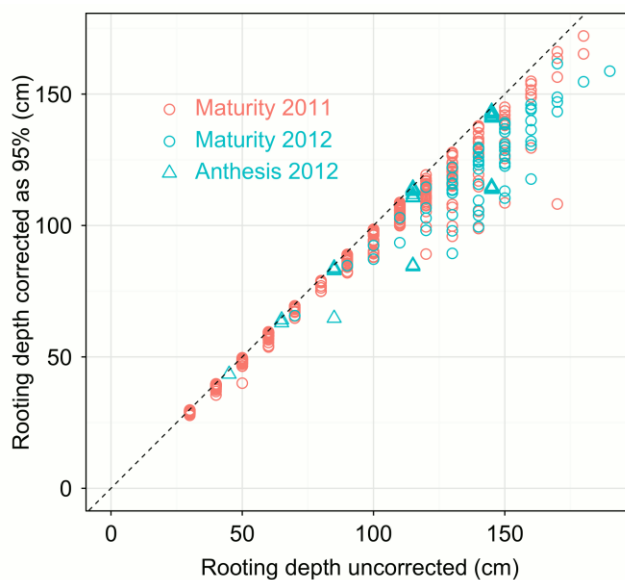


Figure 2.16. The effect of considering maximum rooting depth either to be equal to the depth where the last root is found (rooting depth uncorrected) or to be equal to the depth where plants accumulate, from the soil surface, 95% of their roots. Data comes from plots sampled at anthesis (triangles), or at maturity (circles), during 2011 (pale red) or 2012 (pale blue).

2.6.7 Root length per soil depth intervals or the whole soil profile

The total length of roots along the soil profile per unit area of land, RL (km [roots] m⁻² [soil]), was calculated as the integral of root length density (RLD) along the soil profile from the soil surface ($z = 0$) to the rooting depth ($z = RD$):

$$RL = \int_{z=0}^{z=RD} RLD \, dz \quad (2.2)$$

It serves as a total account of root growth by a certain crop, but does not tell where in the soil profile the root length was distributed. To simplify this problem but still have an account of root length distribution along the soil profile, I also calculated values of RL each 40 cm depth by dividing the soil profile into 3 large layers of 40 cm thickness and a last infinite layer: 0 to 40 cm, 40 to 80 cm, 80 to 120 cm, and deeper than 120 cm.

2.6.8 Above-ground biomass and grain yield

Above-ground biomass and grain yield were determined as dry matter, at three stages: stem elongation (growth stage 31; only in experiment 3), flowering (growth stage 65; only experiment 3 and 4) and physiological maturity (growth stage 92; every experiment). We collected biomass by cutting with a serrated knife all above ground shoot, leaves and grain over an area of 0.7 m². This area was measured by sampling twice with a quadrat of 0.5 m width and 0.7 m long. To do so, we discarded the two outside rows and cut biomass from the 8 inner rows of the plot. These rows were adjacent between each other. We later dried these samples in an air-forced oven at 65 °C until constant weight was reached (around 4 days). Yield was determined by threshing the same samples used for biomass with a stationary thresher, and then

weighing the resulting grain as dry matter. I weighed these and the biomass samples in a balance with an error of 0.01 g.

Chapter 3 Using gypsum blocks for phenotyping water use in the field

3.1 Introduction

Gypsum blocks could make possible the continuous logging of soil water suction in field conditions. They can measure continuously because all that is needed is a current passing through them and a device that can record the resistance to that current, a principle first devised by Bouyoucos and Mick (1940). Neutron probe or total domain reflectometry methods can determine soil water content precisely, but they cannot sample in a continuous manner. Moreover, neutron probe sampling close to the soil surface (say, less than 10 cm depth) is risky to the operator because a substantial fraction of the neutrons are radiated to the air and, for the same reason, measuring soil water at these depths becomes inaccurate (Murphy and Lodge 2004). On the contrary, gypsum blocks are advantageous not only because they offer continuous logging, but can also be precise while cheap (Johnston 2000). However, they are not usually employed for estimating water use by crops; rather, gypsum blocks are used for estimating the right timing of irrigation, in perennial crops like grapes, where knowing soil water suction is sufficient. The study of Murphy and Lodge (2004) shows how gypsum blocks can be used successfully to predict soil water content on shallow, loose soil layers. We are not aware of their use to estimate water use by crops deeper in the soil, where soil is more densely structured. It is unknown, therefore, whether they can be used for phenotyping deep water use by cereal crops.

Previous tests of gypsum blocks properties, as well as their potential for measuring soil suction, suggested that they were capable of measuring soil water suctions within a range that is relevant to plants, that is, from 30 kPa (around field capacity) to 1500 kPa (around wilting point)(Aitchison and Butler 1951). Moreover, it is known that the readings depend on soil temperature, so a calibration to temperature was needed as well (Johnston 2000).

The aims of this Chapter are (i) to test whether gypsum blocks could provide a reliable measure of soil water potential under limits of interest for plants in the field, and (ii) to see if they can be used to estimate volumetric soil water content accurately, provided the errors accumulated after the many steps required to convert soil water suction into volumetric water content are not excessively large.

We proceeded in six steps in order to calibrate and validate the estimation of volumetric water content by gypsum blocks. First, we measured bulk density in two pits in the Creek site (Figure 2.1). Knowing bulk density allowed us to convert gravimetric water content into volumetric water content, as shown later in section 3.2. Second, to avoid sampling every plot by direct soil coring, we measured soil water content with neutron probe. To use the neutron probe we first calibrated it by sampling neutron counts and gravimetric water content side-by-side under a rain-out shelter during 2012 and again, but without a rain-out shelter, during 2013 (section 3.3). Third, by using the parameters published by Johnston (2000), Drs John Passioura and David Deery converted the original resistance values (Ohms) into suction values (kPa), and later did an experiment to calculate how much that suction changes as a function of temperature (section 3.4). Fourth, gypsum blocks were deployed in the field and measurements of soil water

suction were taken almost continuously—one datum every 2 hours—during 2013 and 2014. Fifth, we converted temperature-corrected soil water suction measured by gypsum blocks (kPa) into volumetric water content ($\text{m}^3 \text{m}^{-3}$). To do so, water retention curves were determined in the lab for every soil depth where a gypsum block was buried (section 3.6). Finally, we compared the predicted soil water content—after all the steps required to convert gypsum block's resistance into volumetric water content—with the soil water content measured by neutron probe as a way of validating the predictions of gypsum blocks. We show that a surrogate soil water retention curve determined in the field could be more appropriate than a pressure-plate water retention curve determined in the lab (section 3.7). However, intra-experiment variability in soil physical properties might make both approaches equally uncertain, leaving us with the only hope of using gypsum blocks as sensors of soil water suction, not soil water content. In spite of these uncertainties, we will venture in Chapter 5 to predict water use in two wheat varieties that seemingly vary in rooting depth.

3.2 Measuring bulk density

Bulk density, the dry weight of soil per unit volume ($\text{BD}, \text{g cm}^{-3}$), was needed in order to convert the gravimetric water content ($\text{GWC}, \text{g g}^{-1}$) into the more useful volumetric water content ($\text{VWC}, \text{cm}^3 \text{cm}^{-3}$) by the following:

$$\text{VWC} = \frac{\text{BD} \times \text{GWC}}{\text{WD}} \quad (3.1)$$

where WD is the density of water, which is approximately equal to 1 g cm^{-3} . To sample bulk density, we used a hand-operated device for the top 60 cm (Figure 3.1a), and a 6.5-

cm-wide core, pushed by the hydraulic press, for depths beyond 60 cm until 160 cm depths (Figure 3.1d). Using the hand-operated corer allowed us to sample soil more carefully on the top, looser soil, where it is more prone to breakages given its fragile structure. Using the hydraulic press and the core allowed us to reach depths that would be difficult to get to by a hand corer. At depth, the soil was less fragile and retained its integrity because soil sampled at depth greater than 60 cm had a massive, clayish structure.



Figure 3.1. Procedures followed to sample bulk density. For the top 60 cm layers, a hand corer was used, which allowed more cautioned sampling in those layers that are more prone to crumbling (a). We dug with a shovel between sampling layers 20, 40 and 60 cm depth, avoiding compaction of the soil to be sampled (b, c). For soil layers deeper than 60 cm, we cored with the same hydraulic corer as described for sampling roots, where the coring tube was actually wider (6.5 cm diameter) (d). After removal from the soil, soil samples were levelled with a scraper in order to have a precise, known volume (e).

3.3 Estimating soil water content with neutron probe

Neutron probes work by radiating neutrons into the soil and counting how many are reflected back to the source. The number of neutrons that come back varies with the degree of saturation of the soil. It is possible, therefore, to know the soil water content precisely from a relationship between neutron counts and soil water. There is not a universal relationship as it varies between soils with different textures and structures. Therefore, this technique requires a calibration to work. The calibration consists of generating equations to directly relate volumetric soil water content ($\text{m}^3 \text{m}^{-3}$) to the neutrons counted by the neutron probe. To do so in a robust way, one needs to compare soil water content and neutron counts over a wide range of soil moistures.

Unfortunately, we failed to generate enough data at the dry end of the curve to have precise predictions (Figure 3.2). Uncertainty in these calibrations translated to uncertainty in the estimations of volumetric water content.

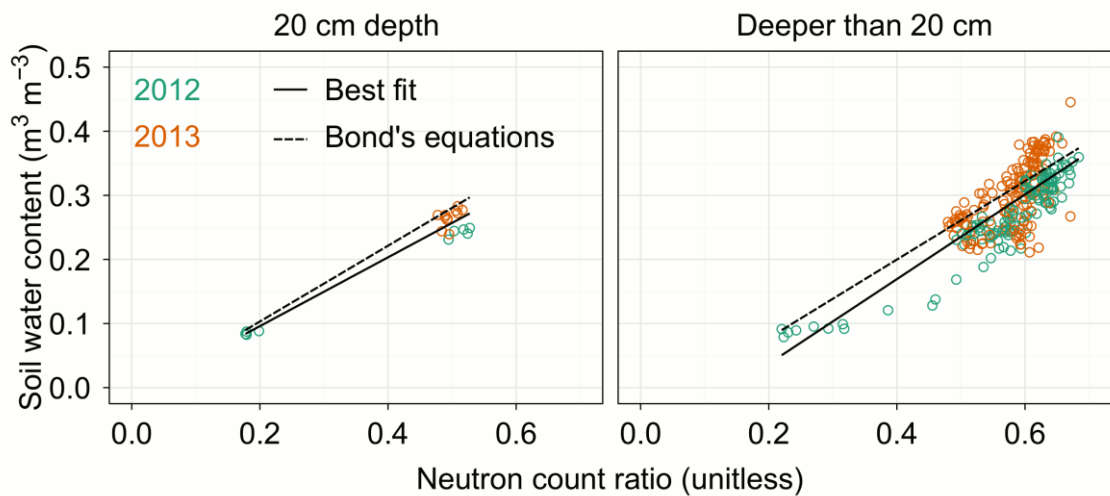


Figure 3.2. Soil water content as a function of the neutron count ratio during 2012 and 2013 for depths of 20 cm and deeper than 20 cm. The full line shows the regression line, best fit, for both years. The dashed lines are the equations by Dr Warren Bond, detailed later in Figure 3.3.

To account for this issue, we compared our fitted calibrations to generic calibrations developed by Dr Warren Bond, from CSIRO Land and Water, who has much expertise working with neutron probes. Warren provided us with a generic calibration that he produced for many different soils (Figure 3.3). According to Warren, using these generic equations to predict soil water content is much more accurate than using an incomplete set of data from the site of the experiments. Our calibrations were similar to those of Warren (Figure 3.2). Given that Warren validated these calibrations in several different soils (Figure 3.4), we used Warren's calibrations rather than ours.

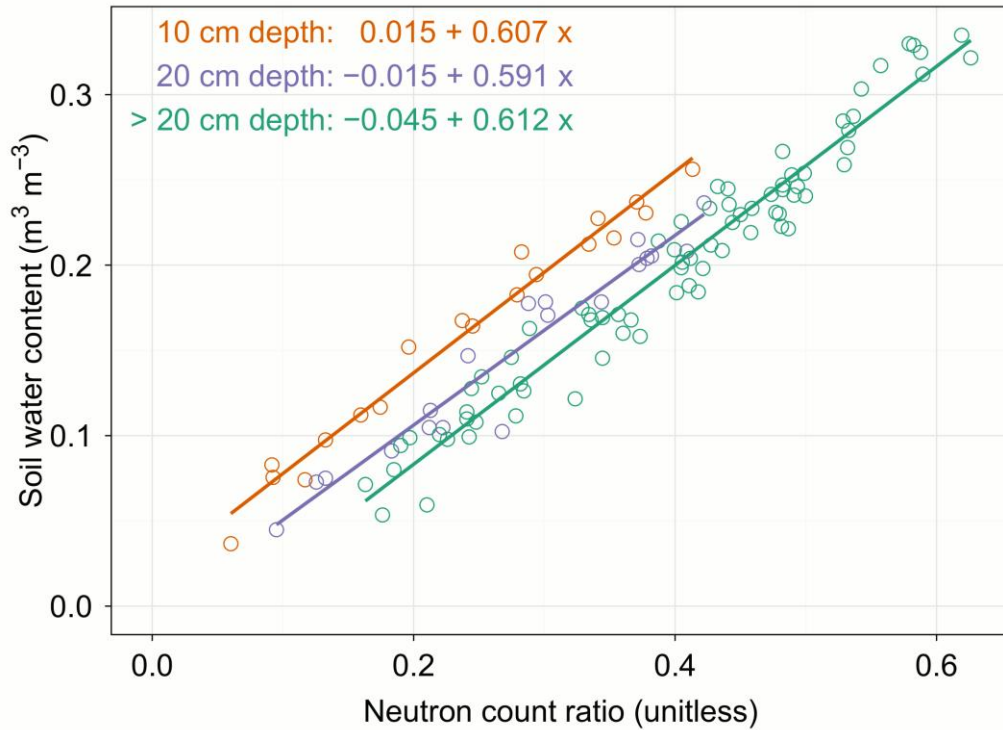


Figure 3.3. Neutron probe generic equations estimated by Dr Warren Bond. The figure shows soil water content as a function of the neutron count ratio, the ratio between the neutrons measured in the soil and the neutrons that can be counted into a tank full of water. The latter is used as a reference measurement to normalise neutron readings that could otherwise vary between devices.

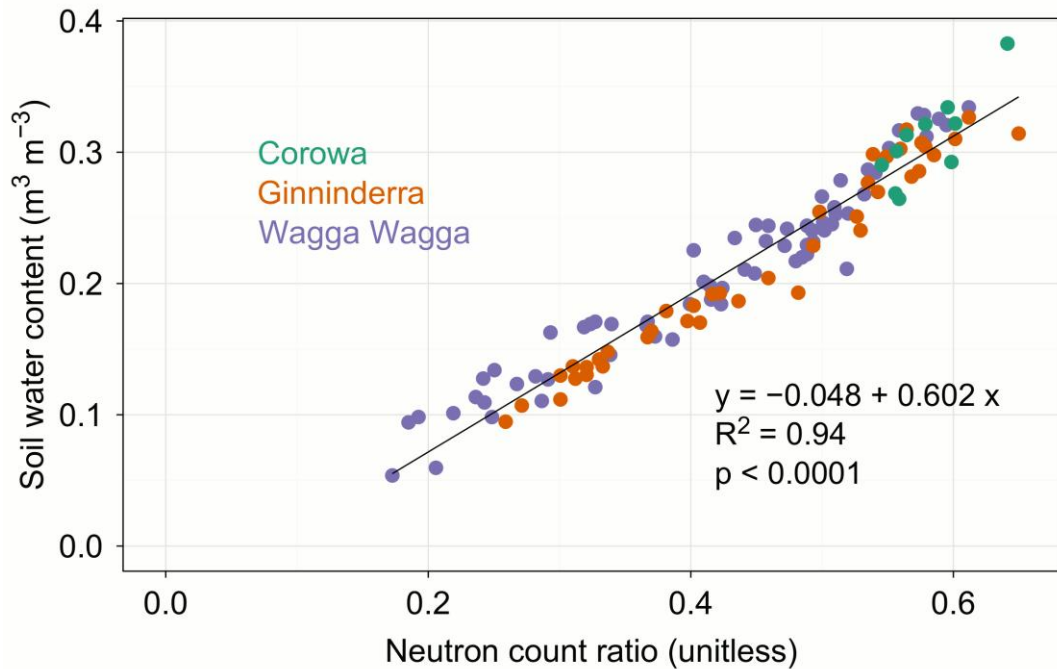


Figure 3.4. Validation of Dr Warren Bond's predictions of soil water content from neutron probe data. The graph shows measured soil water content ($\text{m}^3 \text{m}^{-3}$) as a function of neutron count ratio (unitless) for soil beneath 20 cm at 3 locations in New South Wales: Corowa, Ginninderra and Wagga Wagga. Notice that the parameters of the curve (slope and intercept) are closely similar to those of soil deeper than 20 cm in Figure 3.3

Neutron probe samples were taken by inserting the neutron probe source into an access tube installed in 8 plots in experiment 3 and 16 plots (all) in experiment 4. Access tubes were made of aluminium, 2 m long and wide enough as to allow the source to be inserted (~5 cm). Aluminium tubes were installed again by coring with the tractor, following the same procedures as for root coring. When coring this way, the soil removed produced a hole just wide enough to allow introducing the tube into the soil, and although full soil contact is necessary to prevent preferential infiltration along the external walls of the tube, the collapse of the soil around the tube that usually happens afterwards seals the gaps.

A neutron count ratio was calculated as a ratio between the number of neutrons counted in the soil in each sampling and the reference neutron count that was achieved by measuring inside a 200-L tank full of water with an aluminium access tube inside it. This is used to normalise the neutron probe readings that usually vary from one device to another.

Soil coring to measure soil water content directly was done at the start and the end of the season, which, as mentioned, aimed to generate a set of equations equivalent to those produced by Dr Warren Bond. Cores taken at the start of the season when installing the aluminium tubes provided soil samples that were kept inside plastic bags in 10-cm sections. These samples were transported to the lab where we weighed them fresh (to know initial weight), and we weighed them again after drying for 48 h in an oven at 105 °C (to know the final weight). The difference between final and initial water content was the amount of water in the soil, which divided by the dry weight of the sample (the final weight) gave the gravimetric soil water content. We converted the gravimetric water content (g water g^{-1} soil) into volumetric ($\text{m}^3 \text{ water m}^{-3}$ soil) by multiplying by soil bulk density, measured in experiment 4.

As mentioned, we failed to obtain enough data points in the dry end of the curves (only successful from 20 to 40 cm depth). However, these data were used to validate the soil water content predictions by Warren's equations (Figure 3.5). Data and predictions seemed to agree closely, except for soil layers 50 and 60 where the predicted data were ~5 points higher than the measured data. This could be associated with spatial variation or uncertainty in soil bulk density.

The agreement between predicted and measured soil water content depended on soil depth. For 20, 30 and 40 cm depth, measured and estimated volumetric water content agreed well; for 50 and 60 cm the estimate was greater than the measured content; and for soil depths deeper than 60 cm, both measurements agreed on average (centre of cloud of data points) but it has to be noted that the predicted soil water content changed less than the measured water content, that is, for every unit change in the measured soil water content the predicted changed less than unity. This can happen because of several reasons. Firstly, measured soil water content includes the uncertainty of measuring bulk density (two pits for whole trial), whereas the estimated soil water content bypasses bulk density, for neutrons relate directly to volumetric water content (Warren's data are fitted against volumetric water content and therefore overrides the effect of bulk density). Secondly, installation of the aluminium access tubes may have included air gaps between the outside wall of the aluminium tube and the soil (Evetts *et al.* 2008). During the installation of the aluminium tube down the hole, no slurry was added. Instead we trusted that rainfall would collapse soil into any gaps between the aluminium tube and the soil. This might not have happened and if air gaps were present, neutron count would be less responsive to changes in soil water content. However, while the sensitivity of the response function was underestimated, the average readings agreed (centre of data clouds were the same).

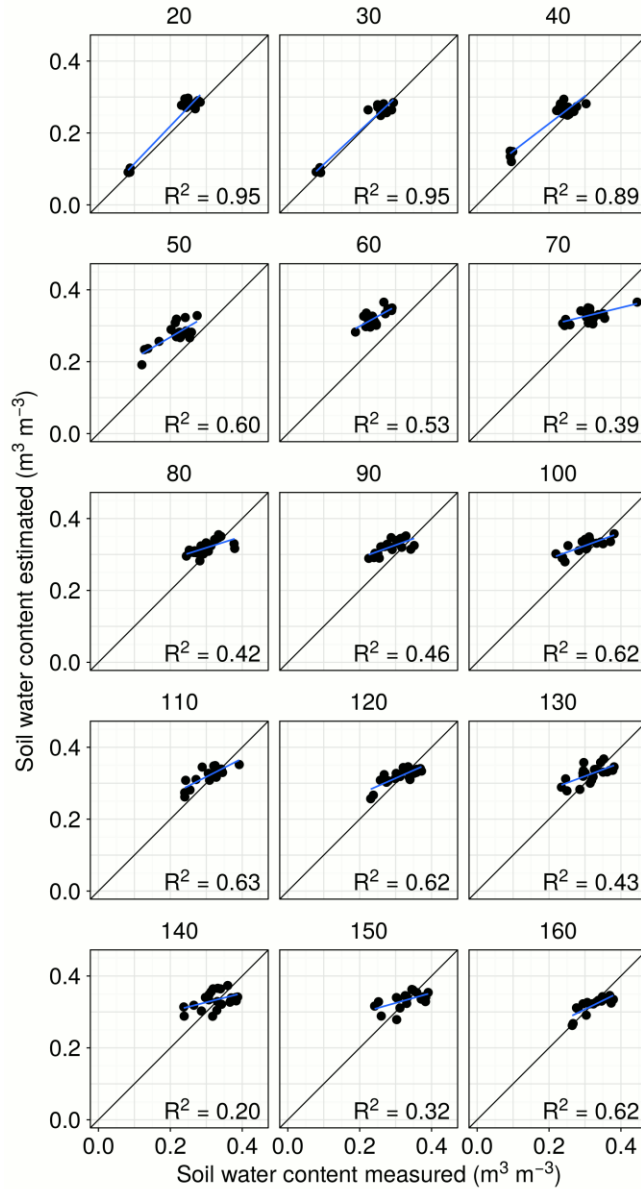


Figure 3.5. Soil water content estimated from Dr Warren Bond's equations (Figure 3.3) against soil water content calculated from gravimetric water contents at the start and end of the season of experiments 3 and 4 and the soil bulk density measured at the end of experiment 4. These comparisons serve as validations of neutron probe predictions against direct coring data. R^2 are indicated for the linear regressions between both variables for each soil layer.

3.4 Converting resistance into suction and correcting for temperature

Gypsum blocks are electrical resistance sensors. They consist of a porous, cylindrical body (2.3 cm diameter by 5 cm length) made of CaSO_4 within which two electrodes are embedded (Figure 3.11d). The sensor wet and dries along with the soil, decreasing or increasing, respectively, the resistance for current flow between the electrodes (Evelt *et al.* 2008). Knowing the resistance therefore solves the water suction. Two types of commercial gypsum block sensors are available in Australia: GBLite and GBHeavy gypsum blocks¹. GBLite are appropriate to measure soil water suction in light-textured soils, for suctions ranging between 0 and 200 kPa. GBHeavy sensors are suited for soils with heavy texture, and measure suctions within the range 50-500 kPa. We used GBHeavy gypsum blocks, and as seen later in the Chapter, this will impair our appreciation of suction readings around field capacity. GBheavy sensors were calibrated to predict soil water suction from resistance by Drs John Passioura and David Deery by using model parameters published in Johnston (2000)(Figure 3.6).

Because electrical resistance in the gypsum blocks is also influenced by temperature, we measured soil temperature in the field, with thermistors logging at the same time steps and the same soil depths as the gypsum blocks (section 3.4). Resistances of a set of gypsum blocks were calibrated in the lab against temperature by Drs John Passioura and David Deery with pressure plate apparatus. The pressure plate and its chamber were immersed in a temperature-controlled water bath set to 5, 15, and 25 °C. A thermistor

¹ Manufactured by Measurements Engineering Australia (MEA):
http://mea.com.au/upload/Brochures/Soil%20Moisture%20Monitoring/Gypsum_Blocks_Web.pdf

placed inside the chamber measured the actual temperature, which was slightly higher than the temperature of the bath, perhaps because the chamber was only partially immersed in the water bath and air was warmer (Figure 3.7 and Figure 3.8). The increase was constantly ~ 1 °C for all temperature sets so it would affect the results of the analysis only negligibly.

A set of 4 gypsum blocks was placed over the pressure plate and surrounded by a small amount of soil to ensure good hydraulic continuity between gypsum blocks and plate. The aim was to compare, within a range of temperatures, gypsum block readings against the pneumatic pressure inside the chamber. At equilibrium, this should equal the actual matric potential of the gypsum blocks. We identified equilibrium when further output of water from the chamber was negligible and the trajectories of the gypsum block readings reached a plateau.

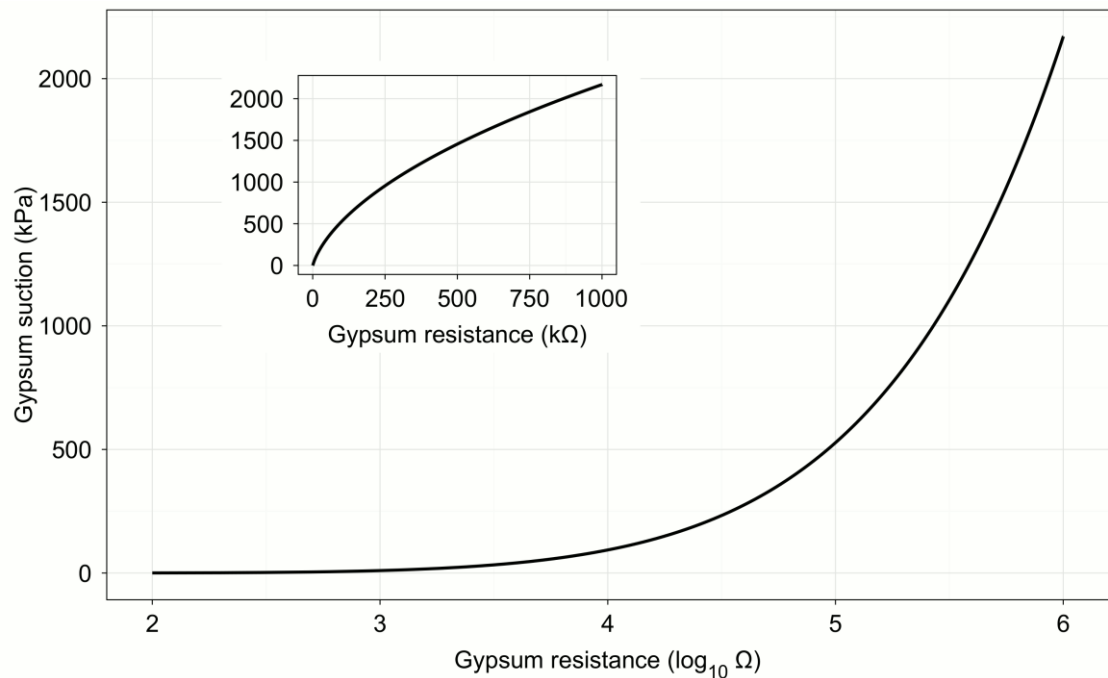


Figure 3.6. Gypsum block suction (kPa) as a function of the logarithm (base 10) of its electrical resistance (Ω , Ohms). The line shows the equation $0.02 r^{7.756}$, where r is the logarithm base 10 of the resistance in Ohms (Johnston 2000). The inset shows the same data in a regular axis for the electrical resistance.

Gypsum block readings are shown over time at 5, 15 and 25 °C, and at pneumatic pressures inside the chamber of 50, 100, 200, 400, 800 (Figure 3.7) and 1500 kPa (Figure 3.8). Readings increased dramatically when bath temperature was reduced from 25 to 15 °C, and again from 15 to 5 °C. Readings of gypsum blocks at equilibrium, the bath temperature, and the pneumatic pressure were recorded and used, as shown in Figure 3.9, to predict the suction reading of the gypsum block from the suction in the pressure plate (the actual suction of the gypsum block) for each temperature. As the y-intercepts were never statistically different from zero, the models were reduced to slopes with a linear dependence on temperature. The equation predicting the actual gypsum block suction from apparent gypsum block suction and soil temperature was

$$\text{Actual gypsum suction} = \frac{\text{Apparent gypsum suction}}{-0.023(\text{Soil temperature}) + 1.472} \quad (3.2)$$

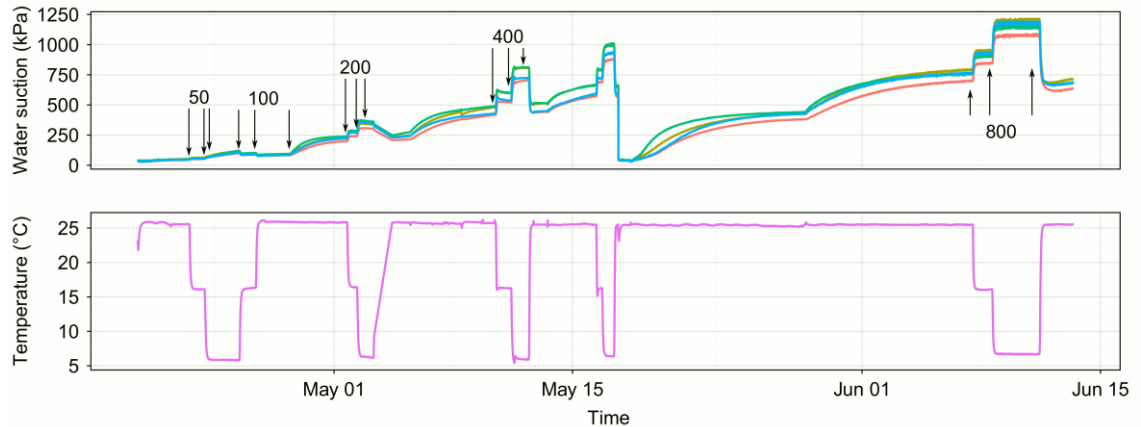


Figure 3.7. Trajectories of water suction readings (up) and the pressure-chamber temperature (down) during the calibrations. Arrows indicate the time when the readings reached a plateau (equilibrium), and hence were recorded. Numbers above those arrows (kPa) indicate the pneumatic pressure inside the chamber by that time. The colour of lines indicates each of the 4 gypsum blocks placed inside the chamber. These sets of 4 suction readings per temperature and per pneumatic pressure recorded at equilibrium are later plotted in Figure 3.9.

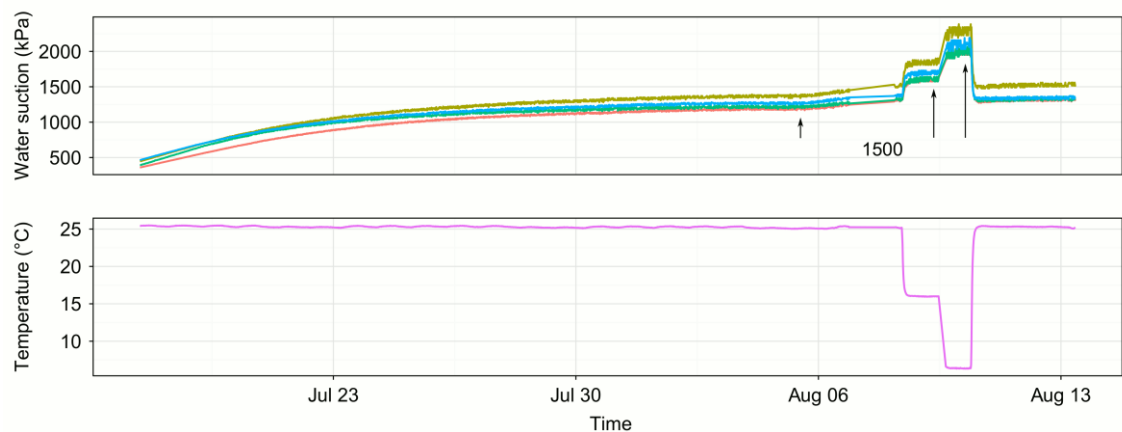


Figure 3.8. Idem Figure 3.7 but for a water suction of 1500 kPa. The figure was separated from Figure 3.7 to show the longer time needed for equilibrium at a greater suction.

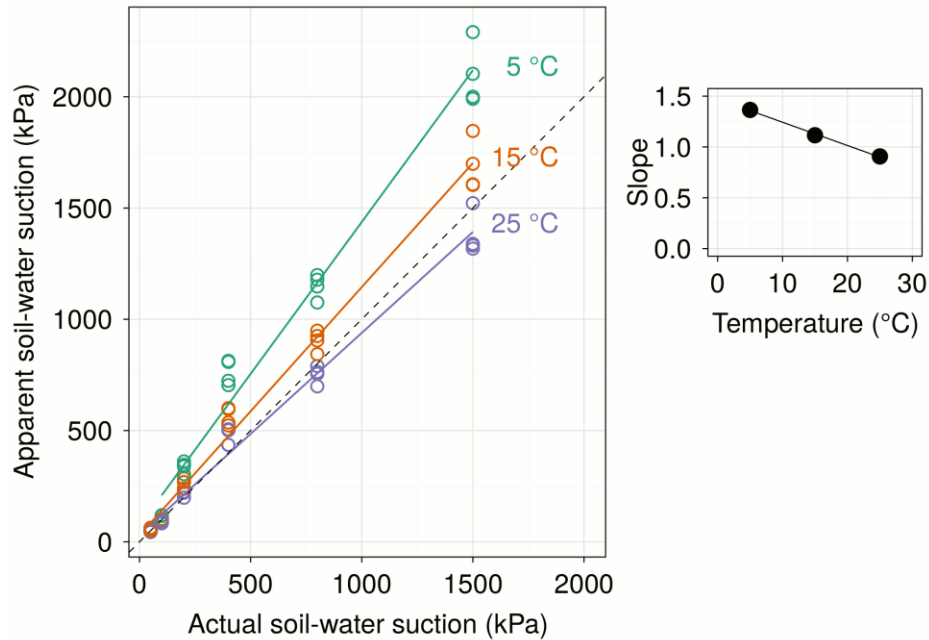


Figure 3.9. Suction given by 4 gypsum blocks as a function of the suction in the pressure plate at three bath temperatures of 5, 15 and 25 °C. The dashed line represents $y = x$. The graph on the right summarises how the slopes of the lines from the graph on the left change as a function of temperature. The latter is the equation that I used to correct suctions by temperature: $y = -0.023x + 1.472$.

After correcting for soil temperature, soil water suction measured by gypsum blocks in the field only changed slightly, as expected from equation (3.2), which states that for every change in 1 °C in soil temperature the actual and the current gypsum block reading will differ by ~2%. For a daily change of ~1.5 °C at 600 kPa, as shown in Figure 3.10, a change of 18 kPa is expected, and at 1200 kPa a change of 36 kPa (double).

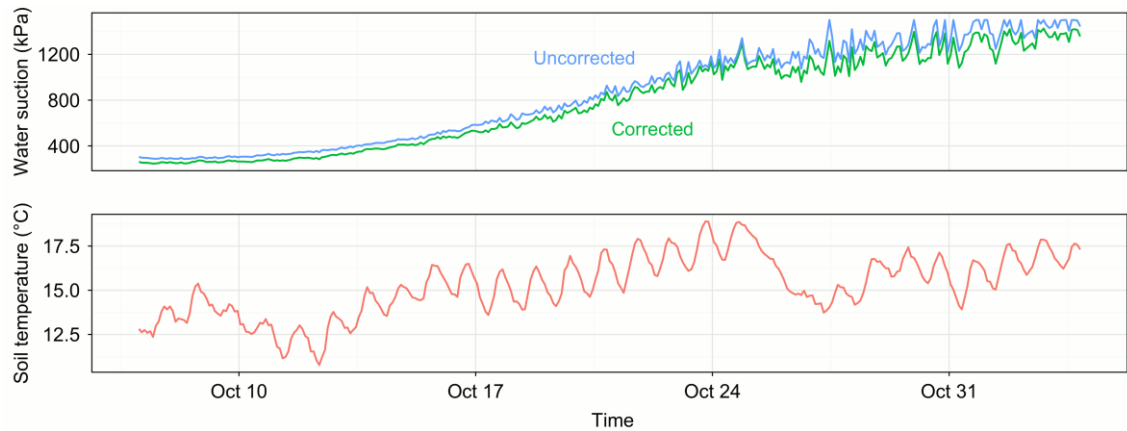


Figure 3.10. Soil water suction, uncorrected or corrected by soil temperature (upper panel), and soil temperature (lower panel) across time for soil at 20 cm depth in experiment 1 during 2011.

3.5 Field measurement of soil water suction with gypsum blocks

In the field, sensors were buried at eight depths in experiment 4 (20, 40, 60, 80, 100, 120, 140, and 160 cm depth) or at six depths in experiment 5 (20, 40, 60, 100, 120, and 140 cm depth). Sets of 6 or 8 gypsum blocks plus a data logger were installed in every plot. Loggers were connected by cables to each of the 6 or 8 gypsum blocks, transmitting the data to a central data station that later uploaded to a website. Gypsum blocks were soaked in water overnight prior to installation. Each sensor was placed into one hole to minimize the preferential flow of water that would be given by only one hole for all gypsum blocks in a plot (Evetts *et al.* 2008). Holes in the soil were made with the same hydraulic device used for soil coring for roots but, instead, a thinner coring tube was used, whose diameter slightly exceeded the diameter of the gypsum blocks (~2.5 cm; Figure 3.11a and b). Soil cores were removed by pushing the tube into the ground until the desired soil depth. Before pushing them into the holes, gypsum blocks

were covered with a thin layer of mud (made from the same soil at the same soil depths as the soil core just removed; Figure 3.11c). Then, gypsum blocks were pushed into the hole with the aid of a thin wooded-stick. After reaching the bottom of the hole, around 5 cm of soil were introduced and pushed with the stick towards the gypsum block to provide intimate contact between soil and gypsum block. Bentonite, a type of clay that is sold commercially, was added to fill up the hole around the cable until reaching the soil surface (Figure 3.11f). Bentonite was chosen because once wetted it expands up to 17 times, minimizing the risk of rainfall running preferentially through the walls of the hole (Evetts *et al.* 2008).

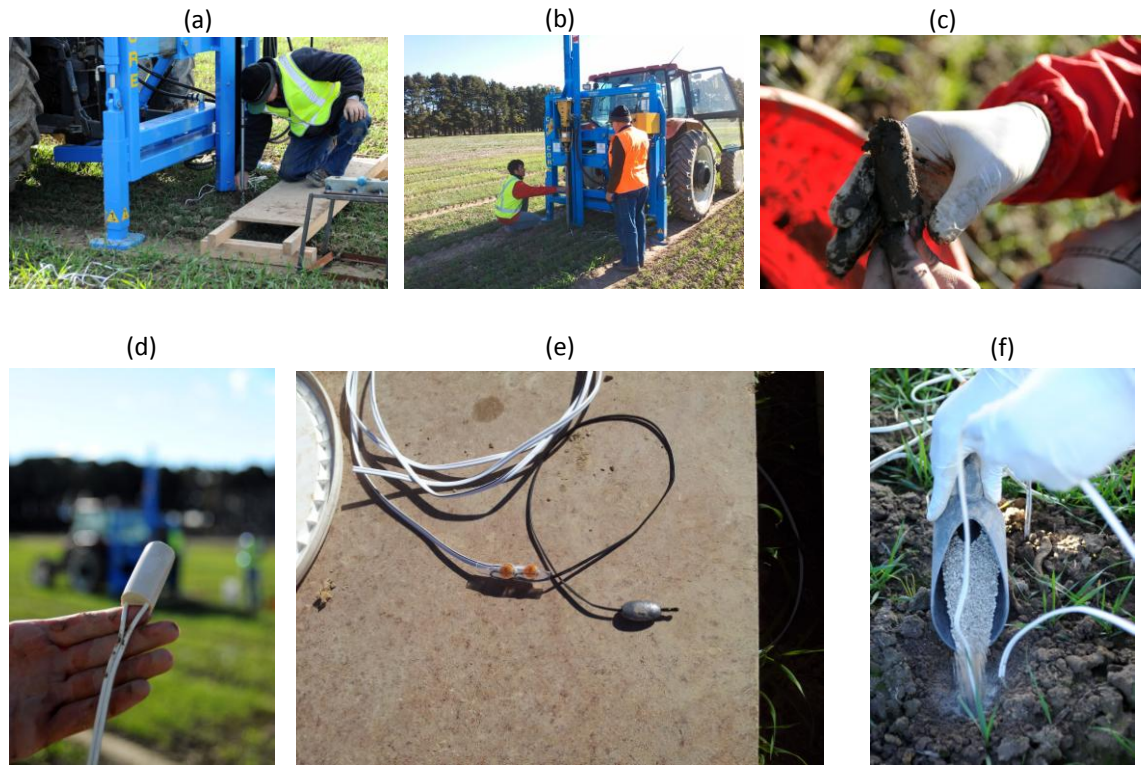


Figure 3.11. Installation of gypsum blocks and thermistors. The same hydraulic press mounted to a tractor that was used for soil coring when sampling roots was used for digging holes in the centre of plots for installing gypsum blocks, albeit a thinner metallic core was used (a, b). Gypsum blocks were soaked in water the night before (d), and covered in mud made from the same soil layer where they were supposed to be buried (c). Thermistors were deployed as well so that soil temperature could be recorded. Frame (e) shows the white cable that worked as an extension necessary to reach the desired soil depth, joint to a thermistor (black wire) with a lead sinker at the tip. After reaching the desired soil depth, the hole where either a gypsum block or a thermistor was installed was filled with bentonite to prevent the preferential flow of water along the walls of the hole (f).

Because of our need to determine soil temperature to allow for corrections of soil water suction, thermistors, which are resistors adapted to give readings of temperature, were installed as well. They were made of a 40 cm black-cable with the thermistor at the tip where we added a fishing sinker made of lead (Figure 3.11e) to ensure that, by its heavy weight, the thermistor reached the bottom of the holes. Holes were made with the same coring tube and same procedures as for gypsum blocks. As shown in Figure 3.11e, the

black cable (the thermistor per se) was connected to a longer white-cable with a silicone sealed joint held together by a heat-shrinkable tube; this was done to connect the thermistor to the data logger and also to prevent water provoking short-circuits. As with gypsum blocks, sets of 8 thermistors were connected to a data logger in 4 plots of experiment 4 (Figure 2.5). Soil temperature did not vary between plots.

3.6 Estimating soil water retention curves for the site

Soil water retention, also called soil water characteristic, describes how soil water content changes as a function of the energy status of water, that is, its suction. As suction was the reading given by the gypsum blocks, we needed soil water retention functions for each soil and soil layer in our study in order to know the soil water content. Knowing soil water content is important in this thesis because root water uptake can be derived from the changes in soil water content over time.

Example soil water retentions are given in Figure 3.12. Plants can only use water held in the soil between 10 and 1500 kPa. Consequently, as shown in the graph, the availability of soil water to plants varies considerably from soil to soil. These upper and lower limits for soil water holding capacity are called, respectively, field capacity and permanent wilting point. Clay soils hold more water at high suctions but their capacity to hold water between field capacity and wilting point is less than, say, a loam soil (Figure 3.12). The amount of water that a sand can hold which is useful to plants is small (Figure 3.12).

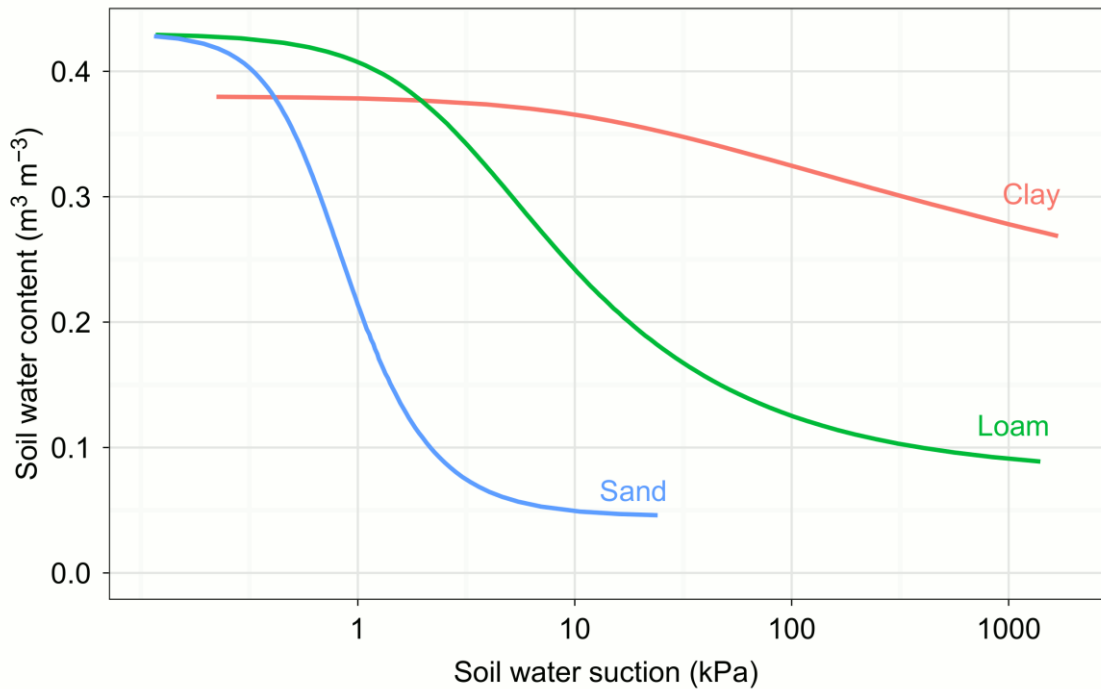


Figure 3.12. Example water retention curves for typical soils. Data were generated from default water retention curves present in the software RETC (van Genuchten *et al.* 1991).

In the experiments in this thesis, changes in soil water retention functions happened mainly between soil layers. Soil water retention can change substantially between soil layers because of textural changes. To account for differences between layers we sampled soil in a similar manner as for bulk density and kept samples for measuring water holding capacity in the lab with a pressure plate. To do this, samples were taken from two positions within the area of experiment 4: one on the north extreme and the other on the south extreme—separated from each other by ~30 m.

To estimate the water retention functions for each soil in the north and the south positions and in several soil layers of 20, 40, 60, 80, 100, and 120 cm, we measured soil water content at six water suctions: 10, 30, 100, 300, 700 and 1500 kPa. For soil

suctions between 10 and 100 kPa, soil samples were handled with caution to avoid compaction, since soil structure is especially important for soil suctions close to field capacity, when the most relevant pores holding water are large enough as to be affected by compaction. For soil suctions higher than 100 kPa, when soil pores cannot be altered by compaction, we ground the samples and sieved through a mesh that allowed us to select only particles smaller than 1 mm; this was done to ensure appropriate hydraulic continuity between the pressure plate and the samples, given that at these high suctions moderate gaps between both can interrupt the water flow and thereby give a false impression of equilibrium.

Soil samples were equilibrated in the pressure plate and chamber using two ceramic plates according to the suction aimed: a coarser one for suctions less than 300 kPa, and a finer one for suctions above it. Two table spoons of soil sample were placed over the pressure plate inside aluminium rings of 1 cm depth and 4 cm wide, in sets of 16 each time. We allocated those 16 rings as 2 soil positions (north and south), 3 soil depths (say, 20, 40 and 60 cm) and 2 replicates per each combination of the first two; replication was done to check for possible problems in samples reaching equilibrium. After that, we added water slowly with a beaker so that samples wetted from the bottom towards the top—this was done, again, to ensure hydraulic continuity between ceramic plate and soil samples. When the top of the soil samples shined, the saturation of the sample was finished and we applied slowly a pneumatic pressure by opening slowly the gauge of an air-gas bottle.

When the soil samples are in equilibrium with the pressure plate at any given pneumatic pressure, the suction in the sample is the same as in the pressure plate, which in turn

equals the pneumatic pressure applied. As water flows out the pressure plate slowly, equilibrium takes some time to be achieved. This time is longer the greater the suction, as the soil water conductivity—that is, how fast the water moves along a gradient of suction (gradient being the ratio between a difference in suction and the distance over which that difference takes place)—decreases exponentially as the suction increases. The pressure plate had a small outlet from which we collected the flow of water coming out and registered the amount every hour (at low suctions at the start of the calibrations) or once a day (at high suctions at the end of the calibration). We considered that the samples reached equilibrium when the trajectory of the outflow coming from the samples over the pressure plate reached a plateau. What we needed to know next was the water content of these samples. Thus, when the plateau was attained, we quickly released the pressure, opened the chamber, collected the soil samples and placed them into small aluminium tins, and weighed in a scale with an accuracy of 0.01 g. Then we placed those tins with the soil inside an oven at 105 °C for 48 h. As when measuring soil water content by direct coring from the field (section 3.2), soil water content was calculated as the difference between the initial wet soil and the final dry soil over the weight of the dry soil. That gravimetric water content (g g^{-1}) was multiplied by the bulk density of the sample (g cm^{-3}) and divided by the density of pure water at 20 °C (1 g cm^{-3}) to obtain the volumetric water content ($\text{m}^3 \text{ m}^{-3}$) (3.1).

Once we gathered all data points of soil water content at soil water suctions of 10, 30, 100, 300, 700 and 1500 kPa, we estimated the water retention curves of the form of van Genuchten's equation (van Genuchten 1980),

$$\begin{aligned} \theta &= \theta_s && \text{if suction} = 0 \\ \theta &= \theta_r + \frac{\theta_s - \theta_r}{(1 + |\alpha \text{ suction}|^n)^{1-\frac{1}{n}}} && \text{if suction} > 0 \end{aligned} \quad (3.3)$$

where θ is the volumetric soil water content ($\text{m}^3 \text{ m}^{-3}$), suction is given in metres rather than kPa (1 m = 10 kPa), θ_s is the water content at saturation ($\text{m}^3 \text{ m}^{-3}$), θ_r is called the residual water content ($\text{m}^3 \text{ m}^{-3}$), which is a water content small enough to be beyond the wilting point and achieved when the function plateaus towards high values of suction, and α (m^{-1}) and n (unitless) are other curve parameters. We fitted these equations by inputting the suction and water content data from the pressure plate into the software RETC (van Genuchten *et al.* 1991). To help the fitting arrive to a solution at suctions smaller than 10 kPa at depths of 20 and 40 cm, and smaller than 100 kPa at depths 60, 80, 100 and 120 cm, we fixed the parameter θ_s according to Paydar and Cresswell (1996). These authors found that, for several Australian soils, a good prediction of θ_s could be obtained by applying the formula

$$\theta_s = 0.93 \left(1 - \frac{BD}{PD}\right) \quad (3.4)$$

where BD is the bulk density (g cm^{-3}) and PD is the average particle density of soils (approximately a constant 2.65 g cm^{-3}); the equation can be rephrased as the saturated water content of a soil is 93% of its porosity, where porosity equals the relative volume of soil that is not a particle $\left(1 - \frac{BD}{PD}\right)$.

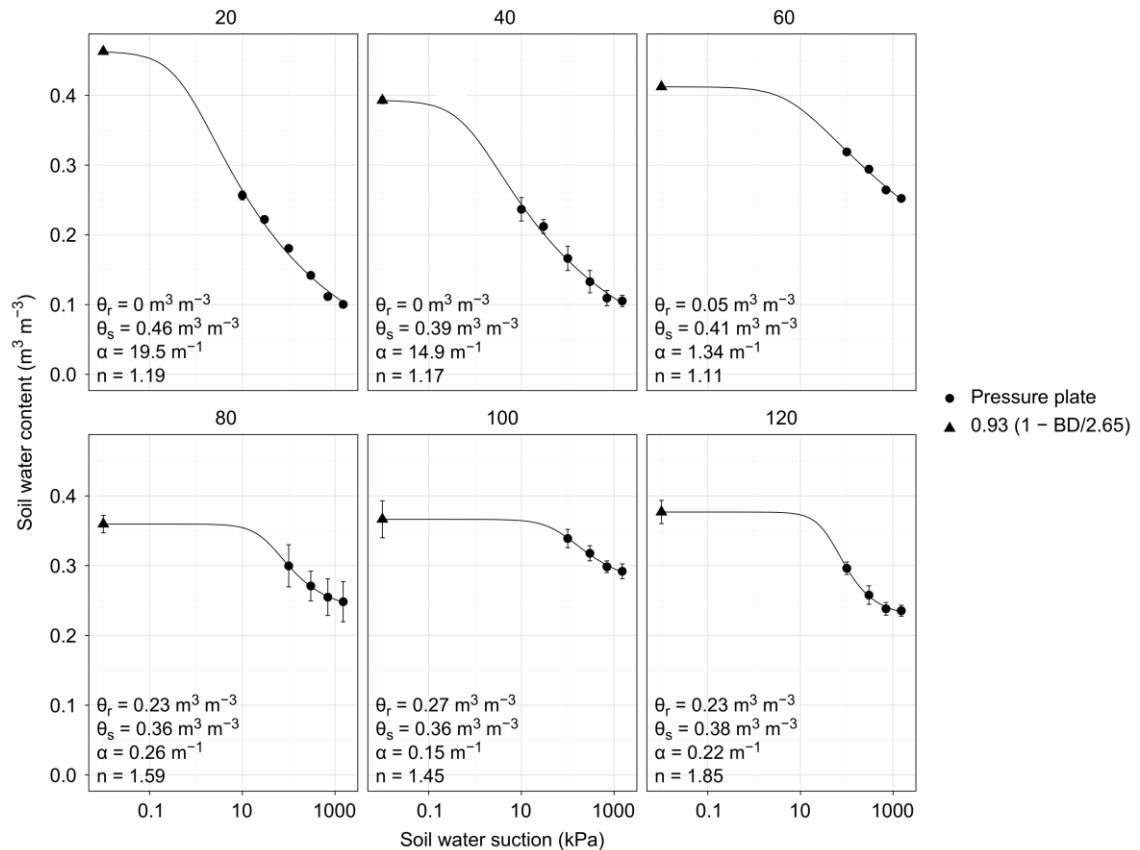


Figure 3.13. Water retention curves estimated for the site in experiment 4. The vertical axis is soil water content and the horizontal axis the soil water suction. Samples in the paddock were taken at two extremes of the experimental area: north and south. Soil water contents at suctions greater than zero were measured in a pressure plate apparatus. Soil water content at complete saturation (i.e. suction equal zero) was estimated as $0.93(1 - \frac{BD}{PD})$ as Paydar and Cresswell (1996).

3.7 Validation against neutron-probe soil water content

As we measured soil water content with a neutron probe within a close proximity to the gypsum blocks (~ 1 m apart, see Figure 2.5 for experiment 4), we were able to compare the predicted soil water content—calculated from the previous water retention curves—with the soil water contents given by the neutron probe (Figure 3.14). Water retention curves did not predict the water content measured by the neutron probe accurately. This

is evident in two ways. First, the most noticeable feature of Figure 3.14 is that, at soil depths of 20 or 40 cm, neutron-probe water contents at suctions less than 50 kPa are too high compared to the predictions of the water retention curve fitted in the lab—reasons for this discrepancy will be discussed later, but for now it can be said that GBHeavy gypsum blocks are not suited for measuring suctions less than 50 kPa. Second, for depths 60 and 100 cm, the predictions of the water retention curves were higher than the measured water contents for the whole range of suctions. This second feature can be due to the fact that soil sampled to determine the water retention curves in the lab might not have been representative of the soil within the experimental area, given the high soil heterogeneity in the field.

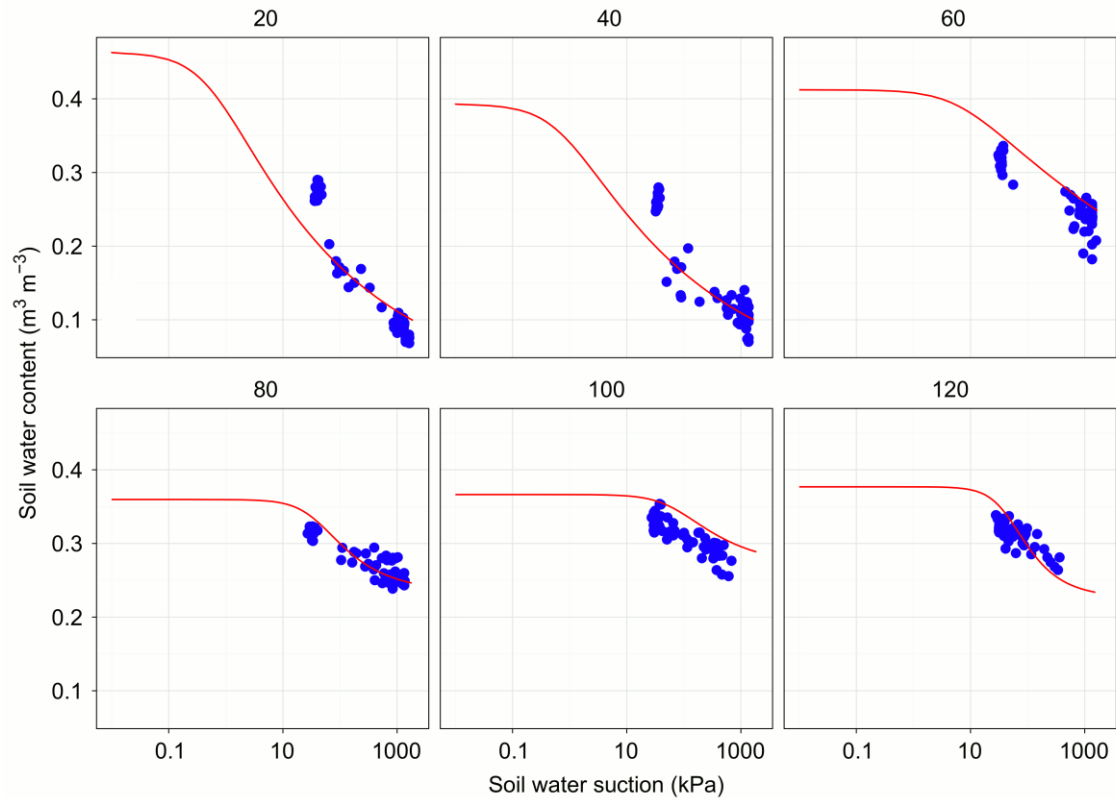


Figure 3.14. Soil water content predicted by the water retention curves (red lines, same curves as in Figure 3.13), and soil water content measured by neutron probe (blue dots), as a function of the soil water suction measured by gypsum blocks.

When having a closer look at the graphs of soil water suction by gypsum blocks over time—shown before when referring to the calibration of gypsum blocks by temperature—one can see that even when supposedly saturated all data points are higher than ~ 50 kPa (Figure 3.15). The principal explanation for this mismatch is that this type of gypsum blocks (GBHeavy) were simply not manufactured for measuring soil water suction under 50 kPa. Another type of gypsum blocks, the GBLite, would be suitable for this task, for their range of measurement is between 0 and 200 kPa. As we were interested in this thesis in estimating water uptake by roots, we chose to use GBHeavy gypsum blocks, which range from 50 to 500 kPa and as such can cover more of the

range where plants take up water. Other explanations for the lack of accuracy below 50 kPa are that some soils, depending on their pore distribution, do not necessarily reach suction = 0 kPa even when saturated, for some soils have such small pores that even when fully saturated water is still under tension. When the material lacks large pores, whose negligible capillary forces when saturated would dominate the soil suction of the whole, then the material is still under some small sort of tension even when saturated. This may be the case for gypsum blocks. Another explanation, though less likely, could be that sometimes air can be trapped inside pores so that the soil—or in this case, the gypsum block—is never fully saturated. This limitation of the gypsum to read suctions under 50 kPa is also supported by Figure 3.16, which shows the very start of the calibration of gypsum blocks against temperature. During the 'glistening point' the soil surrounding the gypsum blocks over the pressure plate was glistening because it was saturated with water. Even when fully saturated gypsum blocks did not show suctions between 0 and ~ 40 kPa.

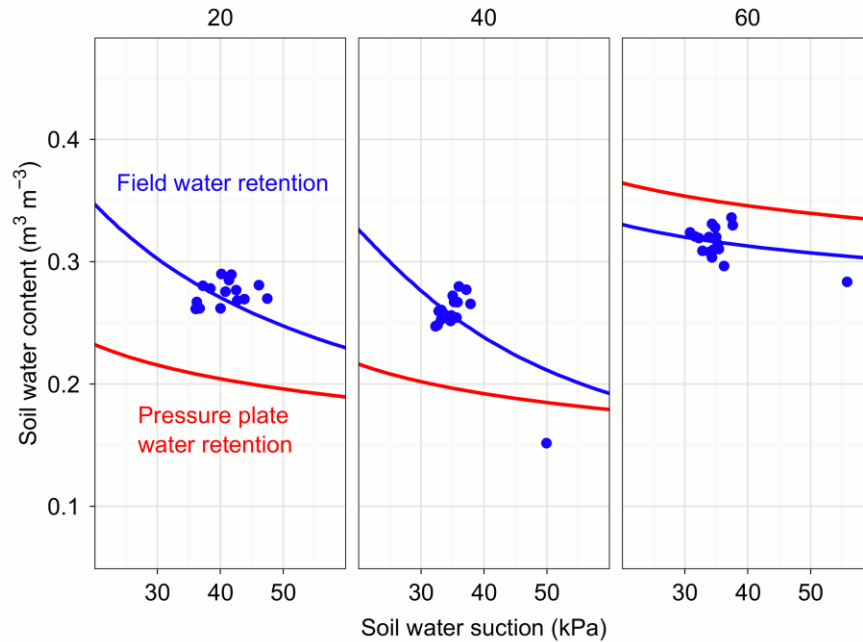


Figure 3.15. A closer look at Figure 3.14, narrowing the focus within soil suctions from 20 to 60 kPa. The graph shows the disagreement between the water retention curves measured in the pressure plate (red line) and the data measured with neutron probe at suctions less than 50 kPa (blue dots), where points cluster at higher values than what the pressure-plate water retention predicts (20 and 40 cm depth). The blue line shows a surrogate water retention curve that results from fitting the gypsum-neutron probe data with RETC (van Genuchten *et al.* 1991). The latter is however unrealistic and will be later discarded, as explained in the main text.

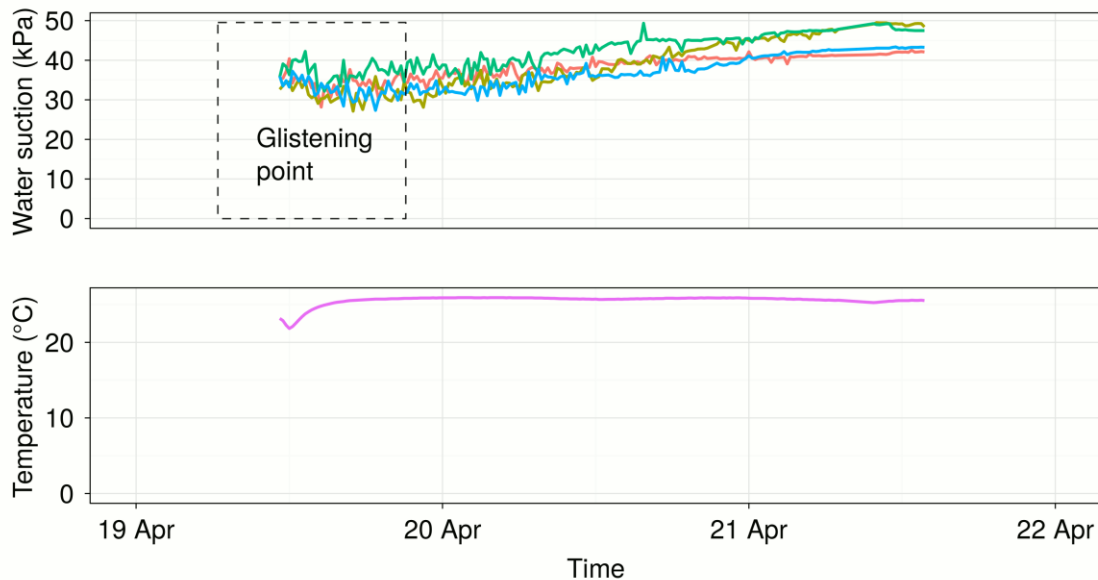


Figure 3.16. The start of the calibration of gypsum blocks, where 'glistening point' shows the approximate period when the soil surrounding the gypsum blocks was shining because of being saturated with water. The graph suggests that, even when fully saturated, gypsum blocks are blind to suctions under c. 50 kPa.

Whichever the cause of the difference at suctions less than 50 kPa between gypsum-blocks-predicted soil water content and neutron-probe-measured soil water content, there was still a disagreement between these two quantities at high suctions (soil depths 20, 40, 60) or along the whole range of suctions (80, 100 cm). We attempted to overcome this disagreement by fitting the van Genuchten model in RETC directly to the neutron probe vs. gypsum blocks data, building in this way a set of surrogate water retention curves tailored to the field data. According to what was discussed, however, two possible surrogate water retention curves could be fitted by considering, or not considering, gypsum blocks blind to suctions less than 50 kPa. These curves are shown in Figure 3.17. Removing data whose suction is less than 50 kPa, albeit still using a fixed θ_s determined as in Paydar and Cresswell (1996), affected the curves at depths 20

and 40 cm. At a depth of 20 cm, fitting the surrogate water retention curve without data smaller than 50 kPa produces a curve similar to the original water retention curve fitted in the lab with the slight difference that in the surrogate one the water content at high suctions is not overestimated (as in Figure 3.14)—which is of course redundant given that the curve was fitted (optimized) to the data. Using all data gives a curve that passes through the cluster of points smaller than 50 kPa, but it is so far from the water contents predicted by the original water retention curve fitted in the lab that it seems unrealistic. At a depth of 40 cm, the surrogate water retention curve that was fitted using all data (i.e. even including data whose suction is less than 50 kPa) looks even more unrealistic: for example, at a soil suction of 10 kPa this curve almost indicate that the soil is saturated (i.e. the curve is close to the plateau) at a soil water content close to $0.40 \text{ m}^3 \text{ m}^{-3}$ whereas both the original water retention (Figure 3.14) and the surrogate fitted without data smaller than 50 kPa indicate soil water contents close to $0.25 \text{ m}^3 \text{ m}^{-3}$. Another feature of this soil water retention curve fitted with all data is that the change in water content per unit change in suction is not smooth like the rest of the curves. Instead, the curve describes an abrupt reduction in soil water content between 10 and c. 600 kPa, and a plateau between 600 and 1500 kPa. This lack of smoothness compared to the other curves suggests as well that including data whose suction is smaller than 50 kPa is inappropriate. The values in the ordinates, soil water contents measured by neutron probe, must be correct, but the values in the abscissas, soil water suction measured by gypsum blocks, must be wrong for suctions less than 50 kPa—gypsum blocks seem to be insensitive to smaller suctions.

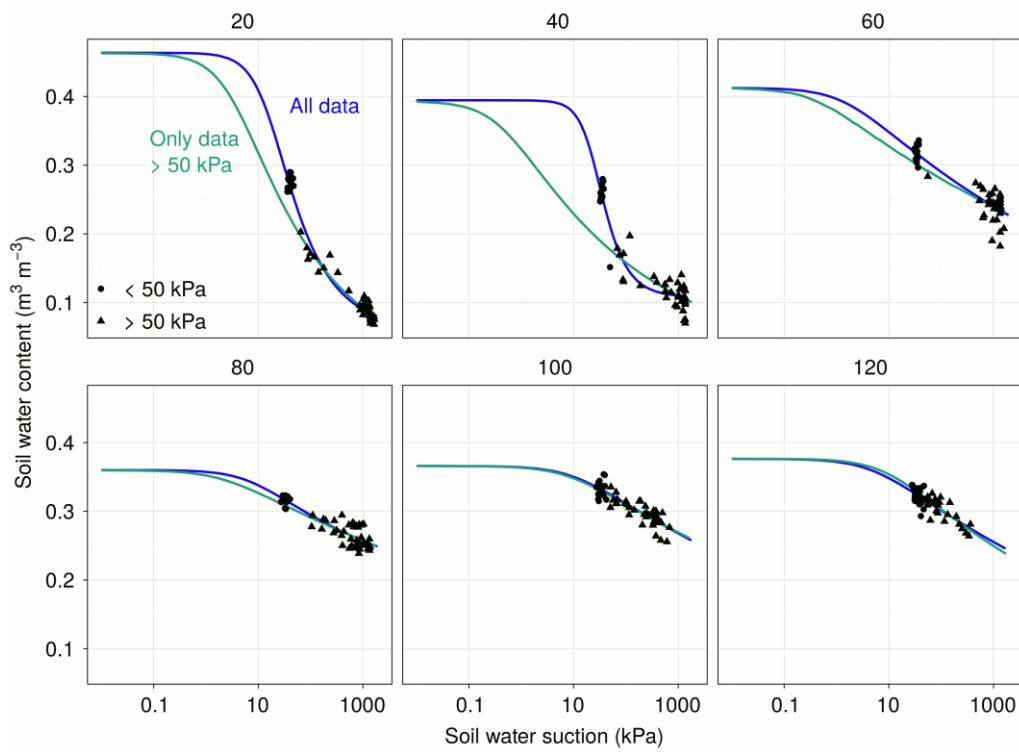


Figure 3.17. Surrogate water retention curves obtained by fitting soil water suction measured by gypsum blocks to soil water content measured by neutron probe in the field. Dots are neutron-probe-measured soil water content (circles are data < 50 kPa, triangles are suction > 50 kPa). Notice that the parameter θ_s was fixed as in equation (3.4). Two possible surrogate water retention curves can be obtained. First, in blue, the lines show water retention curves fitted using all data. Second, in green, the lines show the water retention curves fitted after excluding data < 50 kPa. Reasons for excluding data whose suctions are less than 50 kPa are detailed in the main text and supported by Figure 3.16.

The data of neutron-probe-measured soil water content against gypsum-block-measured soil water suction was not only clustered at around 50 kPa, but also crowded against a ceiling upper limit of 1500 kPa. This is because the calibration of suction against resistance shown in section 3.4 was truncated at a limit of 1500 kPa, since we did not test the gypsum blocks beyond that suction. It is possible, though, that gypsum blocks were reporting soil water suctions higher than 1500 kPa. That would explain why data

points in Figure 3.14 and Figure 3.17 are clustered against a 'wall' of suction at around 1500 kPa.

Perhaps the estimation of suction by GBHeavy gypsum blocks is still valid not only at around 500 kPa (a limit to which they were manufactured) but well beyond a suction of 1500 kPa. For instance, at 60 cm depth, if we try to guess the actual suction of the smallest values of soil water content measured by the neutron probe at around 1500 kPa, we could do it by extending either of the surrogate water retention curves (pretending they are almost straight lines) until they match that value of water content somewhere along the suction scale. That value in the scale of suction would be around 10000 kPa. This value of suction is perhaps too high, but it is interesting that these deviations of neutron-probe-measured soil water content from the water retention curves only happen at soil depths where suction reaches the upper limit of 1500 kPa, that is, at 40 and 60 cm depth; one cannot detect similar deviations at other soil depths, like 80, 100 and 120 cm, which were never as dry as 1500 kPa. All this suggests that gypsum blocks can report suctions much drier than 1500 kPa, but we cannot know how much or how accurately.

Possibly our water retention curves, instead of being separate curves for soil depths at 20 cm intervals, can be simplified to 4 curves: (i) at 20 cm, (ii) at 40 cm, (iii) at 60 cm, and (iv) deeper than 60 cm. Curves at 20 and 40 cm depth are slightly different between each other, both resembling the curves of a loam soil (Figure 3.17). The curve at 60 cm depth matches the pattern of a clay soil, with high water contents even at high suctions—soil water content is c. $0.25 \text{ m}^3 \text{ m}^{-3}$ at 1500 kPa (Figure 3.17). Curves at soil depths beyond 60 cm—that is 80, 100 and 120 cm—look slightly different between each other when calibrated in the lab with pressure plate (Figure 3.13) but when looking

at the surrogate water retention curves fitted to the field data they seem to belong to a unique water retention curve. The latter agrees with our visual observation of the soil when coring, which seemed to be homogeneously equal from 80 cm to the bottom of the profile.

Once we had a set of putative water retention curves, both fitted in the lab or in the field, our next step was to use each of them to predict volumetric water content from gypsum-block's suction measured in the field. As discussed before, we discarded the surrogate water retention curves fitted including all data given that they seemed unrealistic. Two water retention curves were therefore considered: (i) the water retention curve fitted in the lab, with the pressure plate data, and (ii) the surrogate water retention curves fitted to the field data but excluding suction smaller than 50 kPa.

Then, we compared the trajectories of the calculated soil water content of both curves plus the data points of neutron-probe-measured soil water contents. Figures for each soil depth are shown in Appendix B. These figures show data plot by plot. Surprisingly, not even the trajectories of soil water content predicted with the surrogate water retention curves matched the neutron probe data very well—even against the same data that was used for the fitting. This is indicating that the variability in the soil characteristics, and therefore the variability in the water retention parameters, is large within the experimental area. However, this is not unreasonable, since the water retention curves were tailored to the whole data set, not tailored to individual plots. Soil variation can therefore make the fittings disagree with neutron-probe-measured soil water content from plot to plot.

3.8 Conclusions

Calibrating gypsum blocks to measure volumetric water content was a laborious process that, unfortunately, did not yield the expected results—errors at the plot level were too large. This can be seen in the figures in Appendix B. They show that at the plot level neither of the two water retention curves could match the observed soil water contents (here, I considered neutron-probe-measured soil water contents as *observed values* given the proved robustness of this method). However, for the purpose of estimating water use by plants, which is the change in water content over time rather than the actual water content, the use of gypsum blocks might suffice. The figures in Appendix B show that the mismatch between estimated and observed soil water contents was not a mismatch between changes in water content. Consequently, we attempt in Chapter 5 to calculate water use by crops by estimating changes in soil water content with gypsum blocks.

We confirmed that gypsum blocks can report soil water suctions within the limits where plants use water under field conditions. Our lower limit for soil water suction measured by gypsum blocks was around 50 kPa, which is the lower limit reported by the manufacturer and is not far from the limit of 30 kPa reported by Aitchison and Butler (1951). Differences in the porosity of the materials used for the manufacturing of gypsum blocks between their and our study might be responsible for this difference. In the case of the upper limit of suction, readings from the GBHeavy gypsum blocks did not only match with water content determined by neutron probe in the field at 500 kPa—the upper limit reported by the its manufacturer—but seemed to be valid still around 1500 kPa.

The fact gypsum blocks can quantify soil water status within field capacity and permanent wilting point—though both measures are loose, not precisely defined—is encouraging since phenotyping for deep water use could be aimed at measuring soil water suction rather than water content. Using suction, it would not be possible to calculate an accumulated metric over time, such as the amount of water used by crops. But it might be possible to select crop genotypes that are successful in using deep water by looking at some features of the dynamics of soil water suction over time. For instance, one could quantify the onset and rate of drying of a given soil layer as Dardanelli *et al.* (1997, 2004) did for the dynamics of soil water content. Under this framework, the onset of the water withdrawal from a given soil layer might indicate when the root length density in that layer was sufficient to make the water uptake substantial—a sort of threshold root length density. On the other hand, once the onset of drying started, a rate of change in soil water suction over time for that soil layer could indicate how effective a certain genotype is in using soil water. The shape of these putative relationships may be non-linear, since water is withdrawn at a diminished rate over time (Passioura 1983) and on top of that the relationship between water content and suction is exponential (Figure 3.12). Calculating the rate of change of the logarithm of suction, rather than the rate of change of suction *per se*, might help to linearize these relations and therefore have the rate of change (slope) as a parameter that summarises how effective in using water a given genotype is. However, in order to use this technique, sowing crops under rain-out shelters is a must, since the infiltration of rain into the soil would disrupt the drying of the layer and make the calculation of the rate and onset impossible.

In summary, we calibrated gypsum blocks to predict volumetric soil water content. Neither pressure-plate water retention curves nor surrogate, neutron-probe water retention curves were able to predict soil water accurately. However, the lower and upper limits of available water sometimes varied in congruence—for instance, when the lower limit was 5% higher than what the neutron probe measured, the upper limit was 5% higher as well. This indicated that predicted available water was the same. This encouraged us to still use the gypsum blocks to measure water uptake by roots in Chapter 5.

Chapter 4 Searching for genetic diversity in rooting depth and its relationship with crop growth and yield

4.1 Introduction

In previous Chapters I introduced the matter of deeper roots into a framework of water use and yield (Chapter 1), I explained how we sampled roots, biomass and yield in the field (Chapter 2), and how we developed a way of estimating soil water content continuously in the field by using gypsum blocks (Chapter 3). This Chapter is the first of two experimental Chapters, where I aim to address the question of whether we can find—by sampling roots using a soil coring technique—genetic diversity in rooting depth, and its relationship to yield, in wheat and triticale growing in the field.

The background for this Chapter is the idea that breeding grain-crops with deeper roots might increase yield by making plants more able to capture soil resources. While this idea is widely accepted, cases where genetic variability for rooting depth is both proved and validated in field conditions are rare. Moreover, the presence of roots deep in the soil does not guarantee effective use of deep water (Jordan and Miller 1980; Kirkegaard *et al.* 2007); for example, roots can clump together inside macro-pores in the soil, reducing their water uptake (White and Kirkegaard 2010).

The results of some studies suggest that deep roots have been responsible of grain yield progress in the past. In maize, computer simulations suggest that yield increments in the

United States corn-belt have only been possible by both more erect leaves and deeper roots (Hammer *et al.* 2009). In wheat, experiments in 120-cm-deep root observation chambers showed that genotypes developed to resist drought had longer root system in deep soil layers (Manschadi *et al.* 2006). Field experiments also showed that wheat breeding in Mexico caused crops to be more effective in extracting water from deep soil layers (Pask and Reynolds 2013). Furthermore, breeding progress facilitated by roots may be achieved without a yield penalty during seasons with adequate water supply, as suggested by a computer simulation of wheat genotypes possessing a hypothetically higher deep-water extraction capacity (Lilley and Kirkegaard 2011). These examples support the notion that grain yield could be increased by breeding wheat varieties with deeper root length.

Our aim in this Chapter is to test whether genetic diversity exists in current germplasm in field conditions. To explore a wide range of phenotypes we deliberately included four functional groups of genotypes supposed to have increased root growth. The first group were triticales (\times *Triticosecale*), a hybrid from wheat and rye (*Secale cereale*), which grows more vigorously at early stages of crop development and in so doing could grow more roots. Studies have demonstrated the resilience of triticale crops when compared to wheat growing in water-limited conditions (Giunta *et al.* 1993).

The second group were wheat lines bred for increased early vigour. The early vigour trait and its concomitant faster leaf area expansion has been studied in wheat by Rebetzke and Richards (1999) and Rebetzke *et al.* (2004), and the root systems of these vigorous wheats have been shown to improve early nitrogen uptake (Liao *et al.* 2006; Palta and Watt 2009).

The third group were near isogenic lines of wheat with a range of plant heights; "overgrowth" mutants of the *reduced height* genes (*Rht*) responsible for the semi-dwarf phenotype that made the Green Revolution possible. These genotypes could grow more root length or depth by saving carbon that otherwise would be invested in stem mass (Chandler *et al.* 2002; Chandler and Harding 2013).

The fourth group were near isogenic lines of wheat with and without the *tiller inhibition* (*tin*) gene (Duggan *et al.* 2005; Mitchell *et al.* 2012; Kebrom and Richards 2013). The photoassimilate saved from the production of tillers could be directed into the growth of more roots. Considering grain yield, this advantage is double if the tillers saved were going to be unproductive, as they usually are. A study of *tin* lines in tubes showed increased partitioning to, and weight of, the root system to the five leaf stage (Duggan *et al.* 2005). This increase was associated with the seminal root system; the effect on the nodal root system, the development of which is closely associated with tiller emergence, is unknown (Klepper *et al.* 1984). A study in the field showed increased root depth associated with the *tin* gene, but only to the mid tillering stage (Richards *et al.* 2006).

We hypothesize that (i) triticales and wheat genotypes that contrast in early vigour, tiller number and plant height, will differ in rooting depth, and that (ii) those genotypes having deeper roots will produce more biomass and grain yield.

4.2 Materials and methods

The majority of the details about materials and methods pertaining this Chapter were already described in Chapter 2. But briefly, we measured rooting depth, total root length, shoot biomass and grain yield in 3 field experiments, during 2011 and 2012 in the Ginninderra area, Canberra, Australia (Figure 2.1).

Methods specific to this Chapter are those of statistical analyses, which were as follows.

Data were analysed by analysis of variance and linear, or non-linear, regressions with the R statistical software (R Core Team 2014). For analysis of variance, we used linear mixed-effects models because they allowed us to test, and account for, the effects imposed by spatial variability of soil conditions—which, as shown later in the results section, have a large effect over root variables. These models were fitted with the R package ASReml-R (Butler 2009). Three different, but similar, statistical models were used for the analysis of variance of root and shoot variables. First, there was a combined model for experiments 1 and 2, because these two experiments share the same 36 wheat and triticale varieties. The model was

$$y_{ijkmn} = \mu + b_i + s_j + g_k + sg_{jk} + C \times m + R \times n + \epsilon_{ijkmn}, \quad (4.1)$$

where y_{ijkmn} is the response variable (e.g. rooting depth) for replicate (block) i ($i = 1 \dots 4$), site j ($j = \text{Valley or Creek}$), genotype k ($k = 1 \dots 36$), column m , and row n ; μ is the overall mean; b_i is the effect of block i ; s_j is the effect of site j , g_k is the effect of genotype k , sg_{jk} is the effect of the interaction between site j and genotype k , C is the linear effect over a gradient of columns m ; R is the linear effect over a gradient

of rows n ; m is the column where the corresponding plot is located, and n is the row where the corresponding plot is located; ϵ_{ijkmn} is the error. Terms modelled as fixed effects are site, genotype, their interaction, the linear trends of the column and of the row. Random effects terms in the model are the block ($b_i \sim N(0, \sigma_b^2)$)—that is, b_i is a variable that distributes normally with mean equal zero and variance equal σ_b^2 —and the error ($\epsilon_{ijkmn} \sim N(0, \sigma_e^2)$). The linear trend effects of column and row were tested for significance and also for the influence that they have on the residuals of the model. If without the linear effects of the column ($C \times m$) or the row ($R \times n$) the residuals showed a trend across the column or row of the trial, but after including them (i.e. $C \times m$ and $R \times n$) in the model the trend in the residuals disappeared, then they were included as terms in the model. Otherwise, they were removed. When they were included as part of the model, they accounted for the spatial trends inside the experimental area, and, as such, helped to remove random variation from the treatment variance: the environmental (site) and genotypic variances.

Second, we fitted a model for experiment 3, which is similar to the previous one but lacks the effect of the site, given that the varieties in this experiment were sown in only one site. In this regard, some varieties were shared by all 3 experiments but they were only five, too few to draw conclusions about genotypes and genotypic groups. As a result, we didn't analyse those five varieties across the 3 experiments. We analysed, instead, experiments 1 and 2 combined, and experiment 3 apart. That made analysis of experiment 1 and 2 more robust, because of the large number of genotypes (36) and 2 sites. The model for analysis of variances in experiment 3 was therefore

$$y_{ikmn} = \mu + b_i + g_k + C \times m + R \times n + \epsilon_{ikmn}, \quad (4.2)$$

where the components can be understood from the previous model and an explanation would be redundant.

Third, for analysing differences between groups of genotypes in experiments 1 and 2, we added a fixed group term to model (4.1), and modified the genotypic term g_k to be random—a random subset of genotypes from within each group of genotypes:

$$y_{ijlmn} = \mu + b_i + s_j + t_{l(k)} + st_{jl(k)} + C \times m + R \times n + \epsilon_{ijlmn}, \quad (4.3)$$

where $t_{l(k)}$ is the effect of the group of genotype l ($l = (k)$), that is, l which is in turn a function of the genotype k ; see Table 2.5 for groups of genotypes sown in 2011). $st_{jl(k)}$ is the effect of the interaction of the site j with the group of genotypes l (which in turn depends on the genotype k).

Explicit formulae for the preceding models was written in the R programming language and are detailed in Appendix A.

For linear regressions we used the "base" R package (R Core Team 2014). For non-linear regressions we used the "minpack.lm" R package (Elzhov *et al.* 2013). Non-linear regression was applied to predict root length density from root count density, as detailed in section 2.6.5.

4.3 Results

4.3.1 Differences in shoot and root traits between genotypes and environments

As a first step to investigate differences in rooting depth between wheat and triticale varieties, we looked into how crops distributed their root length along the soil profile, i.e. the root length density distributions. Root length density distributions varied much more between experiments than between genotypes (Figure 4.1). Part of the variation was due to changes in soil textures and structures between the Creek and Valley sites in experiment 1 and 2 (Figure 2.1), and another part was due to a greater rainfall during 2012 than 2011 (Figure 2.4). No statistical difference was detected when comparing root length densities, at any given soil depth, between genotypes. The standard errors, either due to errors in sampling or to the roots inherent distribution, were simply too large. The site in experiment 2 markedly reduced root growth, both as root length per soil layer as rooting depth. The top 20 cm of soil were similarly explored by all genotypes, no matter in what site. For genotypes that were sown in all three experiments, it can be seen that root length density was larger in experiment 1 than 2, and larger in experiment 3 than 1. Because experiments 1 and 3 shared the same location, changes in root length density between seasons can be attributed to other factors than soil—e.g. rainfall (Figure 2.4).

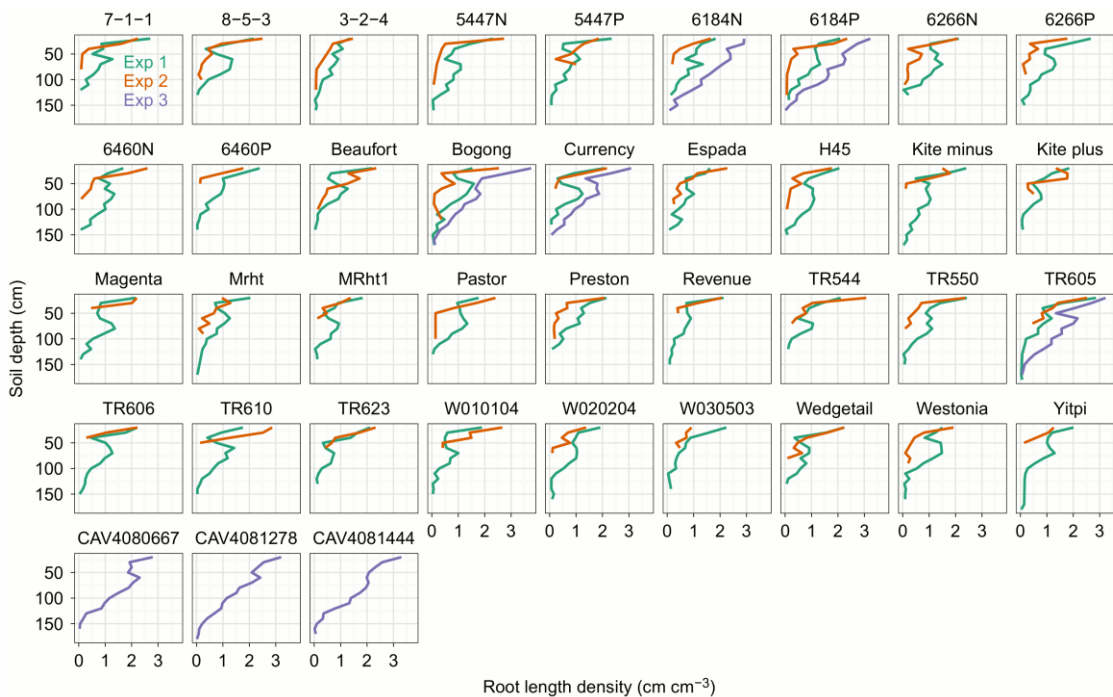


Figure 4.1. Root length density distributions across experiments and genotypes. Lines represent root length densities every 10 cm, each of which is a mean of 4 replicates. Experiments are designated as colours, as in the top-left first panel. Genotypes are detailed in the title of each panel. From those, Bogong and Currency are triticales; the rest are wheat varieties.

4.3.2 Genotypic differences in rooting depth, total root length, biomass and yield

In this section, the root length density distributions presented previously are aggregated (i) along the soil profile, or (ii) within soil depth intervals of 40 cm. When analysed along the soil profile the variables under consideration are total root length (km m^{-2}) and maximum rooting depth (cm). When analysed within 40-cm intervals, the variables are root length from 0 to 40 cm, root length from 40 to 80 cm, root length from 80 to 120 cm and root length deeper than 120 cm (km m^{-2}). Between genotypes, rooting depth differed in experiments 1 and 2 ($p < 0.10$; given the large errors associated with root traits, we accept a statistical threshold of $p < 0.10$ as a difference worth considering) but

not in experiment 3 (Table 4.1). Root length, as a total per m², did not differ between genotypes in experiments 1 and 2, but it did in experiment 3, where the triticale genotype Currency had shorter root length than the rest of the genotypes ($p < 0.05$, Table 4.1). Shoot biomass differed between genotypes in experiments 1 and 2 ($p < 0.001$) and experiment 3 ($p < 0.05$, Table 4.1). Grain yield also differed between genotypes in all experiments ($p < 0.001$, Table 4.1). Both biomass and yield were remarkably higher in triticales, particularly Bogong, than in wheat.

Between experiments, root and shoot growth were larger in experiment 1 than 2 (Table 4.1). For instance, rooting depth was deeper ($p > 0.001$), root length longer ($p < 0.001$), shoot biomass ($p < 0.01$) and grain yield were higher ($p < 0.001$) in experiment 1 than 2 (Table 4.1).

By analysing experiments 1 and 2 together, we were able to disentangle how the groups of genotypes, originally proposed to contrast in shoot growth patterns—namely, triticales, early vigour, MAGIC, ‘overgrowth’ and tin-gene wheat—differed from each other. Groups shown in Figure 4.2 are those that seemed to differ between each other; groups that did not differ, like early-vigour and MAGIC, are not shown. In that respect, triticale produced higher rooting depth ($p < 0.10$), higher shoot biomass ($p < 0.001$), and higher grain yield ($p < 0.001$) than the commercial spring wheat (Figure 4.2).

‘Overgrowth’ wheat groups, grouped as ‘short’, ‘intermediate’, and ‘tall’, differed with each other for rooting depth, shoot biomass and grain yield (Figure 4.2). The ‘short’ genotype produced higher rooting depth ($p < 0.10$), less shoot biomass ($p < 0.10$) but higher grain yield ($p < 0.05$) than ‘tall’ genotypes (Figure 4.2). Wheat isogenic line pairs did not differ between each other when having (*tin* plus) or not having (*tin* minus)

the *tin* gene, although there was a slight tendency of rooting depth and root length to be more in *tin* minus, and for that reason they were included in the figure (Figure 4.2).

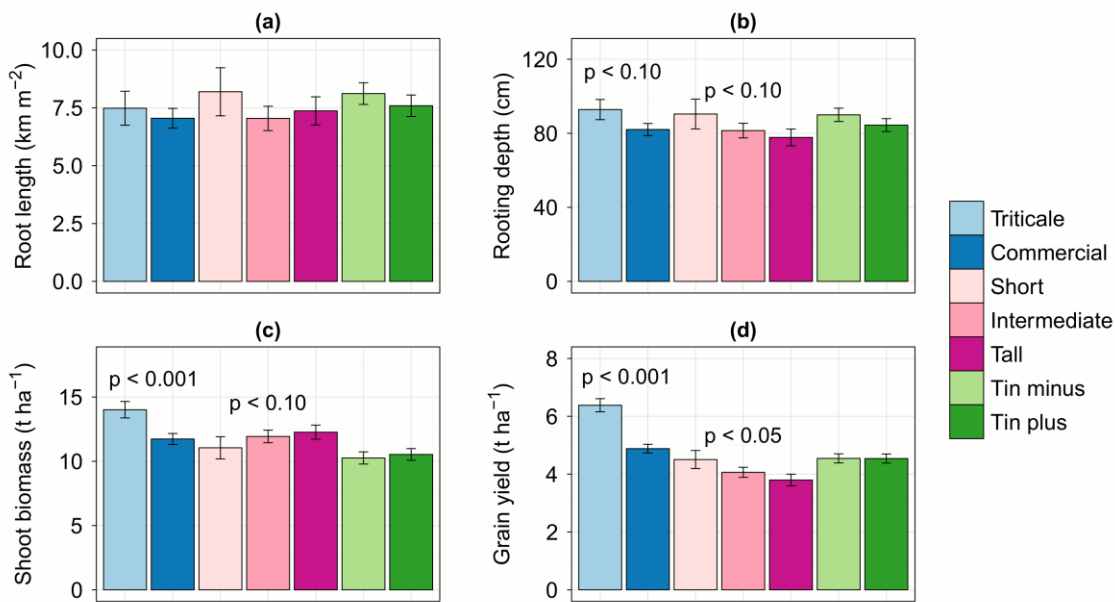


Figure 4.2. (a) Root length, (b) rooting depth, (c) shoot biomass and (d) grain yield for each group of genotypes in experiments 1 and 2. Each bar is the predicted mean, generated by the ASReml model, of the genotype group when combining experiments 1 and 2. Error bars are standard errors for each mean. Above and in the middle of group bars to be compared, p-values indicate significance of their differences; where none is present comparisons are not statistically significant.

Table 4.1. Predicted genotypic means of rooting depth, root length per unit area, shoot biomass and grain yield per experiment. Asterisks (*) or a single dot (.) indicate statistical significance, for genotype, experiment and the interaction between both, as follows: 0 '****' 0.001 '**' 0.01 '*' 0.05 '.' 0.1 'NS' 1. Values within brackets are the least significant difference, calculated as twice the maximum standard error for pairwise comparisons given by the ASReml model.

Group	Genotype	Rooting depth (cm)			Root length (km m ⁻²)			Shoot biomass (g m ⁻²)			Grain yield (g m ⁻²)			
		1	2	3	1	2	3	1	2	3	1	2	3	
Short	TR550	112.0	72.3		11.50	4.89		1240	945		499	415		
Medium	MRht 1	118.0	43.7		8.15	3.18		1440	1010		472	326		
	TR544	103.0	53.7		9.01	6.15		1430	1000		401	363		
	TR605	123.0	53.9	141.0	10.20	7.48	21.60	1380	1200	1800	513	379	594	
	TR623	106.0	44.0		8.92	5.69		1130	1210		397	385		
Tall	Mrht	116.0	37.5		9.54	2.68		1250	1190		411	354		
	TR606	114.0	31.8		11.00	3.76		1340	1160		403	364		
	TR610	120.0	39.0		10.00	6.75		1230	1240		408	354		
Spring	Espada	124.0	37.6		8.84	2.77		1370	995		564	369		
	H45	120.0	56.5		11.60	3.58		1420	1270		573	472		
	Magenta	118.0	31.5		10.30	4.57		1180	761		536	401		
	Pastor	108.0	54.0		10.20	5.15		1340	950		567	393		
	Westonia	125.0	48.6		11.30	3.88		1480	1110		602	405		
	Yitpi	117.0	39.0		9.57	2.50		1210	968		551	397		
Long spring	Beaufort	113.0	75.0		8.46	8.12		1360	869		583	432		
	Preston	104.0	72.2		9.75	4.54		1370	1170		615	497		
Winter	Revenue	103.0	45.3		8.65	4.17		1270	1280		650	536		
	Wedgetail	108.0	67.9		9.14	6.22		1330	920		629	357		
T in minus	5447N	134.0	69.3		11.20	3.71		1240	713		495	423		
	6184N	114.0	50.4	137.0	11.00	3.68	23.70	1340	742	1940	635	300	695	
	6266N	118.0	70.8		12.00	5.58		1100	1080		453	427		
	6460N	121.0	51.4		12.10	5.29		1240	799		574	407		
	Kite minus	138.0	41.2		12.40	4.49		1180	960		506	352		
	T in plus	5447P	124.0	61.0		8.78	6.14		1140	868		553	372	
T in plus	6184P	124.0	69.5	134.0	11.70	4.92	21.20	1310	860	1890	571	372	666	
	6266P	117.0	57.1		12.90	3.79		1320	891		473	410		
	6460P	105.0	36.6		10.10	3.28		1080	778		512	358		
	Kite plus	99.5	54.8		8.32	6.01		1190	1070		459	458		
	Vigour	3-2-4	113.0	64.0		8.65	2.91		1120	812		452	330	
	7-1-1	91.4	53.8		8.65	4.54		1170	884		438	369		
W010104	8-5-3	106.0	62.9		10.20	5.63		1190	852		440	318		
	W010104	129.0	43.1		7.26	6.35		1450	645		541	337		
	W020204	115.0	47.1		10.10	3.58		1220	578		464	339		
	W030503	104.0	52.5		6.96	3.22		1220	986		426	407		
MAGIC	CAV4080667			128.0			20.30			1670			484	
	CAV4081278			148.0			22.00			2000			739	
	CAV4081444			134.0			21.20			1800			604	

Triticale	Bogong	130.0	82.9	145.0	11.40	5.20	20.60	1660	1360	2070	792	651	714
	Currency	118.0	47.3	137.0	8.90	4.37	18.30	1360	1270	1900	595	522	628
	<i>Genotype (G)</i>	· (26.5)		NS	NS		*	*** (216)		*	*** (93)		***
	<i>Experiment (E)</i>	*** (5.5)			*** (0.74)			** (110)			*** (36)		
	<i>G×E</i>	NS			NS			*** (353)			* (149)		

4.3.3 Relationships between rooting depth, total root length, biomass and yield

Shoot and root traits, gathered together across the three experiments, correlated with each other (Figure 4.3). The greater the rooting depth, the greater the shoot biomass ($p < 0.001$, Figure 4.3a) and grain yield ($p < 0.001$, Figure 4.3c). The relationships were curvilinear, and thus while moving from 50 to 100 cm depth corresponded with a biomass increase of ~3 t and a yield increase of ~1 t, changing rooting depth from 100 to 150 cm depth corresponded with a change in biomass of ~8 t and a change in yield of ~2 t.

Shoot biomass and grain yield also correlated with total root length (Figure 4.3b and Figure 4.3d). The larger the total root length, the greater the biomass ($p < 0.001$, Figure 4.3b) and the greater the yield ($p < 0.001$, Figure 4.3d). This time the relationships were better represented by a straight line.

At the same rooting depth or root length, triticale genotypes produce more biomass and yield than wheat genotypes (Figure 4.3). This was more apparent in the case of yield, where triticale, at the same rooting depth or root length, produced ~1 t more yield than wheat in experiments 1 and 2 (Figure 4.3). Differences between biomass and yield

between triticale and wheat having the same rooting depth or root length were smaller in experiment 3 (Figure 4.3).

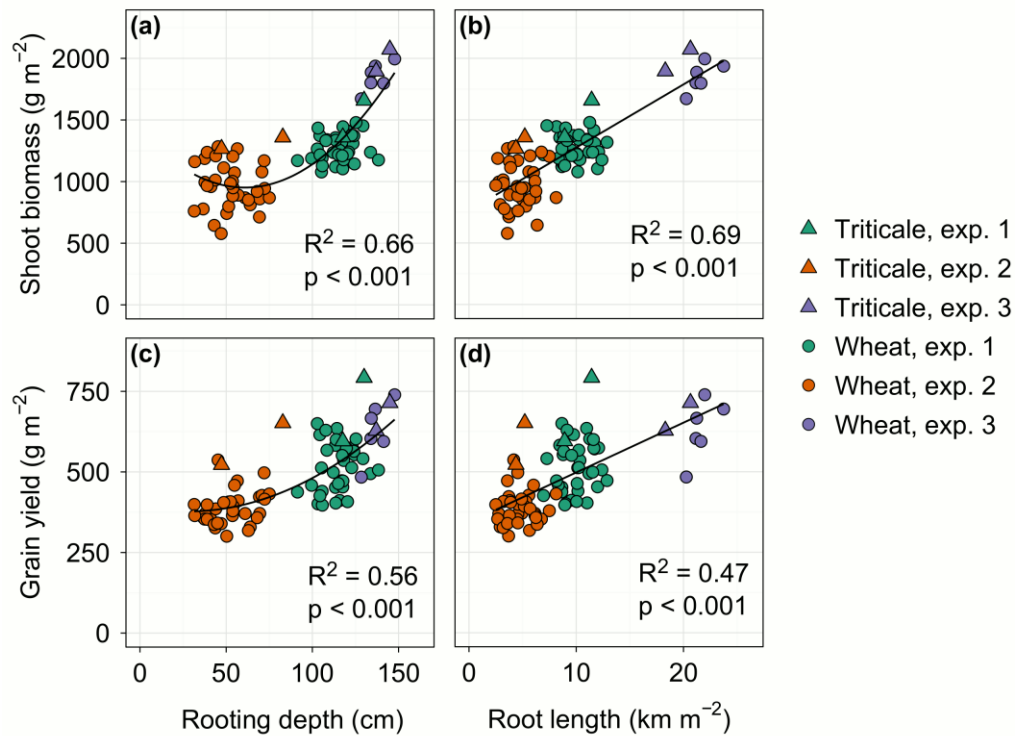


Figure 4.3. Relationship between shoot and root variables at physiological maturity. (a) Shoot biomass, or (c) grain yield, as a function of rooting depth, the maximum soil depth reached by roots, and (b) shoot biomass, or (d) grain yield, as a function of root length, the total root length per unit area. Points are the predicted means, generated by the ASReml model, for each wheat (circles) or triticale (triangle) genotype in each experiment. In (a) and (c) the quadratic term was significant and thus a quadratic model was fitted. In (b) and (d) it was not significant, thereby a linear model was fitted.

When analysing all experiments together, root length deeper than 120 cm was directly related to shoot biomass and grain yield, but not harvest index (Figure 4.4). When fitting these relationships per experiment rather than altogether, root length deeper than 120 cm was directly related to shoot biomass ($p < 0.05$), grain yield ($p < 0.01$) and harvest index ($p < 0.01$) only in experiment 3 (Figure 4). In experiments 1 and 2 these

relationships were not statistically significant (Figure 4.4). The more root length was produced in that deep layer the more biomass and yield crops produced in experiment 3 (Figure 4.4). Correlation does not imply causation, but shoot biomass and grain yield were larger in experiment 3 than experiment 1 and 2, and root length in that deep soil layer was larger as well. It is likely that crops in experiment 3 had more available water in the subsoil and thus more root growth there produced more above-ground growth. The relationships did not seem to be driven by genotypes in experiments 1 and 2, but they did in experiment 3. In that experiment, shoot biomass and grain yield correlated closely with deep root length ($p < 0.05$ and $p < 0.01$, respectively), and, given that data are predicted genotypic means, the variability is mostly caused by genotypes. This means that genotypes drove the relationship between deep root length and shoot and grains growth (Figure 4.4).

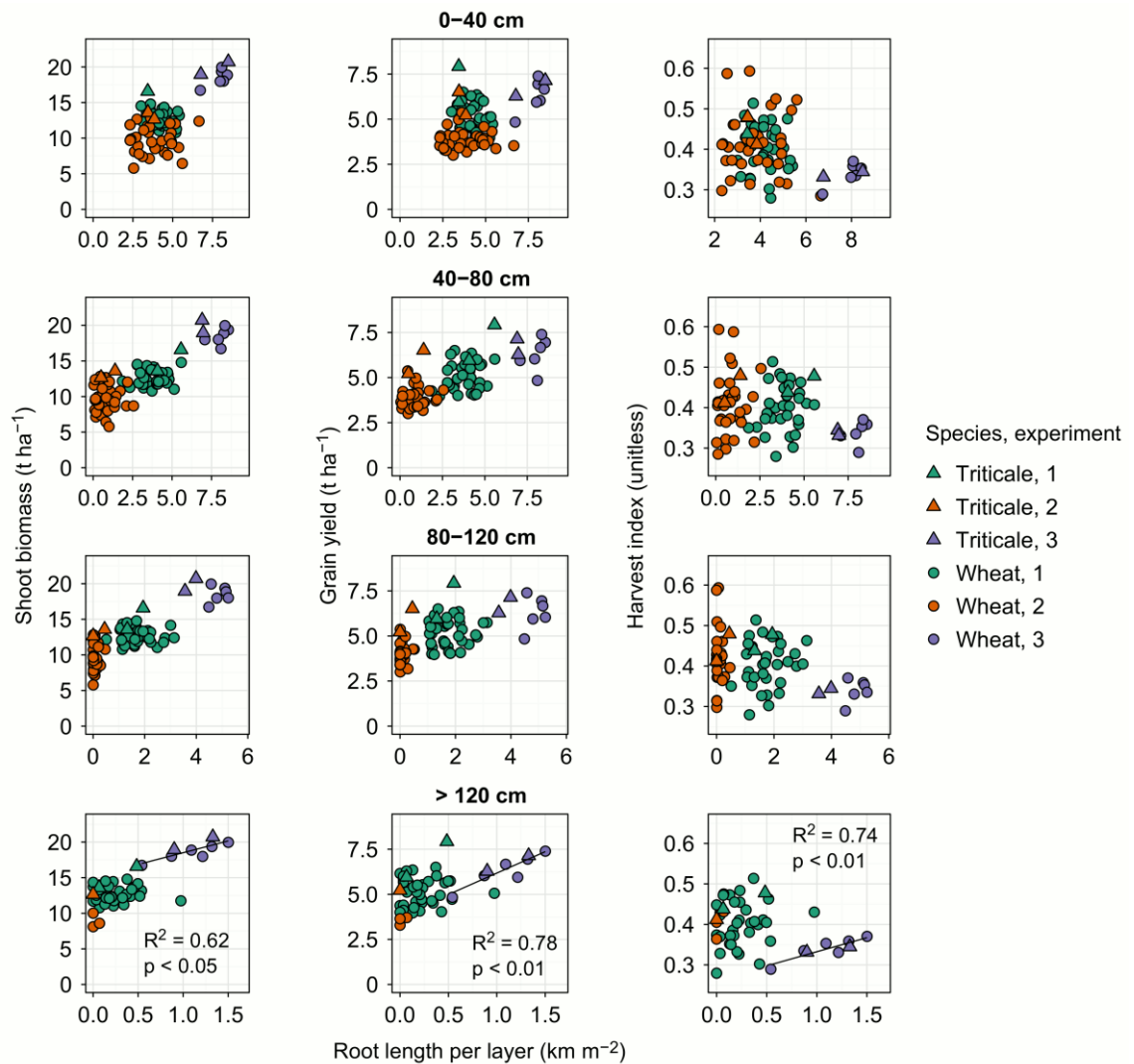


Figure 4.4. Shoot biomass (left), grain yield (centre) and harvest index (right) as a function of the root length per soil layer (rows) in each of the three experiments. Points are the predicted means, generated by the ASReml model, for each genotype in each experiment. R^2 is the adjusted R-squared and p is the p -value for the straight-line fit relating either shoot biomass or grain yield with root length deeper than 120 cm only at experiment 3. Note the change in scale in the x -axis across depth intervals.

4.3.4 Plant height, root and shoot growth

To further investigate the differences in rooting depth, biomass and yield between ‘short’, ‘intermediate’ and ‘tall’ wheat genotypes, we related those variables to canopy height measured just after anthesis (when the maximum height of the crop is achieved). There were trends suggesting a direct relationship between shoot biomass and plant height ($p < 0.07$) and a negative relationship between rooting depth and plant height ($p < 0.06$; Figure 4.5). Grain yield correlated negatively with plant height ($p < 0.02$; Figure 4.5). However, the shortest genotype, TR550, represented a leverage point for the linear fittings in Figure 4.5: without it there would not be any trends. Nevertheless, the trends seem to suggest that wheat with shorter stems have less total above-ground growth (biomass) but higher yield and deeper rooting depth.

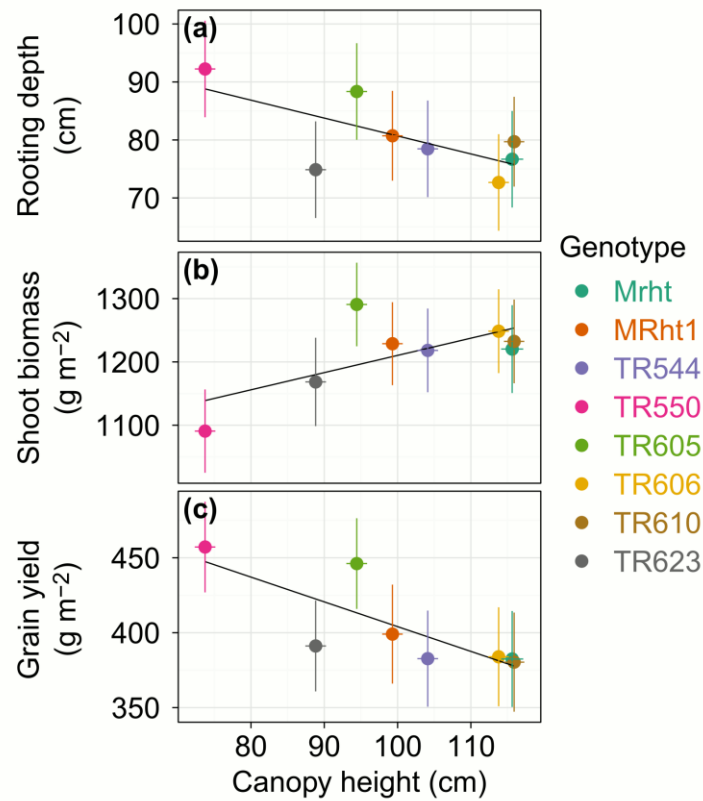


Figure 4.5. Predicted genotypic means, modelled from experiments 1 and 2 combined, of rooting depth (a), shoot biomass (b), and grain yield (c) as a function of final canopy height achieved by crops after anthesis. Bars are the standard errors of the predicted means. The 8 genotypes evaluated are those differing in point mutations for the dwarfing genes (Chandler and Harding 2013). Lines represent the best fit with the following statistics: (a) $R^2 = 0.47$, $p < 0.06$; (b) $R^2 = 0.44$, $p < 0.07$; (c) $R^2 = 0.63$, $p < 0.02$.

4.4 Discussion

We found that triticale and wheat genotypes differed in rooting depth when evaluated in field conditions. However, differences were much larger between experimental sites or years than between genotypes. This may be due to the fact that soil physical properties, water and nutrients availability have a great influence over root growth which could override any genotypic effect. In order to detect differences between varieties, this study suggests that a greater effort has to be placed in making proper statistical designs that can account for soil and season variability.

We found, however, differences in rooting depth between genotypes. These differences were most evident when comparing different species, that is, triticale and wheat. Indeed, triticales produced deeper roots and above-ground growth than commercial wheats. Although introgressing these characteristics of deep roots from triticale to wheat is challenging, the results are encouraging since they support the notion that a more vigorous shoot, by faster leaf area expansion and biomass accumulation, can increase root growth. This breeding objective was already undertaken by (Rebetzke and Richards 1999; Rebetzke *et al.* 2004). However, the early vigour varieties that we evaluated in this thesis did not produce deeper rooting than other wheats. This may be due to the fact that these varieties were not particularly high biomass producers, which can diminish root growth; they had a more dwarf type of plant (genotypes 7-1-1 and 8-5-3) and a planophyle leaf structure (that is, leaves closer to an horizontal rather than vertical angle) which could help in preventing direct soil evaporation by quickly covering the soil, but were not producing high biomass and it seems that neither high root length and depth.

Between wheat genotypes, differences in rooting depth were only noticeable amongst those genotypes that through mutations in the *Rht* genes showed a range of plant heights. For breeding purposes the genetic mechanisms behind these changes are promising because they were given by a change in only one gene. This is not only interesting because of genetic simplicity and its consequent ease of breeding, but also for the possible mechanism behind. It is likely that shorter genotypes were producing deeper roots and more yield by taking advantage of the same trade-off that during the Green Revolution increased yield in wheat, that is, by sacrificing stem growth and favouring grain growth and in this case root length as well. If this mechanism is truth it may still be possible to reduce excessive growth of stems in tall plants while increasing root growth. This should also be true in the case of the prevention of extra tillers by means of the *tin* gene. But unlike Duggan *et al.* (2005), reducing the growth of extra tillers did not increase root growth and yield in our field experiments. These authors, however, found differences in root growth in a wheat isogenic line pair that we did not evaluate (Banks). There were no differences when they tested the isogenic lines Kite + *tin* against Kite, a pair that we did evaluate in this study. Most important perhaps is the distinction that Duggan *et al.* (2005) measured root growth in tube experiment in 50-days old plants whereas we did it in the field in plants that reached maturity. Differences in root growth between isogenic line pairs with and without the *tin* gene might disappear towards older stages of crop development.

Crops with deeper roots certainly yielded more. But because one's aim is to improve yields by breeding, one must wonder how much of the variation in rooting depth and yields was provoked by genotypes. The answer is that it was not much. Most of the

variation was caused by environments. For example, in Figure 4.3 yield and biomass were both related to rooting depth and total root length, but data points were clustered according to the experiment where they belonged. Within each cluster, i.e. within each experiment, genotypes did not drive the relationships (that can be seen in the lack of correlation between a given abscissa value and a given ordinate value *per experiment*). This means that rooting depth and total root length were associated with biomass and yield, but genotypes had little responsibility over these relationships—environmental factors had greater impact.

Genotypic effects on the relationship between deep root length and crop above-ground growth might have taken place in experiment 3. These can be seen in Figure 4.4, where only in experiment 3 there were significant regressions between shoot biomass, grain yield and harvest index with the length of roots beyond 120 cm depth in the soil. Data points are distilled, predicted genotypic means and therefore the source of variation comes mostly from genotypes. Breeding for more root length deep in the profile, at least according to experiment 3, can increase biomass and yield.

4.5 Conclusions

Increasing rooting depth has been proposed as a way of increasing wheat yield, both in water limited and in high yielding conditions. However, examples where it differs between genotypes growing in field conditions are rare. We showed that rooting depth and root length deeper than 120 cm can vary between triticale and wheat genotypes and these differences in turn correlate with biomass, harvest index, and grain yield. Between genotypes, the greatest differences in root and shoot growth were between triticale and

wheat. Within wheat, the greatest differences were between isogenic lines that differ in point mutations conferring them a range of plant heights. In that respect, a trend is suggested, where shorter plants produced less biomass but greater rooting depth and yield, which could signify that a reduction in stem growth results in more assimilates being available for root and grain growth. To corroborate the existence of this trade-off more experiments should be conducted, where several wheat isogenic lines (more than the number tested in this study) are tested in the field for differences in stem biomass and root growth and root depth. Ideally, these lines should vary along a gradient of plant heights so that several lines fall under the 'short', 'intermediate' and 'tall' classes, for assessing only one line (TR550) in the 'short' class proved to be a weakness of the analysis in this study. Validating the existence of this negative relationship between stem biomass and root growth would conform with the concept of ideotypes by Donald (1968) and encourages the exploitation of this trade-off under other circumstances, like reducing tiller number (Mitchell *et al.* 2012) or overproduction of roots in shallow soil layers (Zhang *et al.* 1999).

In summary, there were genotypic differences in rooting depth, they correlated with grain yield, and we were able to detect them by soil coring. Soil coring was challenging because it was time consuming and genotypic differences were elusive because of the strong environmental effects over root growth. The careful design of experiments accounting for spatial variation in soil properties to distil the genotypic effects from the soil effects may prove highly useful in phenotyping for deep rooted genotypes in the field.

Chapter 5 Relating deep-root length with water use, canopy temperature and grain yield

5.1 Introduction

Whether we can detect genotypic differences in rooting depth in current germplasm growing in field conditions, and if those differences have value for grain yield, was addressed in the previous Chapter 4. That was done by sampling roots by soil coring, a technique that is of utmost importance but is very time consuming. In this Chapter I aim to find an alternative, or a complementary approach, to detect deep roots by measuring canopy temperature, as well as analysing the relationship between canopy temperature and water use determined with the gypsum blocks sensors, whose calibration was previously detailed in Chapter 3. This approach is important if we are to incorporate the selection of deep roots into breeding programs.

In farming systems where soil water limits grain yield, crops with deeper roots are expected to yield more grain if water is available deep in the soil. Nevertheless, selecting for them by directly quantifying roots in the field is too slow and it lacks the precision required by breeding programs. Although high throughput soil coring methods have been developed in the field that can assess rooting depth in large numbers of genotypes or treatments, the soil spatial variability even within the same general area is an issue which requires greater replication or smarter designs to overcome (Wasson *et al.* 2014). Hence, we need to develop high-throughput field phenotyping methods for

deep water uptake by roots if we are to incorporate this trait into crop improvement programs. There are several possibilities that may be useful proxies for rooting depth. The most widely discussed ones are canopy temperature (Olivares-Villegas *et al.* 2007; Reynolds *et al.* 2007; Lopes and Reynolds 2010; Pinto and Reynolds 2015) and green leaf area retention (Borrell *et al.* 2000; Christopher *et al.* 2008), both of which should be related to root systems being able to access deep soil water. Differences in canopy temperature are probably most feasible due to the availability of cheap infrared thermometers and thermal imaging cameras that can be used. These are useful because the temperature of a canopy results from a balance between heat gain and heat loss, and a large fraction of that loss is latent heat associated with evaporation from the leaves (transpiration). Hence, cooler canopies indicate higher transpiration rates and greater stomatal conductance (Choudhury *et al.* 1986; Dunin *et al.* 1991) and thereby an effective root system with access to soil moisture. Although water captured anywhere in the soil profile can supply transpiration, there are examples in wheat where cooler canopies correlated specifically to deep water use and deep roots in landraces and genotypes belonging to a breeding population (Reynolds *et al.* 2007; Lopes and Reynolds 2010; Pask and Reynolds 2013).

In water-limited environments, water used by a wheat crop is often more valuable after anthesis, when most of the current assimilates produced by the crop are partitioned directly to grain growth. Indeed, the efficiency with which wheat converts water use into grain is around 22 kg of grain ha⁻¹ mm⁻¹ over the whole season (French and Schultz 1984; Sadras and Lawson 2013), but can be more than doubled, between 55 (Manschadi *et al.* 2006) and 59 kg of grain ha⁻¹ mm⁻¹ (Kirkegaard *et al.* 2007), during the grain-

filling period. Therefore, if the top soil is dry but water is available at depth a wheat crop with deeper roots during grain filling is expected to have a cooler canopy, use more water, and produce more grain through a higher-than-usual water-use efficiency.

A low canopy temperature can therefore be used as a surrogate for roots accessing soil water at depth in some environments. Taking spot measurements of canopy temperature in field plots is useful to provide a snapshot of variation but it does not give dynamic information on canopy temperature over time. Moreover, canopy temperature depends on air temperature and vapour pressure deficit. To account for the effect of both, we used the approach of calculating a crop water-stress index as proposed by Idso *et al.* (1981) and Idso (1982) and used elsewhere (Cárcova *et al.* 1998). In this Chapter, I have studied the dynamics of canopy temperature, the crop water-stress index, and soil water status of two contemporary wheat varieties grown in Australia known to vary for their rooting depth in the field at maturity. We report this together with variation in biomass and yield. We hypothesize that (i) continuously monitored canopy temperature, and expressed in the form of a water-stress index, can be used to detect deep water use in high-yielding wheat varieties, and that (ii) the wheat genotype shown to have deeper roots will have a cooler canopy temperature and deeper water use, which will result in more above-ground growth, including grain yield.

5.2 Materials and methods

5.2.1 Growing conditions

The experiments were designated as experiment 4 (2013), and experiment 5 (2014), and were conducted in the field in the Ginninderra region, ACT, Australia (Figure 2.1).

Plots were machine sown on the 5th June in both 2013 and 2014, and were 6 m long and 1.8 m wide. Each plot was 10 rows wide with 0.18 m between rows. This is typical for wheat growing in this region. Plots were fertilized, in all experiments at sowing, with a mix of 15-12-0-12 Croplift 15® (percentages of N, P, S and K, respectively) at a rate of 100 kg ha⁻¹. Other abiotic (nutrients) or biotic (weeds, diseases) stresses were avoided by sound management, since we aimed to achieve growing conditions where only radiation, temperature and water limited growth of the crops.

Air temperature and vapour pressure deficit were measured with a weather station next to the experiments. Vapour pressure deficit (VPD) was calculated as the difference between the saturated vapour pressure that would correspond to the actual air temperature and the actual vapour pressure in the air, which was registered by the weather station. Rainfall was registered by the weather station as well.

5.2.2 Measuring canopy temperature

Canopy temperature was measured with 2 infrared thermometers positioned on one side of every plot, pointing at their centres with a North direction (Figure 5.1). The infrared thermometers had a built-in data logger that registered one datum every hour.

Thermometers were first calibrated against a black body apparatus that served as a

reference temperature. Then, canopy temperature, air temperature, and VPD were matched together according to time of measurement and were used to calculate canopy temperature deviation (CTD), the temperature of the canopy minus the temperature of the air (°C); the more negative the CTD the cooler the canopy with respect to the air. This is an important distinction as other researchers have used 'canopy temperature depression', which equals the temperature of the air minus the temperature of the canopy (Amani *et al.* 1996). Using 'canopy temperature deviation', as we do, is consistent with the pioneering work of Idso *et al.* (1981), and gives us the chance of further calculating a crop water-stress index.



Figure 5.1. Pictures showing the infrared thermometers used to measure canopy temperature hour after hour. On the left, it can be better appreciated that they were positioned in a 45° angle from the vertical line. On the right, it can be seen more about its construction: a PVC tube inside which the electronic components are installed, and a frontal aluminium head with a hole in the middle where the infrared sensor lays.

5.2.3 Calculating a crop water-stress index

To normalise CTD by VPD, we calculated a crop water-stress index as proposed by Idso *et al.* (1981) and Idso (1982). Crop water-stress index (CWSI) will adopt values between 0 (no stress) and 1 (fully stressed), and is defined as

$$\text{CWSI} = \frac{\text{CTD} - \text{CTD}_{\text{LL}}}{\text{CTD}_{\text{UL}} - \text{CTD}_{\text{LL}}} \quad (5.1)$$

where CTD is the current canopy temperature deviation on a given day (°C); CTD_{LL} is the CTD lower limit (°C), representing the non-water-stressed baseline; and CTD_{UL} is the CTD upper limit, which is the CTD that would be achieved when transpiration is zero (°C). Therefore, CTD_{LL} is the minimum CTD that can be achieved by a well-watered crop at the current level of VPD. This would ideally be measured in a well-watered crop in our experiments, but we lacked that type of plot. As a substitution, we

used a prediction equation determined by Idso (1982) for wheat, which, as shown later, matched our data well (Figure 5.8). The prediction equation was

$$CTD_{LL} = T_c - T_a = a + b \text{ VPD} \quad (5.2)$$

where T_c is canopy temperature ($^{\circ}\text{C}$), T_a is air temperature ($^{\circ}\text{C}$), $a = 3.38$ $^{\circ}\text{C}$ and $b = -3.25$ $^{\circ}\text{C kPa}^{-1}$, as detailed in Idso (1982 p. 62). While this equation was originally developed for wheat during pre-heading, and our canopy temperature data are for post-heading, using this pre-heading equation matched our data better than a post-heading one. Therefore, we used this curve. Reasons for this disagreement could be due to the fact that our more modern wheats are retaining more green leaf area during post-anthesis than the durum wheat (*Triticum durum*) that Idso (1982) used for his calibration.

CTD_{UL} is the maximum CTD that can be achieved when transpiration is nil. While this cannot be measured experimentally, it can be estimated from equation (5.2) as

$$CTD_{UL} = a + b \text{ VPD}' \quad (5.3)$$

where VPD' is vapour pressure deficit determined with help of parameter a , as in the following equation

$$\text{VPD}' = \text{VP}_{T_a+a} - \text{VP}_{T_a} \quad (5.4)$$

where VP_{T_a+a} is vapour pressure determined at a temperature equal to $T_a + a$, and VP_{T_a} is vapour pressure determined at air temperature. VPD' is therefore only a function of air temperature. The concept of CWSI is represented graphically in Figure 5.2.

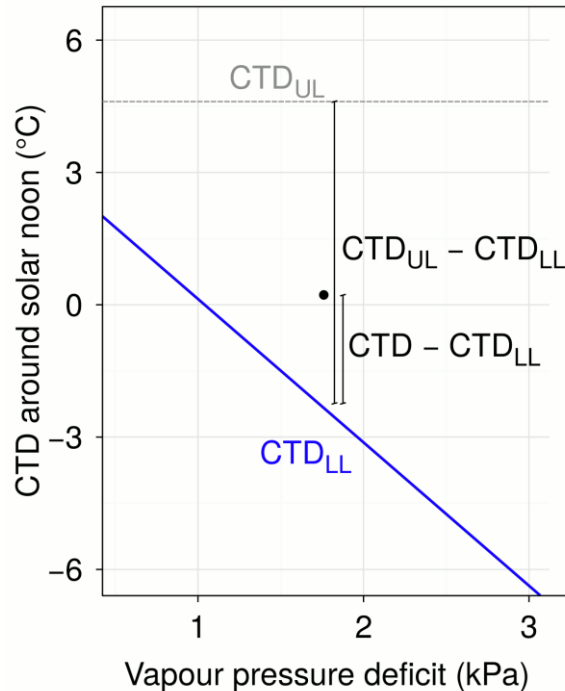


Figure 5.2. Graphical depiction of the concept of crop water-stress index (CWSI) developed by Idso *et al.* (1981) and Idso (1982). The CWSI is a ratio between how far the current CTD of a crop is from the non-water-stressed CTD, and the maximum possible difference in CTD with the non-water-stressed CTD. The current CTD of the crop is exemplified in the graph as a black point. The non-water-stressed CTD (CTD lower limit = CTD_{LL}) is determined by equation (5.2) and is represented by the blue line. The maximum CTD at the current air temperature (CTD upper limit = CTD_{UL}) is the top grey line. The segment representing the distance between CTD and CTD_{LL} is the numerator, and the segment between CTD_{UL} and CTD_{LL} the denominator, of equation (5.1).

5.2.4 Calculating water use and the fraction of plant available water

Water use was determined from the gypsum blocks data, as shown in Chapter 3, where I described how we calibrated the gypsum blocks to read volumetric water content (VWC) of the soil every 2 hours at several soil depths. Then, from the trajectories of VWC over time, we calculated the mean VWC per layer for each day. Because studying the system in one dimension is enough, we calculated the millimetres of water that corresponded to each soil layer by multiplying VWC by the thickness of the soil layer

(200 mm). We established that every negative change in mean VWC (or mm of water) between two successive days equalled root water uptake and soil evaporation (i.e. evapotranspiration = water use). This has the drawback that water use can be confused with internal soil percolation, but as rainfall events were not large (Figure 2.4) we assumed percolation was negligible. Because our measuring time was post-anthesis, it can be assumed that, under full canopy cover, direct soil evaporation would be nil, and water use would be equivalent to transpiration, that is, root water uptake.

The fraction of plant available water (FPAW) was calculated as the ratio between the actual plant available water at a given time (PAW) and the maximum PAW that the soil profile can hold (PAW_{max})

$$FPAW = \frac{PAW}{PAW_{max}} \quad (5.5)$$

Both PAW and PAW_{max} were initially calculated per soil layer and later for the whole soil profile by adding the individual values of every soil layer until a depth corresponding to the maximum rooting depth of the corresponding trial (140 cm in 2013, and 100 cm in 2014). For each individual layer, PAW was estimated as the amount of water held above wilting point. Wilting point was estimated as the VWC when soil water suction is 1500 kPa. Also for every soil layer, PAW_{max} was estimated as the amount of water than can be hold between field capacity and wilting point, where field capacity was estimated as the VWC when soil water suction was 30 kPa. To calculate the VWC at each of those suctions, we used equation (3.3).

5.2.5 Measuring root length density along the soil profile

Root length density was estimated by counting roots by the core-break technique, performing root washing and root scanning (as detailed previously from sections 2.6.2 to 2.6.5).

5.3 Results

5.3.1 Growing conditions

Seasons differed in water availability, as 2014 was drier than 2013 (Figure 2.4). Rainfall was less during spring in 2014 than 2013. Both seasons, however, had more rain than the average season when compared to long term means from 1889 to 2014 (Figure 2.4). Both seasons were similar in terms of thermal regimes (Figure 2.4).

5.3.2 Root length density distributions

Root length densities were greater in soil layers near the surface than deeper in the profile. The maximum depth reached by roots was higher in 2013, probably in response to a wetter spring (Figure 2.4). Variability in root length density was high, and differences between genotypes were not statistically significant in any soil layer (as evidenced by the large standard error bars, Figure 5.3). However, in all three experiments, Gregory had consistently higher mean root length densities below 1 m depth than Derrimut (Figure 5.3).

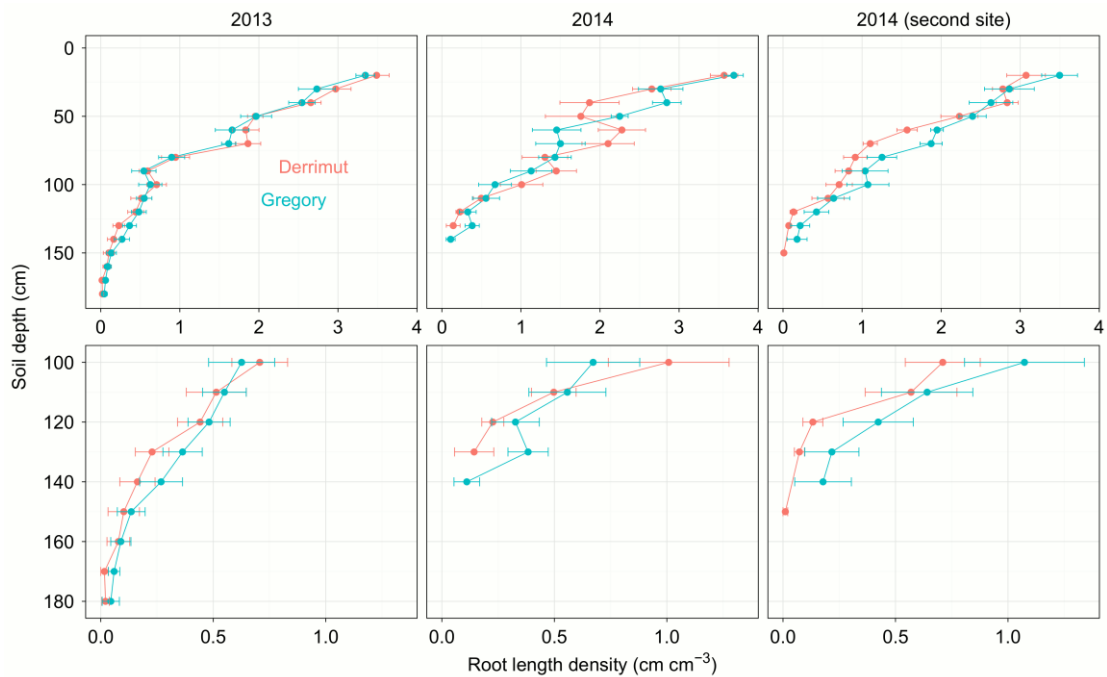


Figure 5.3. Root length density distributed along soil depth for the varieties Derrimut and Gregory during 2013 (left) and 2014 (centre and right). The complete profile is plotted on top, and a subset, at 100 cm and deeper, is plotted at the bottom for better appreciation of small root length density values. Points are means, and horizontal bars are standard errors, of 8 replicates. For data from 2014, an extra site is shown (right). For that extra site only data of root length density is shown in this thesis, since air temperature and soil water characteristics were not measured, making estimations of canopy temperature deviation and soil water content inaccurate.

5.3.3 Canopy temperature and water use

Canopy temperature deviation from air temperature (CTD) around solar noon was consistently more negative for Gregory than Derrimut, for both 2013 and 2014 (Figure 5.4), indicating that Gregory's canopy was cooler than Derrimut's. Before anthesis, CTD around solar noon was closer to negative values than after anthesis. CTD became progressively more positive towards maturity while VPD was increasing. This may have been partly caused by senescence of leaf area, a quantity that we did not measure. Mean CTD around solar noon was similar between both genotypes during a rainfall

event, since rain would have cooled down the foliage to a common temperature—e.g. most evident the 8th, 10th and 11th November 2013, and 15th, 16th and 24th November 2014. When rain was largely absent, as it was for long periods pre- and post-flowering in both years, CTD became more negative as water use per day increased. CTD also responded to VPD, becoming more negative as the latter increased—e.g. between 4th and 6th October, and between 7th and 10th October 2013 (Figure 5.4).



Figure 5.4. Trajectory of canopy temperature deviation from air temperature (CTD) at solar noon \pm 2 hours, during 2013 and 2014 (top); water use per day during 2013 and 2014 (middle); vapour pressure deficit (VPD) at solar noon \pm 2 hours; and rainfall per day during 2013 and

2014 (bottom). Rainfall bars are stacked on top of each other when coinciding between years. Anthesis and physiological maturity dates are indicated, respectively, by a vertical, dashed line the 22nd October and another the 12th December. For CTD and water use, points are the means, and bars the standard errors, of 8 replicates.

Water use per day was greater in many instances for Gregory than Derrimut, both during 2013 and 2014 (Figure 5.4). During 2013, water use per day had two peaks, one at the beginning of booting (Zadoks 40; Zadoks *et al.* (1974)) and another at mid-grain filling (at around Zadoks 80; Zadoks *et al.* (1974)), during the end of November (Figure 5.4). In both peaks water use per day surpassed 4 mm day⁻¹. During 2014, water use per day had one main peak just after anthesis, during the end of October and the start of November. Values were less than during 2013, never reaching 4 mm day⁻¹.

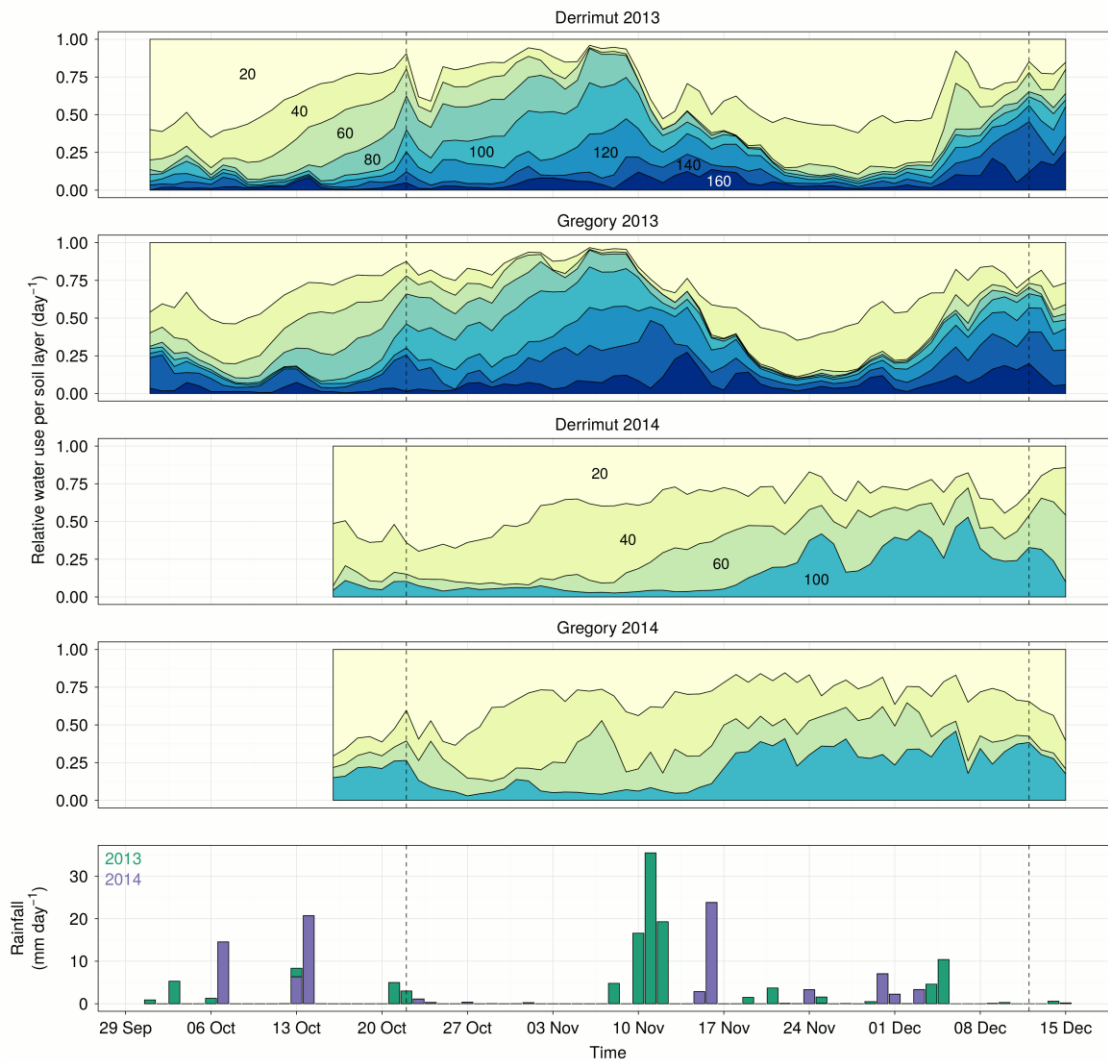


Figure 5.5. Relative water use per soil layer and per day for Derrimut and Gregory during 2013 (top) and 2014 (middle), and rainfall per day (bottom). Water use is relative to the total water use per day, and it is indicated by coloured areas. Numbers inside those areas are their soil depths, in cm. Rainfall bars are stacked on top of each other when coinciding between years. Vertical, dashed lines across panels indicate anthesis (left) and physiological maturity (right) dates as in Figure 5.4. Relative water uses per soil layer are means of 8 replicates.

In addition to typically capturing more water, Gregory used relatively more water from deeper soil layers than Derrimut (Figure 5.5). During 2013, Gregory took up proportionally more water from the 140 and 160 cm layers than Derrimut (Figure 5.5). These results of day after day relative water uptake were confirmed later, when water

use per soil layer was accumulated for the whole grain filling period (Figure 5.6). Accumulated water use in Gregory was greater than Derrimut at depths of 100 and 140 cm ($p < 0.05$, Figure 5.6). Moreover, these data given by gypsum block sensors were supported by data given by neutron probe, which showed a slightly higher (but not statistically significant) water uptake of Gregory between 100 and 140 cm depth (Figure 5.7). During 2014, root water uptake was shallower than 2013 for both varieties, but Gregory, again, had proportionally more water uptake at the deepest, 100 cm, depth than Derrimut (Figure 5.5). Those differences were however non-significant when accumulated during the whole grain-filling period, where mean water use was seemingly larger in Gregory but not statistically significant from Derrimut (Figure 5.6). Unfortunately, we did not use a neutron probe during 2014 that could confirm our lack of differences in accumulated water use estimated from gypsum blocks.

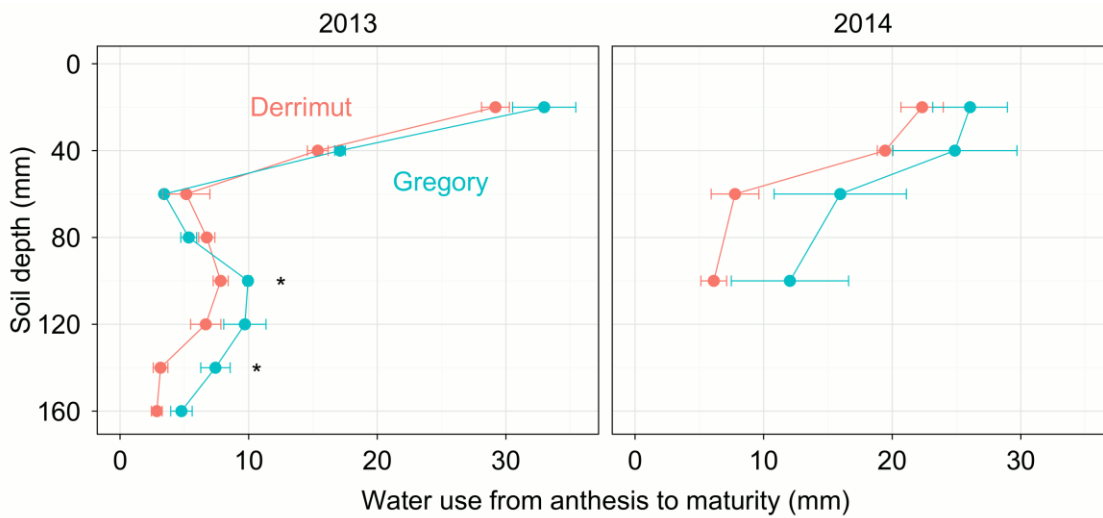


Figure 5.6. Accumulated water use from anthesis to maturity along the soil profile for Derrimut and Gregory during 2013 (left) and 2014 (right). Accumulated water use was determined as the sum of every negative change in volumetric water content ($\text{m}^3 \text{m}^{-3}$) measured by gypsum blocks between two successive days. Points are means, and horizontal bars are standard errors, of 8 replicates. Asterisks at soil depths 100 and 140 during 2013 indicate statistically significant differences ($p < 0.05$). Other soil depths during 2013 and 2014 did not differ statistically.

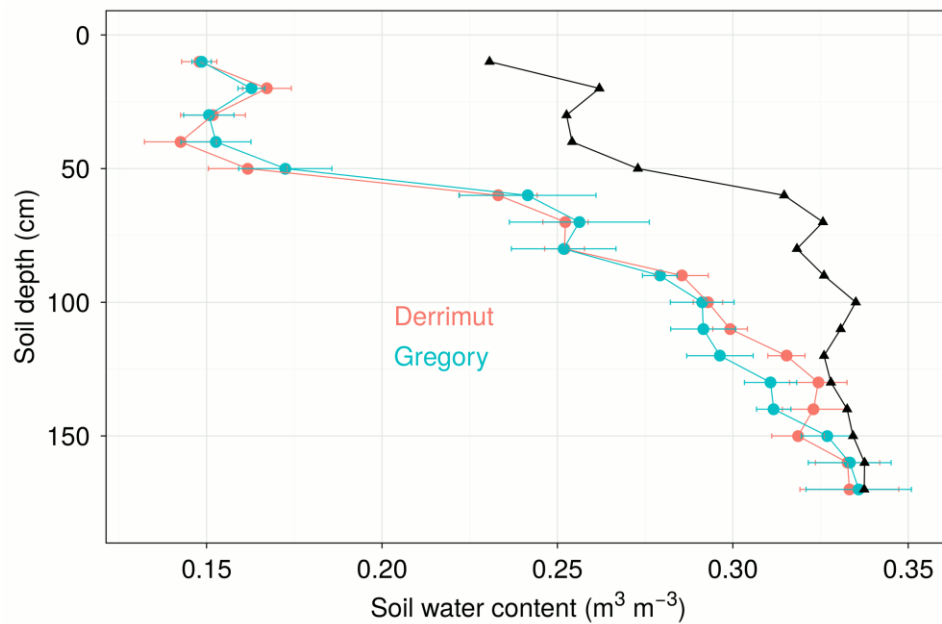


Figure 5.7. Soil water content along the soil profile, at the start of the season (black line and triangles), and at maturity of each genotype (coloured points and lines) measured by neutron probe during 2013. Points are the means, and horizontal bars the standard errors, of 8 replicates in the case of soil water content at maturity. Initial soil water content is a mean of all plots in the trial, as they did not vary appreciably.

5.3.4 Crop water-stress index

Because CTD is affected by VPD, we followed the method of Idso *et al.* (1981) and Idso (1982) for calculating a new variable that normalizes the effects of both air temperature and VPD: the crop water-stress index (CWSI), as explained in section 5.2.3.

When our data of CTD was placed within the framework of Idso (1982), it matched well, as the field data fitted within the lower (CTD_{LL}) and upper limits (CTD_{UL}) (Figure 5.8). This gave reassurance that predicting CTD_{LL} from the model published by Idso (1982 p. 62) was appropriate. There were, however, some values of CTD that were more negative than the CTD_{LL} baseline (Figure 5.8). This could be due to the effect of

variables not included in the calculation of CWSI that can still affect CTD, like wind speed. The upper limit of CTD, the CTD_{UL} , increased as VPD increased, which is an expected output given that both are a direct function of air temperature.

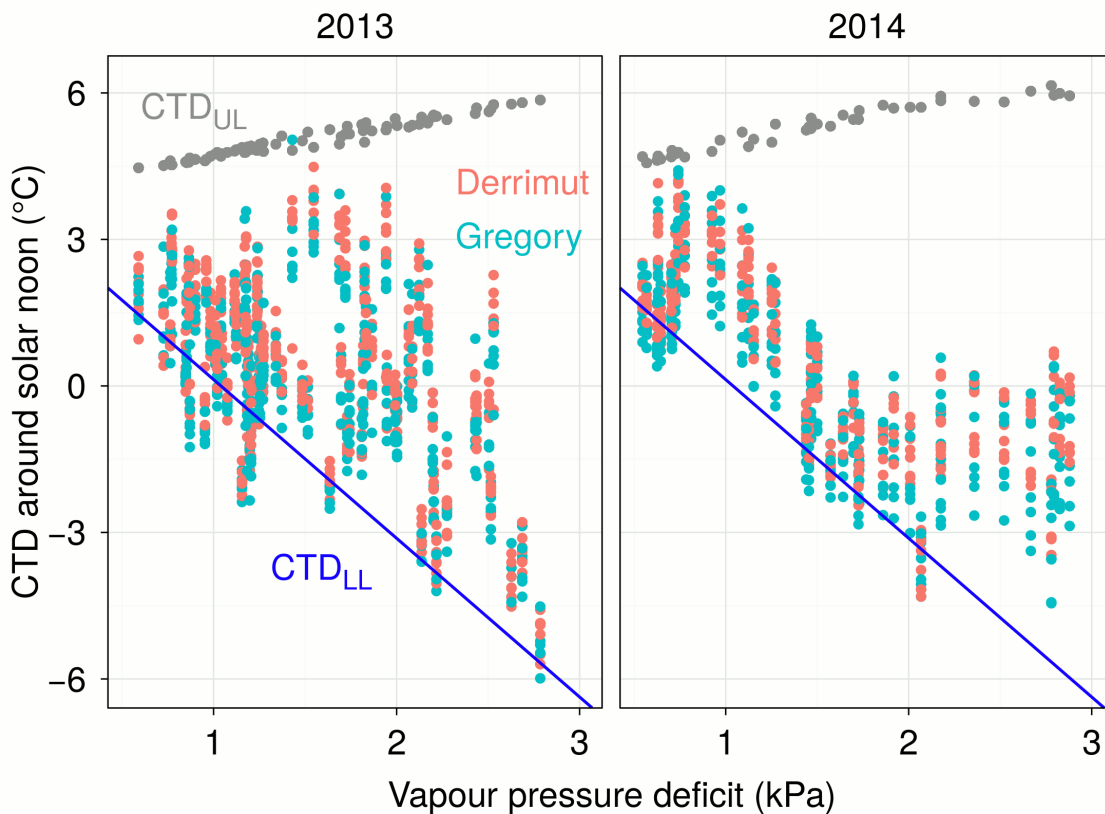


Figure 5.8. Canopy temperature deviation around solar noon (CTD) when fitted within the framework of Idso *et al.* (1981) and Idso (1982) during our experiments in 2013 and 2014. Each individual point is the CTD of each of 8 replicates per genotype, either Derrimut (pale red) or Gregory (pale blue). CTD_{UL} and CTD_{LL} represent, respectively, the CTD upper limit and CTD lower limit as explained in Figure 5.2.

To further analyse how CWSI behaved over time, we compared it with the trajectory of the fraction of plant available water (FPAW) for each genotype and experiment. During 2013, CWSI started from close to zero (no water stress) at the beginning of October. As the soil progressively dried, as shown by FPAW, the CWSI started to rise (Figure 5.9).

The occurrence of rainfall on any given day abruptly reduced the CWSI, as shown, for example, a couple of days before 21st October. The sharp reduction in CWSI during 17th October was caused by cloudiness. It must be noted, however, that CWSI data during a rainfall event or cloudy day is meaningless. The main aim for me to show this data in Figure 5.9 is to verify the occurrence of the reduction of CWSI during rainfall or cloudiness. Then, following with the CWSI data, there are unfortunately missing data from 20th October to 7th November due to malfunction of the infrared thermometers' data loggers—a misfortune considering that it must have been an interesting period to look at CWSI when FPAW was at its lowest and leaf area, presumably, still fully green. When data logging was recovered the 7th November, CWSI reached its maximum value at around 0.7, which matched FPAW being at its minimum level of c. 0.3 during October and November (Figure 5.9). Soon after the 76 mm of rainfall around 11th November, say, the 14th November, the soil profile recovered FPAW to c. 0.6 which corresponded to a reduction in CWSI to values around 0.5. Subsequently, rainfall events during the rest of the growing season were not large enough as to increase FPAW substantially. In part this was due to our inability to determine FPAW in the topsoil, since our shallowest gypsum block was buried at 20 cm from the soil surface. Therefore, these small rainfall events might have reduce the CWSI slightly (for instance, the 20th November) but increases in FPAW were undetected because they happened shallower than 20 cm depth. The same behaviour just described was observed during 2014, where CWSI increased (more water deficit) as FPAW diminished over time. This time the need to determine soil water content shallower than 20 cm was more evident, since, for example, the 27 mm rainfall happening during 15th and 16th

November reduced the CWSI from about 0.7 the 12th November to 0.5 the 18th November, without a substantial increase in FPAW (Figure 5.10).

For both Figure 5.9 and Figure 5.10 it must be clarified that after the middle of the grain filling period—say, from 19th November onwards—the increase in CWSI is most likely caused by leaf senescence, that while reducing transpiration must have increased the amount of net radiation that is partitioned to sensible rather than latent heat, increasing canopy temperature. Unfortunately, we did not measure green leaf area index to validate this assumption.

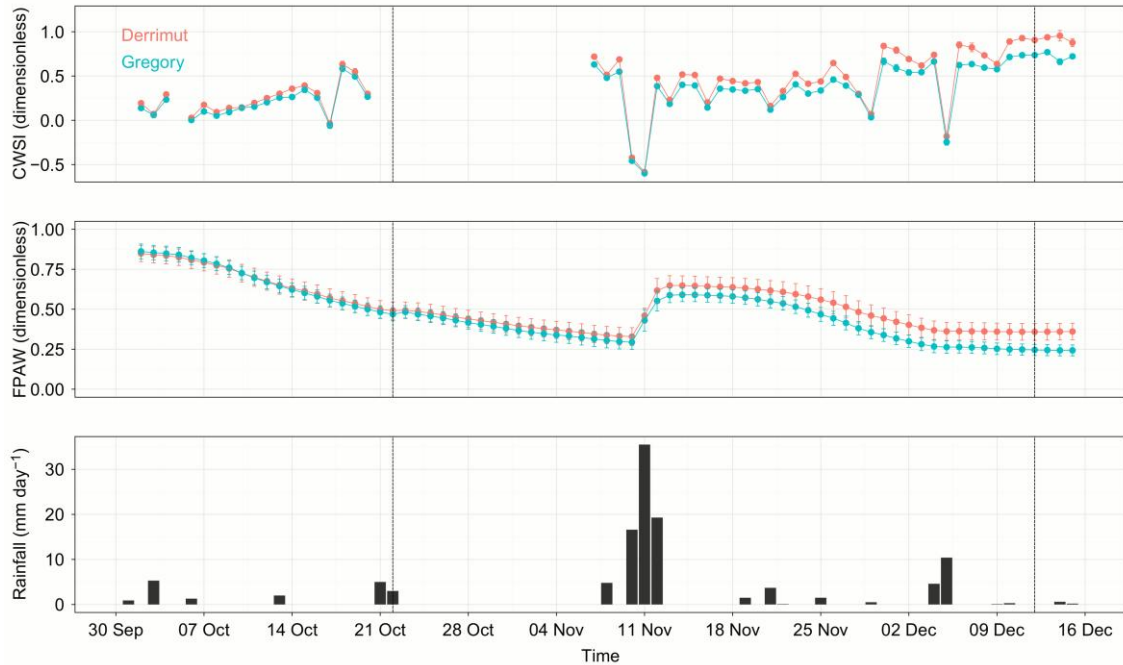


Figure 5.9. Crop water-stress index (CWSI) calculated from canopy temperature (top), fraction of plant available water (FPAW) (middle), and rainfall per day (bottom) across time during 2013. Vertical, dashed lines across panels indicate anthesis (left) and physiological maturity (right) dates as in Figure 5.4. For CWSI and FPAW, points are the means, and bars the standard errors, of 8 replicates. For CWSI, data are missing between 20th October and 7th November due to malfunction of the infrared thermometers' data loggers.

One might now wonder which is a better surrogate of the water status of a crop: CTD or CWSI? To help answering this question we compared CTD and CWSI as functions of FPAW (Figure 5.11). We excluded for this purpose data during periods when crop senescence was high. Without having quantified green leaf area index, we deliberately excluded data after mid grain-filling. It seems from Figure 5.11 that CWSI captures more of the variation in FPAW than CTD alone. Both during 2013 and 2014, the R^2 for the relationships between CWSI and FPAW were higher than the R^2 of the relationships between CTD and FPAW (Figure 5.11). In particular, it is remarkable how, for the relationship of CTD as a function of FPAW during 2013, the data points align when

CTD is replaced by CWSI (Figure 5.11). Not so remarkable as 2013, but also during 2014 the data points align slightly better when the FPAW is expressed as a function of CWSI rather than as a function of CTD. The biggest disagreement in the relationships between CWSI and FPAW seem to happen at high values of FPAW (around 0.8), with positive outliers during 2013 and several possible values of CWSI at the same level of 0.8 FPAW during 2014. This might happen because at this high values of soil available water it is not the soil who limits transpiration but the demand from the atmosphere. Although those likely changes in atmospheric demand for water must impact CWSI, they are certainly independent of soil water status. Thereby, we can observe several possible CWSI at the same level of (non-limiting) FPAW. This value of CWSI should however be lower than 0.8, as the FPAW below which gas exchange is reduced is around 0.4 (Sadras and Milroy 1996). This could be caused by our several sources of uncertainty when using the framework of Idso (1982); namely, uncertainty when calculating CTD_{LL} from a model rather than measuring in a well-watered wheat plot, and uncertainty in soil water content predicted by gypsum blocks.

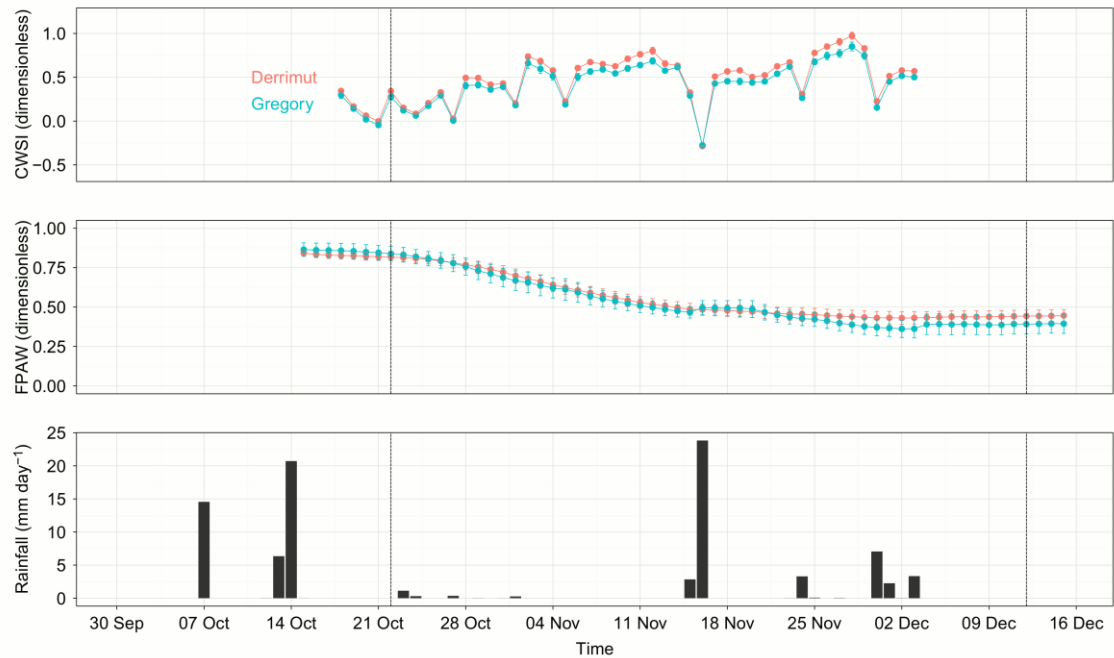


Figure 5.10. Crop water-stress index (CWSI) calculated from canopy temperature (top), fraction of plant available water (FPAW) (middle), and rainfall per day (bottom) across time during 2014. Vertical, dashed lines across panels indicate anthesis (left) and physiological maturity (right) dates as in Figure 5.4. For CWSI and PAW, points are the means, and bars the standard errors, of 8 replicates.

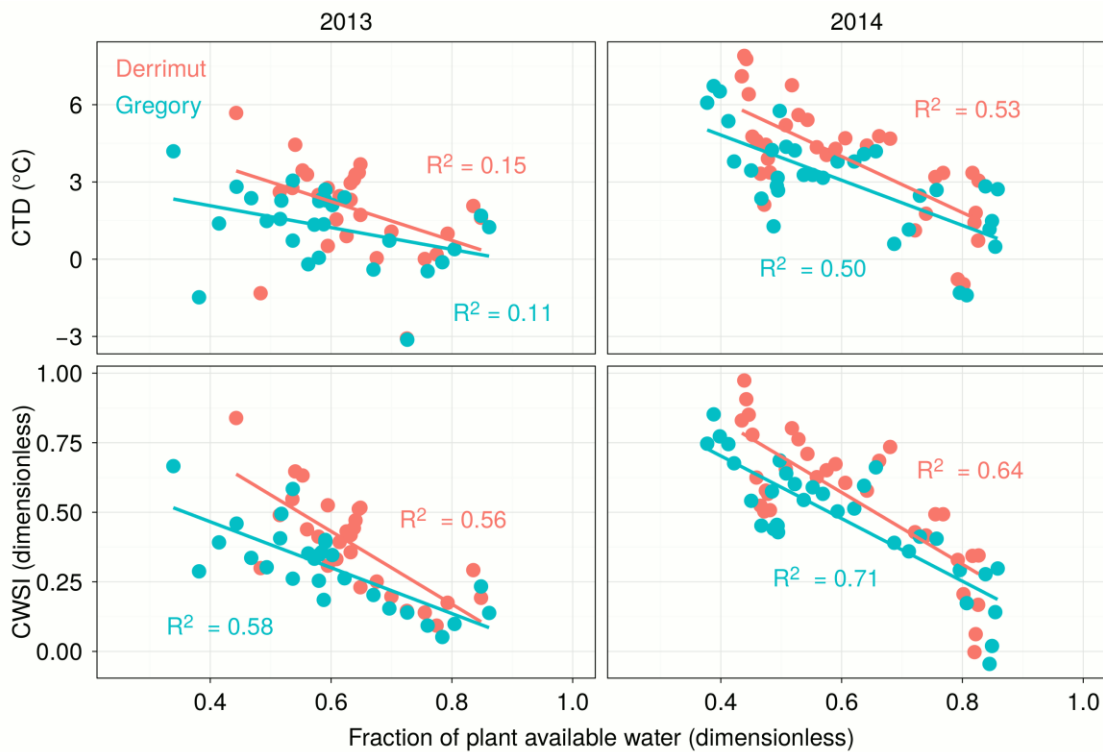


Figure 5.11. A figure showing how crop water-stress index (CWSI) is a better predictor of the fraction of plant available water than the canopy temperature deviation from air temperature (CTD) alone. The figure shows either CTD (top row) or CWSI (bottom row) as a function of the fraction of soil available water (soil water held between suctions from 30 to 1500 kPa) during 2013 (left) or 2014 (right). Each data point is the mean of 8 replicates per genotype, for genotypes Derrimut (pale red) or Gregory (pale blue). R^2 are the r-squared values fitted per genotype per year.

An increase in water use in a given day must reduce the CWSI on that day. To confirm this we analysed how a difference in CWSI from one genotype to the other in any given day impacted on their respective differences in water use on that day. To do that, we took the data shown in Figure 5.11 (i.e. belonging to the first half of the grain-filling period) and calculated each day the difference between the mean CWSI of Gregory and the mean CWSI of Derrimut, and the difference in mean water use per day of Gregory and the mean water use per day of Derrimut. The comparison is shown for both years in Figure 5.12. The differences in CWSI between Gregory and Derrimut did not correlate

with the differences in water use between them (Figure 5.12). This is striking, for a higher water use, which equals transpiration under full canopy cover, must reduce canopy temperature and therefore CWSI. Possibly, again, this is obscured by the large level of uncertainties accumulated after every sequential step when calculating changes in volumetric water content per day from soil water suction values coming from gypsum blocks (Chapter 3). These uncertainties might have greater impact over a rate variable, like water use per day, than over a state variable, like soil water content and therefore FPAW—day to day changes might simply carry proportionally larger errors than soil water content.

Nevertheless, most data fell within the quadrant where Gregory used more water and had cooler canopy than Derrimut. Although there is no correlation, this is interesting because it means that Gregory, the genotype that on average had less CWSI, also had more water use per day (Figure 5.12).

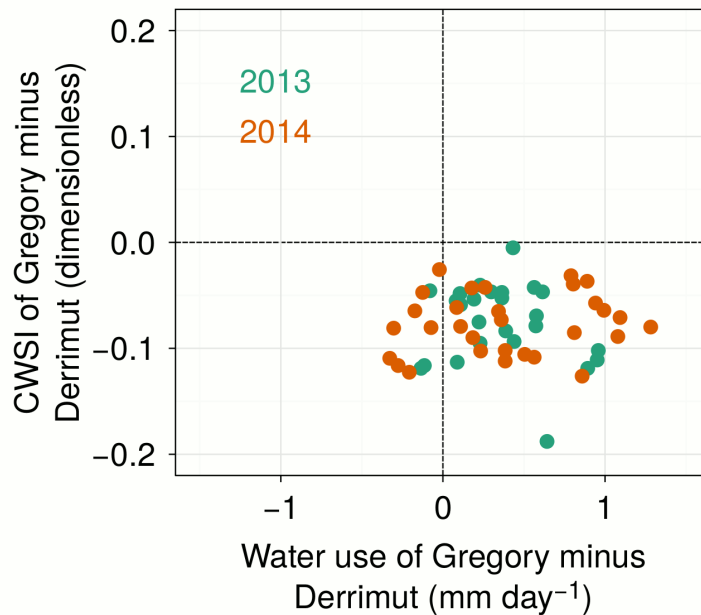


Figure 5.12. Crop water stress index (CWSI) of Gregory minus Derrimut, as a function of water use of Gregory minus Derrimut during 2013 and 2014. Axes are the values of Gregory minus the values of Derrimut—i.e. $CWSI_{Gregory} - CWSI_{Derrimut}$, and $(water\ use\ Gregory) - (water\ use\ Derrimut)$. For instance, a value in the y-axis of -0.1 could mean that the CWSI of Gregory was 0.3 (less water-stressed) while the CWSI of Derrimut was 0.4 (more water-stressed). Correlation between ordinate and abscissa is nil, but data fall within the quadrant of negative difference in CWSI corresponding to positive difference in water use between Gregory and Derrimut—more water use corresponded with less water stress.

5.3.5 Crop growth and water use

Shoot biomass at maturity and grain yield were higher during 2013 than 2014 (Table 5.1). Gregory and Derrimut did not differ statistically in shoot biomass or grain yield, though Gregory tended to produce more biomass ($p = 0.06$, Table 5.1). Moreover, despite the lack of significance in the year \times genotype interaction, the mean biomass and yield from Gregory during 2013 and 2014 were higher than Derrimut (Table 5.1). Therefore, both varieties produced more biomass during 2013 but the ranking between them was maintained in both years: Gregory more than Derrimut. Harvest index was the same within both varieties, and slightly higher during 2014 than 2013 (not significant,

Table 5.1). Interestingly, total water use accumulated between anthesis and maturity was higher during 2013 than 2014 ($p < 0.05$) and higher in Gregory than Derrimut by 11 mm ($p < 0.05$, Table 5.1). Interactions year \times genotype were again non-significant but followed, remarkably, the same ranking as biomass and yield, that is, Gregory 2013 > Derrimut 2013 > Gregory 2014 > Derrimut 2014 (Table 5.1).

Table 5.1. Means of shoot biomass, grain yield, harvest index, and cumulative water use during grain filling, per year (top 3 rows), per genotype (middle 3 rows), and per year \times genotype combination (bottom 5 rows). P values are specific to the rows above them. n.s. indicate comparisons that were not significant.

Year	Genotype	Shoot biomass (t ha ⁻¹)	Grain yield (t ha ⁻¹)	Harvest index (unitless)	Water use grain filling (mm)
2013		16.7	6.8	0.41	82.8
2014		12.1	5.1	0.42	63.3
<i>P value</i>		< 0.0001	< 0.0001	n.s.	< 0.05
	Derrimut	13.0	5.4	0.42	66.6
	Gregory	14.4	5.9	0.41	77.7
<i>P value</i>		0.06	n.s.	n.s.	< 0.05
2013	Derrimut	16.2	6.6	0.41	78.5
	Gregory	17.3	7.1	0.41	88.8
2014	Derrimut	11.4	4.8	0.42	54.8
	Gregory	12.9	5.3	0.41	70.7
<i>P value</i>		n.s.	n.s.	n.s.	n.s.

The consistent ranking in biomass, yield and water use during grain filling for each of the year \times genotype combinations suggest that they correlate with each other, and that Gregory, while having extra deep water use (Figure 5.5 and Figure 5.6), was able to uptake on average an extra 11 mm that translated into almost half a tonne of grain yield

(Table 5.1). Indeed, at a plot to plot level, grain yield was related to water use during grain filling with a slope of $54 \text{ kg ha}^{-1} \text{ mm}^{-1}$ (Figure 5.13).

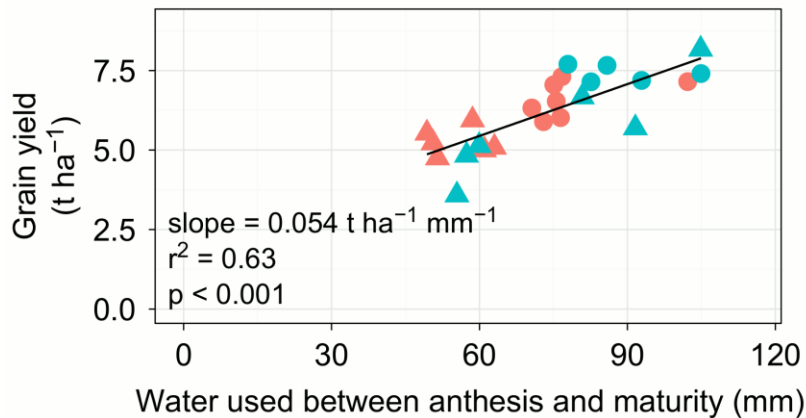


Figure 5.13. Grain yield as a function of water used from anthesis to maturity for the varieties Derrimut and Gregory during 2013 (circles) and 2014 (triangles). Each data point is one replicate. The slope of the regression line, as well as its r-square and p-value, are shown.

5.4 Discussion

Two high yielding commercially grown spring wheat cultivars were chosen in this study. Both are very competitive in the market place as they are high yielding in Australian environments, have very good disease resistance, and have very acceptable grain quality. Previous studies had detected subtle differences in them in that Gregory had a reputation of extracting more soil water.

It was therefore expected that the techniques used in this study would need to be very discriminating in order to detect differences in root systems, water extraction and stomatal behaviour.

Measurements made at maturity on both cultivars for grain yield, above-ground biomass and harvest index were not significant at $p = 0.05$. The yield of Gregory was higher than Derrimut but it just failed at $p = 0.05$. Above-ground biomass of Gregory was also higher. Hence, this study was contrasting two very similar performing cultivars. The finding that Gregory performed slightly better than Derrimut was consistent with all aspects of this study, which measured root growth, canopy temperature and soil water use.

5.4.1 Water use was higher in Gregory than Derrimut, but differences in root length were not demonstrable

Gregory had higher root length densities beneath 1 m than Derrimut, but this could not be shown to be statistically significant. Gregory also had higher water use in deep soil layers than Derrimut (during 2013: $p < 0.05$). While these results are encouraging in the sense that they suggest a correlation between deep roots and deep water use, alternative explanations are possible. For instance, differences in deep water use could be a result of a higher canopy conductance to water vapour in Gregory than Derrimut. Assuming this alternative is true, higher deep water use in Gregory would be a result of a more water-demanding shoot rather than a more efficient root system.

On the other hand, if the reverse is true, that is, if higher deep-water use is a result of higher root length density in those layers in Gregory, then very small differences in root length density must have produced differences in water uptake. The physiologically relevant root length density for wheat has been reported at 0.1 cm cm^{-1} (Kirkegaard *et al.* 2007). There is a degree of randomness in the sampling compounded with variability

in root distribution in response to soil heterogeneity. Thus we cannot conclude with confidence that the root length density values for Gregory fall beneath that threshold at any of depths observed (to 180 cm). The same cannot be said for Derrimut, which does appear to fall below that threshold at 170 cm in 2013 and 150 cm at the second site in 2014 (Figure 5.3).

In response to the greater water use of Gregory, yield increased $54 \text{ kg ha}^{-1} \text{ mm}^{-1}$, similar water-use efficiencies that were estimated by simulation modelling by Manschadi *et al.* (2006) and measured by Kirkegaard *et al.* (2007).

5.4.2 Canopy temperature was cooler in Gregory than Derrimut

Canopy temperature in Gregory was consistently lower than in Derrimut (Figure 5.4). Given that water use was also typically higher in Gregory, this would seem to indicate that, as expected, the canopy temperature result is linked to higher evapotranspiration. However, the two measures did not correlate on a daily basis (discussed below) and the fact that only 2 varieties were evaluated in this study limits our capacity to discern the reasons for cooler canopy temperature. The cooler canopy temperature of Gregory could also be due to other features of the canopy, such as canopy height, as found by Rebetzke *et al.* (2012). Higher canopy height is supposed to reduce the resistance to the removal of sensible heat by the wind. Thus, taller canopies dissipate heat quicker, and this heat may be sensible (not latent) and as such unrelated to water use. Therefore, we cannot assure that higher water use was the cause of a cooler canopy in Gregory than Derrimut. Several genotypes would be needed in order to disentangle the contribution of water use to canopy temperature by phenotyping in the way described in this study. I suggest that

more genotypes should be evaluated together, so that canopy height and other above-ground attributes confounding the relationship between canopy temperature and water-use can be removed.

5.4.3 CWSI was a better surrogate of plant water-status than CTD

Using CWSI rather than CTD, or even more, canopy temperature per se, captured more of the variation in plant available water (Figure 5.11). This happens because vapour pressure deficit is one of the main drivers of transpiration, and by normalizing by it, CWSI becomes an independent variable and has thereby more predictive value than canopy temperature alone.

It is curious why such an easy to calculate variable is not used in breeding programs. Perhaps it is because correct use would require determining the non-stressed baseline of CTD (CTD_{LL}) in a well-watered crop. This is not difficult if we consider that these baselines might be species-specific but not varying between genotypes, as found in maize (Cárcova *et al.* 1998). Once some plots are set up with irrigation, the baseline functions relating CTD_{LL} to VPD can be measured directly, and extrapolated to the whole breeding trial if assuming they are equal in all plots. Then, the variables needed in order to determine CWSI per plot are canopy temperature, air temperature, and air relative humidity.

5.4.4 Daily changes in CWSI did not correlate with water use

Low canopy temperature has been presented as a surrogate for transpiration maintained through access of roots to water deep in the soil profile (Reynolds *et al.* 2007; Lopes

and Reynolds 2010; Pinto and Reynolds 2015). We replaced canopy temperature by CWSI, which showed to be a more robust metric. However, although both canopy temperature deviation (CTD) and CWSI were lower for Gregory, which used more water than Derrimut, day-to-day changes in CWSI did not correlate with day-to-day changes in water use. The reason could have been that the effect of the genotype over water use was not large enough. Or perhaps they were caused by both errors accumulated when calculating CTD_{LL} from a model rather than measuring in a well-watered wheat plot, or the uncertainty in soil water content predicted by gypsum blocks.

Despite CWSI was related to the fraction of plant available water (FPAW), this lack of day-to-day correlation challenges the use of canopy temperature per se for phenotyping wheat with higher water use and, incidentally, deep roots. Further conceptual models are needed that can account for differences in canopy architectures between genotypes. For example, the estimation of latent heat, and consequently evapotranspiration, by heat balance as done by Choudhury *et al.* (1986) and Dunin *et al.* (1991), may be more appropriate for phenotyping than canopy temperature per se. This is because heat balance takes into account the height of the canopy for calculating the aerodynamic resistance of the crop, and as such could potentially normalise the effect of canopy height between Gregory and Derrimut. However, these two studies were done in large field plots covered by a homogeneous wheat crop rather than as we did in the current study, where of 12 m²-plots were arranged in a mosaic. Mixing canopies with different heights in a mosaic may result in unpredictable aerodynamic resistances, and hence highly uncertain estimations of evapotranspiration.

5.4.5 Trial size is more important than continuous monitoring for detecting overall differences between genotypes—but continuous monitoring can reveal genotype interactions with time

One might wonder whether measuring canopy temperature continuously, as we have done with the infrared thermometers fixed to each plot, is more convenient than measuring in discrete times, e.g. 4 to 10 days during the whole season (Rebetzke *et al.* 2012; Pinto and Reynolds 2015). The cost of equipment, time and labour limits the number of sensors that can be applied to plots in a trial, hence limiting the size of the trial. However, once installed, the sensors can provide continuous monitoring of water uptake over an extended period of time (barring data loss as experienced in 2013). Such monitoring can provide information on genotype interactions with time but is limited in its ability to detect genotype differences that are constant over time (genotypes main effects) where the number of genotype replicates becomes more important. In cases where having continuous monitoring of canopy temperature is not crucial, measurements of canopy temperature by means of unmanned aerial vehicles equipped with hyperspectral cameras may allow the sampling of a large number of plots. Sampling many plots within a short period of time is important so that variations in atmospheric conditions are minimised (e.g. VPD and solar radiation), which, as shown in this Chapter can greatly influence canopy temperature.

Obviously, data must be collected over time in order to investigate genotype by time interactions. Data collected over more time points also provides greater residual degrees of freedom for the statistical detection of significant genotype by time

interaction effects—although the improvement in statistical power experiences diminishing returns as the residual degrees of freedom increase.

It should also be noted that observations made on the same plots at different time points may exhibit strongly autocorrelated random behaviour, so that observations on subsequent days do not represent independent observations of the plots over days—this reduces the effective residual degrees of freedom gained from each subsequent days' observations (Greenhouse and Geisser 1959). For our 2014 trial, an autocorrelation of approximately 0.65 was observed between successive days. Observations made over larger time intervals (such as weekly intervals) are likely to be less strongly autocorrelated.

5.4.6 Trial size also remains important for detecting smaller genotype by time interactions overall

For detecting time-independent differences between genotypes (genotype main effects), observations made over time have limited impact in improving accuracy compared to trial size. In the relevant repeated measures analysis of variance of the data, the significance of a genotype main effect is tested against the observed variance of the replicated plots. Under the assumption of no autocorrelation between time points, the observed variance is given by $\sigma_p^2 + \sigma^2/n$, where σ_p^2 is the true plot-to-plot variance (the 'plot variance component'), and σ^2/n is the contribution to the observed variance from the random variation (of variance σ^2) between n time points observed within plots.

Collecting data from more time points (increasing n) will only reduce the second term above—the variance σ_p^2 remains constant. The benefit to collecting more time points is therefore limited by the relative sizes of σ_p^2 and σ^2 . As previously, the presence of autocorrelated random behaviour will further reduce the improvement in accuracy (via reduction of σ^2/n) obtained from each subsequent time point observed. In our 2014 dataset we observed no increase in the estimated standard error of the difference between Gregory and Derrimut as we included more days of data into our analysis.

5.5 Conclusions

In summary, we showed that two high-yielding commercial wheat varieties seemed to differ in deep root length, and had different canopy temperatures. Using a crop water-stress index (CWSI), rather than canopy temperature per se or canopy temperature deviation from air temperature, gave better predictions of plant water-status—at least concerning the amount of plant available water present along the soil profile. The CWSI of the variety with deep roots, Gregory, was lower than the one with shallower roots, Derrimut. Gregory also used more water, but the difference in water use per day between both varieties did not correlate with their difference in canopy temperature. Extra water use in Gregory came from deeper in the soil, and was used during grain filling to grow more grain at a rate of $54 \text{ kg ha}^{-1} \text{ mm}^{-1}$. When compared to average values of transpiration efficiency from sowing to maturity (c. $24 \text{ kg ha}^{-1} \text{ mm}^{-1}$), the yield produced per unit of water used during grain filling is doubled. This indicates that deep

roots can be detected by CWSI and can increase yield by taking advantage of water during grain filling when it is most efficiently used.

Chapter 6 General discussion and implications for crop improvement

6.1 Overview of the thesis

The genetic improvement in rooting depth is a major challenge to the on-going effort to improve the yield of crops, particularly those grown in water-limited conditions. The selection for root system traits, especially deep roots, remains challenging because of the difficulties involved in root sampling in field conditions. We also know very little about what to select for when it comes to root systems and how to select for them. In an attempt to help in the solution of these problems, this study aimed to determine whether genetic diversity in rooting depth at maturity existed between wheat and triticale genotypes growing in field conditions. We found that genotypes differed in rooting depth ($p < 0.10$). Differences were larger, however, between species (triticale and wheat) than within a species (wheat). Within a population of wheat genotypes that express a gradient of plant heights, genotypes differed in rooting depth ($p < 0.10$), biomass ($p < 0.10$) and yield ($p < 0.05$). Interestingly, the shorter the plants, the deeper the roots and higher the yield, which suggest that a shift in carbon partitioning from stems towards grain and roots had happened.

These differences in rooting depth, while encouraging, were obtained by soil coring, a very time-consuming process that is difficult to adopt in breeding programs. Thus, our second aim was to investigate whether canopy temperature can be used as a surrogate of

transpiration, and thereby as a predictor of deep water use. Canopy temperature would then be used to select wheat genotypes with deep roots. For this, we compared canopy temperature and water use between Gregory, a wheat with tentatively deeper roots, and Derrimut, a wheat with shallower roots. Both varieties are high-yielding commercial wheats sown in Australia. Canopy temperature reflects an energy balance where many factors are involved, so we calculated a water-stress index that normalized for the main factors affecting the relationship between canopy temperature and transpiration: air temperature and vapour pressure deficit. We found that genotypes did not differ in rooting depth or deep root length, but mean values of these root traits were higher in Gregory than Derrimut in three independent experiments. Indeed, Gregory had deeper water use ($p < 0.05$) and more total water use during grain filling ($p < 0.05$) than Derrimut, and it also had a cooler canopy during that period which corresponded to a lower crop water-stress index. Finally, the crop-water stress index correlated closely with the amount of soil available water, confirming that this index calculated from canopy temperature could be used to select wheat with deeper water use.

In the following sections I will outline the main results of the thesis, (i) highlighting the importance of deep roots for wheat yield, (ii) listing ways in which breeding can increase rooting depth, and (iii) proposing future work that would be interesting to undertake following this thesis.

6.2 The benefits of deeper roots to wheat growth and yield

One of the most significant findings to emerge from this thesis is that rooting depth differed between wheat and triticale genotypes growing in field conditions ($p < 0.10$).

To my knowledge, there are no studies reporting genotypic differences in rooting depth other than this thesis and the study by Wasson *et al.* (2014). Botwright Acuña and Wade (2012) evaluated rooting depth in the field in 24 wheat cultivars growing at 6 locations in Western Australia. They found that the sum of squares given by genotype \times environment interactions was more than 3 times larger than the sum of squares given by genotype, but the latter was not statistically significant. Others have suggested differences in rooting depth and deep root length by inferring them from water use deep in the soil. For instance, Pask and Reynolds (2013) measured water uptake by roots at several soil depths under non-limiting moisture conditions in a set of wheat varieties released between 1950 to 2009. They found that modern wheat varieties take up more water from deep soil than older varieties. There was an increase in water uptake between 60 and 120 cm, but most markedly between 90 and 120 cm. Interestingly, this increase by means of breeding was responsible for gains in yield potential (that is, yield only limited by radiation and temperature, not water or nutrients). However, despite their results being encouraging, these authors measured neither root length density nor rooting depth, as we did in this thesis. Although they suggest that deeper water use was caused by more root length at depth, deeper water use can also be due to an inherently higher stomatal conductance in the modern varieties. In the US corn-belt, Hammer *et al.* (2009) suggested that rooting depth in maize was changed by breeding, although this was not measured directly but rather it was inferred by simulation modelling. The results of this thesis are one of the few showing rooting depth differences among genotypes in the field.

What is also interesting is that those differences in rooting depth and deep root length correlated with shoot biomass and grain yield. Now, it is true that the main source of variation in the data in Figure 4.3 was soil type and the amount of rainfall in each season, with less variation due to genotype. But as shown in Figure 4.4, there was one experiment where shoot biomass, grain yield and even harvest index increased as the root length below 120 cm increased. Interestingly, this experiment was carried out during 2012, when soil available water was not apparently limiting. Pask and Reynolds (2013) also found that biomass and yield correlated with greater water use between 90 and 120 cm depth, and Lopes and Reynolds (2010) found that biomass of deep roots was related to the amount of residual water left at maturity—the greater the amount of deep-root biomass the lesser the amount of residual soil water. Although Pask and Reynolds (2013) and Lopes and Reynolds (2010) did not measure root length density, their results, and the results of this study, highlight the importance of deep water use even in conditions of mild water deficit.

Another interesting finding of this thesis is that, by having deeper roots, genotypes increased total water use during the season, and yield at with a high efficiency (Chapter 5). Though one must be cautious given that this is inferred from two experiments where only two genotypes were evaluated, the results imply that having deep roots is highly valuable in terms of water economy for wheat. The rate of grain yield per unit of water used during grain filling was $54 \text{ kg ha}^{-1} \text{ mm}^{-1}$, more than double the usual $22 \text{ kg ha}^{-1} \text{ mm}^{-1}$ reported for the whole duration of the growing season (French and Schultz, 1984; updated to $24 \text{ kg ha}^{-1} \text{ mm}^{-1}$ by Sadras and Lawson, 2013). This result of higher water-use efficiency during grain filling is similar to results published by Manschadi *et al.*

(2006) and Kirkegaard *et al.* (2007). The fact that water-use efficiency to produce grain is higher during grain filling can be explained by the fact that (i) during that period it is mostly grains that are growing (no vegetative organs), and (ii), as shown by Borrás *et al.* (2004), crops in general (though maize more so than wheat) respond markedly to improvements in growing conditions during grain filling if assimilates for grain growth are limiting. This is because the potential capacity for grain growth is set early in grain filling, so a crop that established a high potential grain size early would respond significantly to alleviations of stresses later during grain filling (Borrás *et al.* 2004).

The current study also suggests that the benefits of deep roots are not exclusive to conditions where drought prevails during early reproductive development or late grain filling (terminal drought). On the contrary, they are still meaningful in an environment with mild or no water stress. This was shown by the range of yields covered in Chapter 4 and 5 (from ~ 3 to 8 t ha⁻¹). But this can be seen particularly in the case of experiment 3, where biomass, yield and harvest index responded to root length density under 120 cm depth while yields ranged between 5 and 8 t ha⁻¹. That yield increases with deeper roots or deeper water use is consistent with the results of Pask and Reynolds (2013).

6.3 Ways of improving root depth by breeding

A key strength of the present thesis was the finding that rooting depth can vary with germplasm. It was usually documented in controlled conditions (Manschadi *et al.* 2006, 2008), but there are a few cases where rooting depth is measured and found to differ between genotypes under field conditions.

A question that emerges is how can breeding increase rooting depth. A reasonable approach to tackle this issue would be to focus on the traits that allowed for greater root growth. Examples of traits to which we engaged in this thesis, as mentioned in Chapter 1, are (i) early vigour, (ii) reduced tillering, (iii) reduced height, as well as, (iv) deeper rooting directly. To tackle these traits and their effects on root growth, we could first classify the genotypic differences that we found in this thesis as interspecific, i.e. between different species (triticale and wheat), or intraspecific, i.e. between genotypes of the same species (wheat differing in height). The distinction is important because to breed wheat by introgressing genes from a different species is far more difficult than introgressing from another wheat genotype.

Concerning interspecific differences, triticale produced deeper roots, more biomass and higher yield than wheat ($p < 0.10$). These results are interesting because they confirm the higher resilience of triticale to drought found by Giunta *et al.* (1993) and Condon (personal communication). However, the application of this knowledge to wheat breeding might be limited considering that introgressing genes from triticale to wheat may prove a challenge. But as proposed in the preceding paragraph, one could better investigate what is the trait that enabled triticale to have such a great advantage in terms of root and shoot growth than wheat. The most evident one seems to be the fact that triticale is just more vigorous early in seedling development, and later those differences accumulate towards a mature plant, which result eventually in higher shoot growth than wheat. Apparently, that above-ground vigour is mirrored by high vigour in the roots as well. If this is the case, then this challenge of increasing early vigour in wheat was already undertaken by Rebetzke and Richards (1999).

Concerning our intraspecific differences, we found that, for wheats differing in height, shorter stems were related with deeper root growth and more yield. It seems, therefore, that alleviating the competition for assimilates between stems and roots increased rooting depth. Taken together, these findings support the concept of the ideotypes and communal plants that was originally drawn by Donald (1968). This is interesting since the change in roots during the Green Revolution is not known. In young wheat seedlings, Wojciechowski *et al.* (2009) showed that *Rht* genes had an effect on root growth without an effect in shoot growth, suggesting that the effect of *Rht* genes on roots is direct. Richards (1992) and Miralles *et al.* (1997), on the other hand, suggested that the effect of these genes was not direct but rather secondary, i.e. by reducing shoot growth more assimilate was available for root growth. In accordance with Richards (1992) and Miralles *et al.* (1997), shoot biomass was reduced as plant height decreased. Miralles *et al.* (1997) also found that, while plant height was reduced, total root length and root dry weight were increased. They suggested that this was due to a surplus of assimilates without a sink to utilise them. Miralles *et al.* (1997) found no difference in root length but rather in root dry weight, that they propose is a result of roots thickening but not elongating. Returning to the results of this thesis, however, these data related to the increase in rooting depth as plant height increased must be interpreted with caution because regressions in Figure 4.5 were only significant if considering $p < 0.10$.

Reduced tillering has been proposed as a way of increasing yield when crops rely on stored soil moisture (Hendriks *et al.* 2015). In this thesis, however, we were unable to detect differences in root growth, shoot biomass or yield between isogenic lines for the *tin* gene. Perhaps this was because our crops had more available water in-season. The

main advantage of *tin* genes in wheat seems to be in crops that rely on in-season rainfall. In this context, while leaf area expansion is reduced in *tin* isogenic lines, so too was the relative amount of rainfall lost by direct evaporation. This trait would be detrimental in the opposite growing conditions, when crops rely heavily in stored soil moisture. Under these conditions, faster leaf area expansion would lead to a greater transpiration before anthesis and a consequent reduction of the amount of water available for grain filling. This in turn would reduce harvest index and grain yield (Passioura 1976). In our conditions, crops did not experience terminal drought during 2011 and 2012, and therefore *tin* lines provided no advantage over lines without *tin*.

Liao *et al.* (2006) found that vigorous lines produced more roots from 20 to 70 cm depth in glass-walled pots, with no differences in rooting depth. Watt *et al.* (2005) found faster root growth in the more vigorous line V18 than the non-vigorous genotype Janz, when sampled at 2 and 5 fully expanded leaf stages. However, the differences declined towards anthesis and maturity (Watt *et al.* 2013). Therefore, early vigour might be beneficial in the same sense as reduced tillering: increasing the fraction of total evapotranspiration that is transpired and reducing direct soil evaporation in environments where wheat relies on in-season rainfall (Palta *et al.* 2011). In a field study during two seasons, Botwright Acuña *et al.* (2002) documented that early vigour increased yield by c. 12% in the wetter year, but there were no effects in the drier year. In a simulation study evaluating increased early vigour by means of increasing specific leaf area (SLA, $\text{cm}^2 \text{g}^{-1}$) in APSIM-Nwheat, Asseng *et al.* (2003) found that increased SLA only increased yields in sandy soils, adding to the notion that early vigour might augment transpiration while reducing direct evaporation from the soil. Therefore, the

contribution of early vigour to greater rooting depth and deep water uptake is uncertain from the start.

Another trait that might increase the potential of wheat to access deep water is the capacity of the root system to penetrate hardpans. Botwright Acuña and Wade (2005) tested in soil columns the ability of wheat roots from several genotypes to penetrate thin wax layers. These wax layers were used to simulate soil hardness. They found genotypic differences in the capacity of roots to grow through the wax layers. Moreover, Botwright Acuña *et al.* (2007) showed that those genotypes with more root length passing through the wax layers were the same genotypes exhibiting the highest rooting depths in the field. This indicates that in some environments the ability of some genotypes to grow roots through soil layers with high mechanical impedance can improve rooting depth and possibly deep water use.

It is important to mention, however, that it is worth defining the target environment where the trait would be of any advantage for grain yield, for it would be useless if it could improve deep root growth but have a detrimental effect over yield. This is provided by a pivotal analysis done by Chenu *et al.* (2013) for wheat grown in the whole Australian wheat-belt. Chenu *et al.* (2013) divided the whole area of the Australian wheat-belt into four environmental types. This is interesting because the environments, rather than being defined solely by their climate and soil conditions, are defined from 'the point of view of a crop facing drought'. This 'point of view' is defined as an index of supply over demand, where supply is calculated as the amount of available water within the rooting depth, and demand is calculated from crop growth rate and the transpiration efficiency (which is species-dependent and normalized by

vapour pressure deficit [the higher the vapour pressure deficit the lower the transpiration efficiency]). The analysis is summarized in Figure 6.1, where, based on the most common patterns of source-demand ratio along the development of the crop (with a centre at anthesis), they defined the four environment types. Those environments were:

- environment 1: no or light stress;
- environment 2: post-flowering mild stress;
- environment 3: stresses that began before flowering but were relieved during grain filling; and
- environment 4: severe stresses that began during the vegetative period and lasted until maturity.

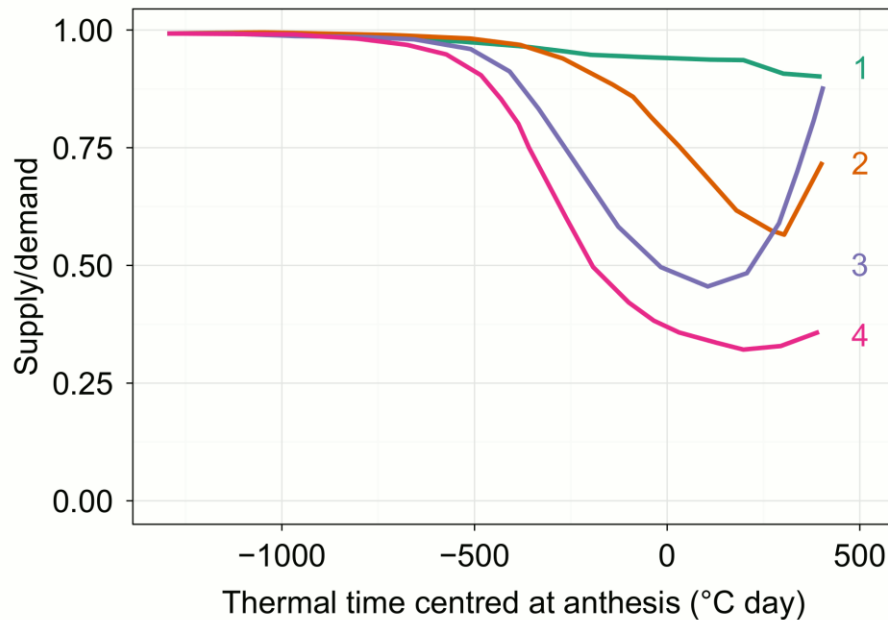


Figure 6.1. Simulated water supply-demand ratio for four environment types that typify the most common water balances for wheat across the Australian wheat-belt as a function of thermal time accumulated from anthesis (base temperature = 0 °C). Numbers indicate 4 possible environment types: environment 1: no or light stress; environment 2: post-flowering mild stress; environment 3: stresses that began before flowering but were relieved during grain filling; and environment 4: severe stresses that began during the vegetative period and lasted until maturity. Redrawn from Chenu *et al.* (2013 fig. 5).

Depending on the environment type where a putative wheat genotype expressing the trait under consideration is grown, the effect on yield will be positive or negative. For instance, a genotype with increased early vigour would only suit environment 1, where a faster leaf area expansion early in the season would minimize water wasted by direct soil evaporation. In this environment, continuous (and perhaps small) rainfall events would guarantee access to water in shallow soil layers with little risk of running out of water for late grain filling. The opposite could be expected for a *tin* wheat genotype with reduced tillering, where limited tillers early in the season would slow down the increase in leaf area index and increase direct soil evaporation. However, in the later

part of the season, there would be more soil water to spend during the reproductive period. A reduced tillering genotype would take advantage of environments 2, 3 and 4. Similarly, a genotype possessing deep roots would be advantageous in these three environment types.

Finally, if traits are genetically independent from each other (i.e. there is no linkage between chromosome regions on which they depend) then they could in principle be combined in the same plant, they can be pyramided (Wilson *et al.* 2015). Therefore, ideotypes can be targeted for each environment type: presence of in-season rainfall (environment 1) = high early vigour, rapid canopy closure, vigorous shallow roots; reliance on stored soil water (environments 2, 3, 4) = reduced tillering, high carbon isotope discrimination (i.e. high transpiration efficiency), and deep roots.

6.4 Phenotyping for deep roots

Continuously measuring canopy temperature proved useful, for it enabled us to calculate the crop water stress index (CWSI) over time and predict soil water availability. In other studies canopy temperature has been measured, roughly, every 3-10 days by operators with hand-held infrared thermometers (Lopes and Reynolds 2010; Rebetzke *et al.* 2012; Pinto and Reynolds 2015). By measuring canopy temperature continuously, we were able to select days when canopy temperature is more representative of transpiration, like clear days with low wind speed. While this can be done by sampling weekly and choosing days with those qualities, investing in devices that allow for continuous sampling could guarantee more days of sampling and perhaps less cost. Moreover, it is somewhat surprising that CWSI is not so widespread in canopy

temperature studies. It would be easy to incorporate CWSI as a selection criteria rather than canopy temperature or canopy-air temperature deviation. All that is required is to know relative humidity of the air, which can be easily obtained.

We found that cool canopy temperature and a low CWSI were related to higher water use which in turn was directly related to grain yield. However, caution is needed in interpreting these results, given that we only evaluated two genotypes. Although other interesting studies have evaluated just two varieties (e.g. Condon *et al.* (2002)), other factors that differed between those two varieties like biomass or plant height (Rebetzke *et al.* 2012) could influence their canopy temperature and its relationship to transpiration. It is crucial to compare genotypes with similar time to flowering, since differences in flowering time would put green leaf area indices out of phase between varieties, some senescing earlier, and some senescing later. Matching green leaf areas would help to eliminate the possible effects of a diminishing leaf area index on transpiration due to senescence. In Condon *et al.* (2002) both time to flowering and plant height were equal between the two genotypes evaluated, Quarrion and Matong. In our study, Derrimut and Gregory differed in plant height, the latter being 20 cm taller. Moreover, these genotypes were some of the top yielding varieties in Australia, and therefore few differences were expected between them. It is suggested that more genotypes should be evaluated together to test whether CWSI offers potential as a predictor of water use and deep root length.

Gypsum blocks were not accurate for determining volumetric soil water content, but they could be employed for phenotyping soil water suction. If one intends to measure water use precisely to relate to canopy temperature or CWSI, the best alternative would

be to use lysimeters. However, this is impractical for selecting between hundreds of genotypes within a breeding program. Therefore, gypsum blocks, in spite of being inaccurate compared with lysimeters, can predict soil water use for many plots, and be used for phenotyping wheat. Errors can be reduced by sowing trials in homogeneous paddocks, or avoiding the need of calculating volumetric water content by just looking at the changes of soil water suction as a way of detecting genotypes with access to deep water. The limits for soil water suction within which plants can take up water was within the measurement range of the gypsum blocks. Gypsum blocks could not reach soil water suctions close to 30 kPa, as is usually assumed for field capacity, but they predicted well between 50 kPa and close to wilting point, at 1500 kPa.

6.5 Future research

6.5.1 Automation of soil coring

One of the questions raised by this thesis is whether sampling roots by soil coring is worthwhile if practiced in the way we did. This involved counting roots by a naked eye and several operators. The fact that root length density was so variable after so much time-consuming sampling might indicate that this is not the best way to phenotype root systems. How roots spread along the soil volume is erratic, as it is strongly influenced by local changes in soil hardness, moisture, and nutrients. But another part of the variation is strictly experimental error when sampling. It could be possible to drastically reduce that experimental error by removing human error by using automated ways of counting. A fluorescence imaging system with root counting software has been

developed for this purpose (Wasson, personal communication). This is promising since the errors in root counting and root length density determination could be reduced and the sampling made more cost effective by reducing the labour requirements.

6.5.2 Measuring root function without measuring roots

Sampling roots is both time consuming and the parameter values are variable. One could be radical and avoid sampling roots altogether. Instead, we could measure root activity rather than roots *per se*. This concept is based on the approach of the pioneer crop modellers De Wit and Penning de Vries (De Wit and Penning de Vries 1983), who proposed 'modelling plant hormone action without modelling the hormones' (Hammer *et al.* 2004). By following these criteria, we could measure root water uptake (i.e. root function) without measuring root length density, inferring, indirectly, root presence from root function.

This was done successfully by Dardanelli *et al.* (1997), who used a model developed by Passioura (1983) to formalise root water uptake from a given soil layer in the same fashion as a soil dries

$$\theta_t = \theta_a e^{-kl(t-t_c)} \quad (6.1)$$

and therefore

$$\log \theta_t = \log \theta_a - kl(t - t_c) \quad (6.2)$$

where θ_t is available soil water content over the wilting point ($\text{m}^3 \text{m}^{-3}$) at any given time t (days); θ_a is soil available water content at the start of soil water extraction ($\text{m}^3 \text{m}^{-3}$); t_c is the threshold time at which water extraction starts; $(t - t_c)$ is time since the

beginning of water extraction; l is root length density (cm cm^{-3}); and k is a parameter with the dimensions of soil water diffusivity ($\text{cm}^2 \text{d}^{-1}$) but actually summarizes an apparent diffusivity of the root-soil combined. It must be noted that, in spite of this parameter k having the same dimensions as soil water diffusivity, it is not soil water diffusivity, which is in turn orders of magnitude larger than k (Deery 2008; Deery *et al.* 2012).

In this way, kl summarizes the capacity of the root system to capture water in a given soil layer per day. It is the maximum water uptake that can be achieved in one day, and is a time constant, or in other words a kl of 0.10 d^{-1} means that today's water uptake is 10% of soil water left in the soil since yesterday, and tomorrow it will be the 10% of what is left after in the soil today. It decays exponentially. The parameter kl is indeed applied by the widely used simulation model Apsim-Nwheat to simulate root water uptake (Keating *et al.* 2001).

The process is shown in Figure 6.2, where it can be seen on the left panel how kl is calculated per soil depth, and on the right panel how kl distributes along the soil profile. What Dardanelli *et al.* (1997) found is that a sunflower commercial hybrid called Contiflor 3 had consistently higher kl than another hybrid called G100. This means that the former hybrid had a root system able to capture more water than the latter, although, because of the inherent properties of the method, it could not be disentangled whether this was due to more root length density or more root hydraulic conductivity.

For kl to be the maximum possible water uptake per day it is necessary that the demand of water by the atmosphere is always greater than the capacity of the soil, interacting

with the roots, to supply it. This was discussed in Chapter 1 where the concept from Cowan (1965) was presented, in which transpiration will be equal to the supply or equal to the demand, whichever is smaller. In other words, the only way of isolating the capacity of roots and soil to provide water for transpiration is by guaranteeing that demand is always larger than supply. This is a drawback because it means that this study needs to be done either under a rain-out shelter or in arid environments.

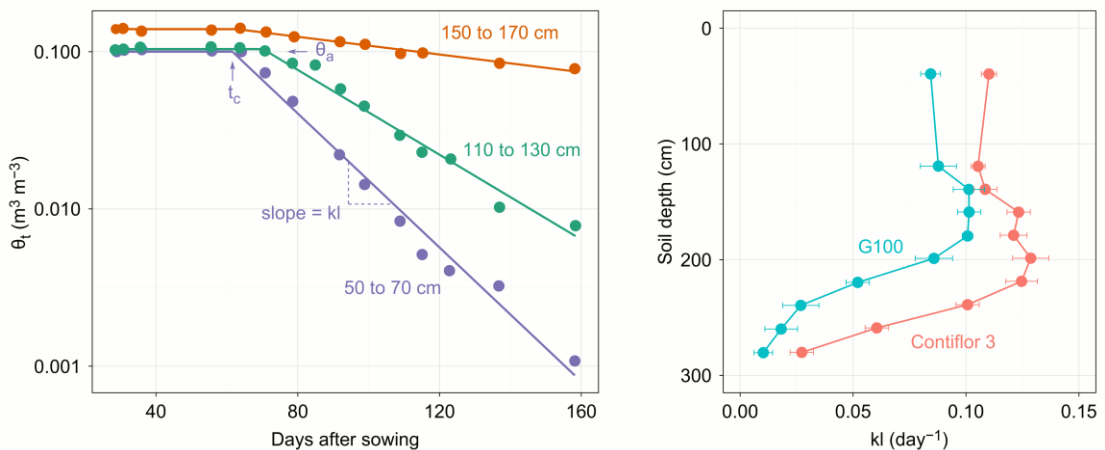


Figure 6.2. Depiction of the method for determining the maximum water uptake per day per soil layer (kl). On the left, the graph shows the available soil water content at a given time t (θ_t) as a function of time since sowing for three soil depths. The parameters of equations (6.1) and (6.2) are indicated as well. On the right, the kl calculated as in the graph in the left are plotted along soil depth for two sunflower hybrids. Bars are standard errors. It must be noted that the data on the left is peanut and therefore does not relate to the data on the right; it only serves as an example. The figure was redrawn from Dardanelli *et al.* (1997).

The rewards may make this technique worthwhile, since, to my knowledge, Dardanelli *et al.* (1997) represents the only study carried out in field conditions where differences in root capacity to capture water were detected between genotypes.

6.5.3 Enhanced root vertical distribution, trade-off-free opportunities and root self/non-self recognition

As previously discussed, a shift of root biomass allocation from shallow to deep soil layers could be more effective for capturing soil water while minimizing the expenditure of assimilates in extra root growth. This shift might already have happened in maize hybrids progressively released in the US corn-belt (Hammer *et al.* 2009).

As suggested by Denison (2012, 2015), breeding should tackle trade-off-free opportunities, i.e. opportunities that were rejected by past natural selection because they were detrimental to individual plants, but are nowadays favourable to agriculture because they benefit the plant population forming a crop as a whole.

Perhaps the key to shifting root growth to deep soil is to investigate into how root tips perceive other root tips: as self or non-self? Self roots would not compete with each other because they would reduce the fitness of their mother plant and the genes causing it, being completely shared by both roots, would be eradicated by natural selection.

Non-self roots, belonging to different plants, might have different genes, and by competing with each other for water or nutrients they might have increased their own fitness and past natural selection have favoured them. Therefore, recognizing whether another root is self or non self must offer advantages, and indeed this sort of recognition exists (Gersani *et al.* 2001; Falik *et al.* 2003).

The most common response to encounters between root tips that belong to different mother plants is branching ending up in root overproduction (Gersani *et al.* 2001; Depuydt 2014). This might explain in part why root length density is usually higher in

the topsoil than the 0.1 cm cm^{-3} (Deery 2008) that is required to maximize water uptake. Thus, it would be useful for plants forming a wheat crop to avoid overproduction of roots in the topsoil by inhibiting the mechanism that enables non-self recognition. But it may not be just a matter of genetic differences between confronting roots, as Gruntman and Novoplansky (2004) found that roots coming from cuttings from the same individual of the perennial grass *Buchloe dactyloides*, were progressively behaving as non-self as the time since the cutting progressed. This suggests that the recognition is not genetic but physiological, possibly mediated by root exudates (Semchenko *et al.* 2014). In either case, the suppression of the non-self root recognition behaviour from crop plants may make them more effective in using water and nutrients by occupying the soil more effectively and relieving extra carbon to enable root growth deep in the profile.

6.6 Conclusion

The unifying hypotheses in this study were that (i) there is genotypic variation in the depth of rooting that can be used to increase growth of the crops and grain yield; and that (ii) canopy temperature and soil water measured continuously can be used to phenotype wheat with deeper water access and incidentally deep roots. Genotypic variation for rooting depth, both interspecific (triticale and wheat) and intraspecific (variable height lines of wheat), were detected in field conditions. Deep rooting was shown to be positively correlated with biomass and yield, and to be associated with increased water uptake and a higher water-use efficiency. Gypsum blocks were not a suitable tool to phenotype water uptake, but may be appropriate where suction is being measured. Continuous measurement of canopy temperature was shown to allow

phenotyping of root systems with superior deep water access, by enabling the calculation of a CWSI that would be challenging to achieve with sporadic measurements. Taken together, these findings can help breeders to produce wheat varieties that can make better use of deep water and improve yield in water-limited environments.

Appendix A ASReml-R models

This section presents specific code written in the R language for data analysis (R Core Team 2014).

Model (4.1):

```
asreml(fixed = biomass ~ genotype * site + at(site, 2):lin(row),
       random = ~ at(site):block,
       rcov = ~ at(site, 1):column:ar1(row) +
         at(experiment, 2):ar1(column):row,
       data = data,
       na.method.X = "include")
```

Model (4.2):

```
asreml(fixed = biomass ~ genotype + lin(column) + lin(row),
       random = ~ block,
       rcov = ~ column:row,
       data = data,
       na.method.X = "include")
```

Model (4.3):

```
asreml(fixed = biomass ~ group * site + at(site, 2):lin(row),
       random = ~ at(site):block + genotype,
       rcov = ~ at(site):ar1(column):row,
       data = data,
       na.method.X = "include")
```


Appendix B Validation of gypsum blocks calibration against neutron probe

calibration against neutron probe

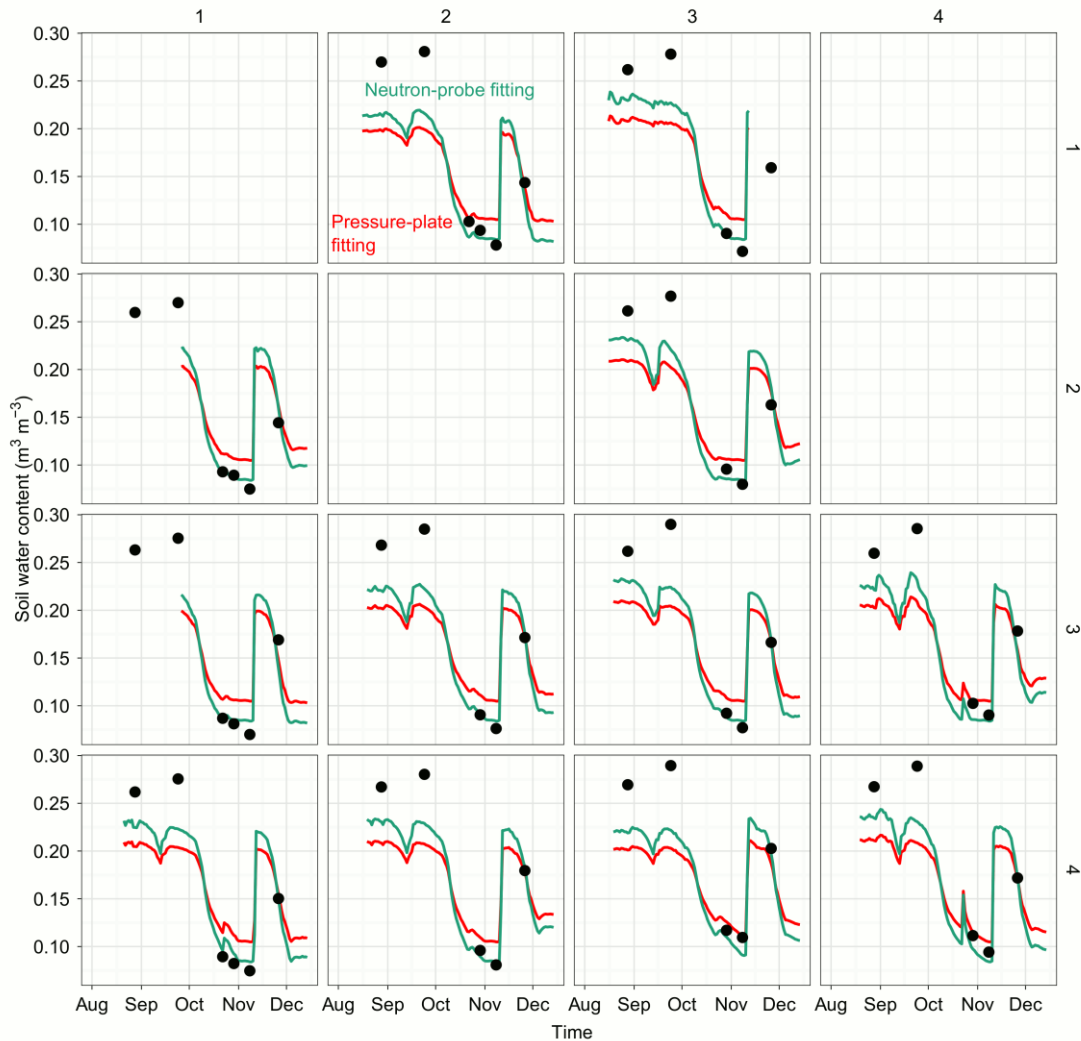


Figure B.1. Comparison of the soil water content estimated by gypsum blocks (lines) with the soil water content estimated with neutron probe (dots) in the soil layer corresponding to **20 cm** depth. The red line is the trajectory of soil water content estimated with gypsum blocks fitted to the water retention curve calibrated in the pressure plate. The green line is the trajectory estimated with the water retention curve estimated by fitting gypsum block suction to soil water content given by neutron probe. Each frame is a plot from experiment 4 (2013), where column numbers are 'columns' and row numbers are 'rows' of that experiment (see Figure 2.11 for a detailed map).

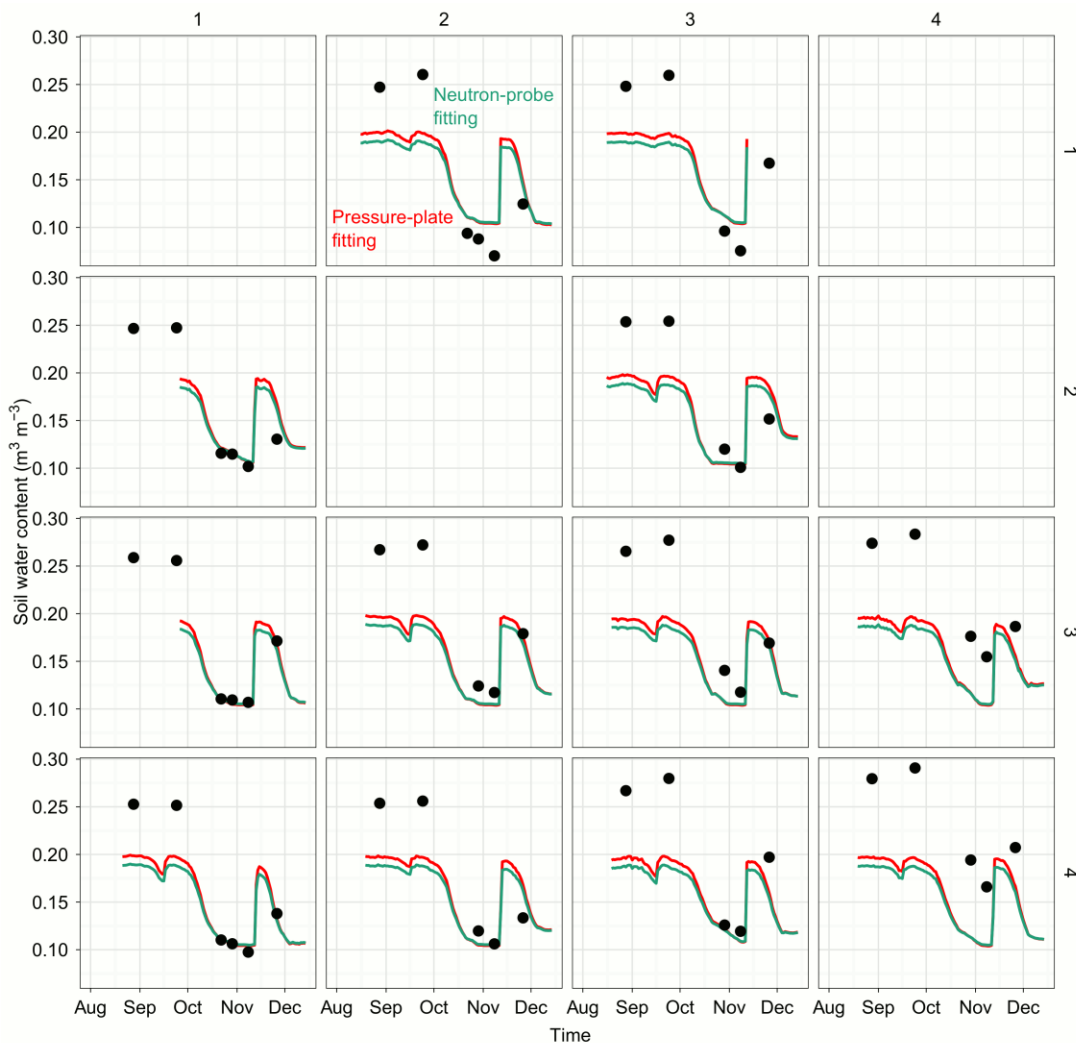


Figure B.2. Comparison of the soil water content estimated by gypsum blocks (lines) with the soil water content estimated with neutron probe (dots) in the soil layer corresponding to **40 cm** depth. The red line is the trajectory of soil water content estimated with gypsum blocks fitted to the water retention curve calibrated in the pressure plate. The green line is the trajectory estimated with the water retention curve estimated by fitting gypsum block suction to soil water content given by neutron probe. Each frame is a plot from experiment 4 (2013), where column numbers are 'columns' and row numbers are 'rows' of that experiment (see Figure 2.11 for a detailed map).

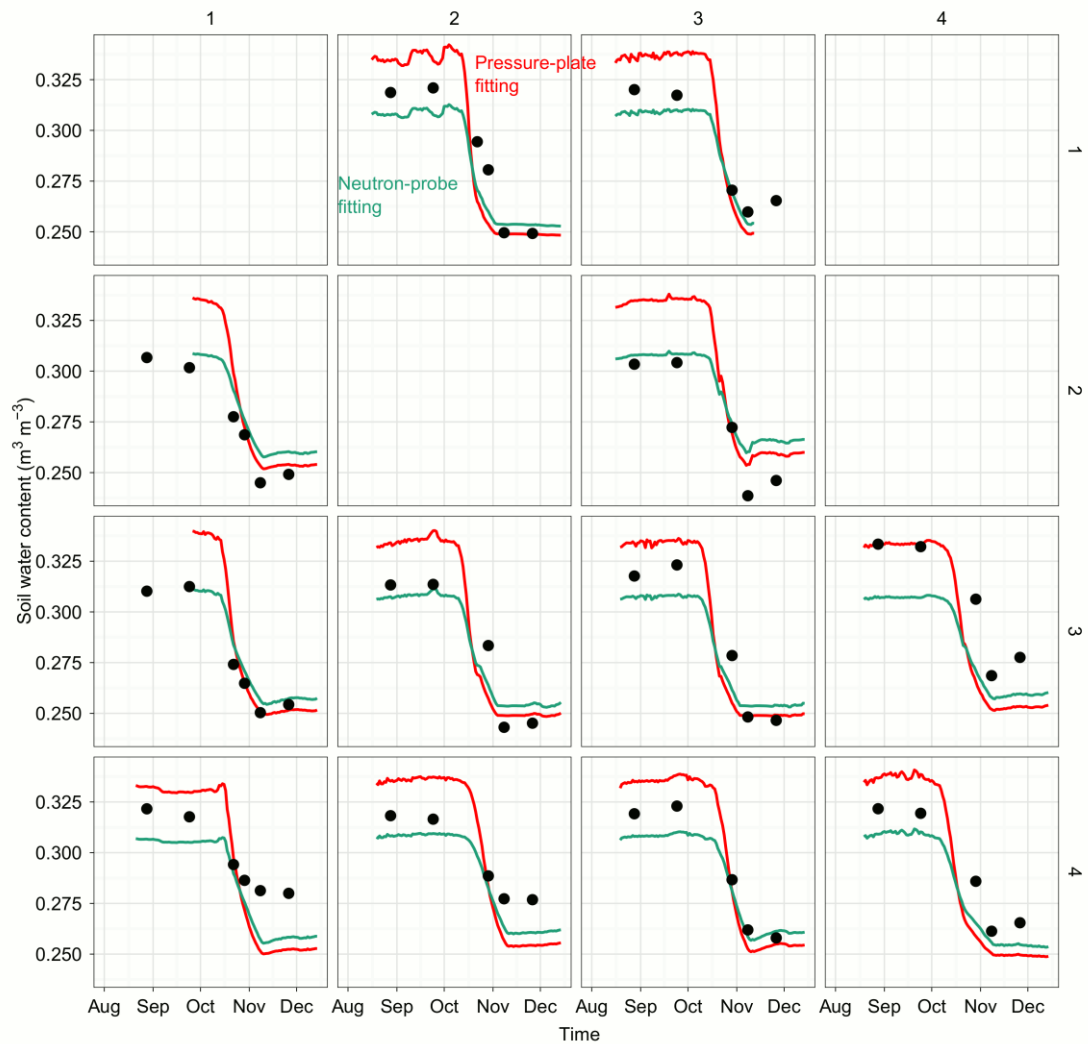


Figure B.3. Comparison of the soil water content estimated by gypsum blocks (lines) with the soil water content estimated with neutron probe (dots) in the soil layer corresponding to **60 cm** depth. The red line is the trajectory of soil water content estimated with gypsum blocks fitted to the water retention curve calibrated in the pressure plate. The green line is the trajectory estimated with the water retention curve estimated by fitting gypsum block suction to soil water content given by neutron probe. Each frame is a plot from experiment 4 (2013), where column numbers are 'columns' and row numbers are 'rows' of that experiment (see Figure 2.11 for a detailed map).

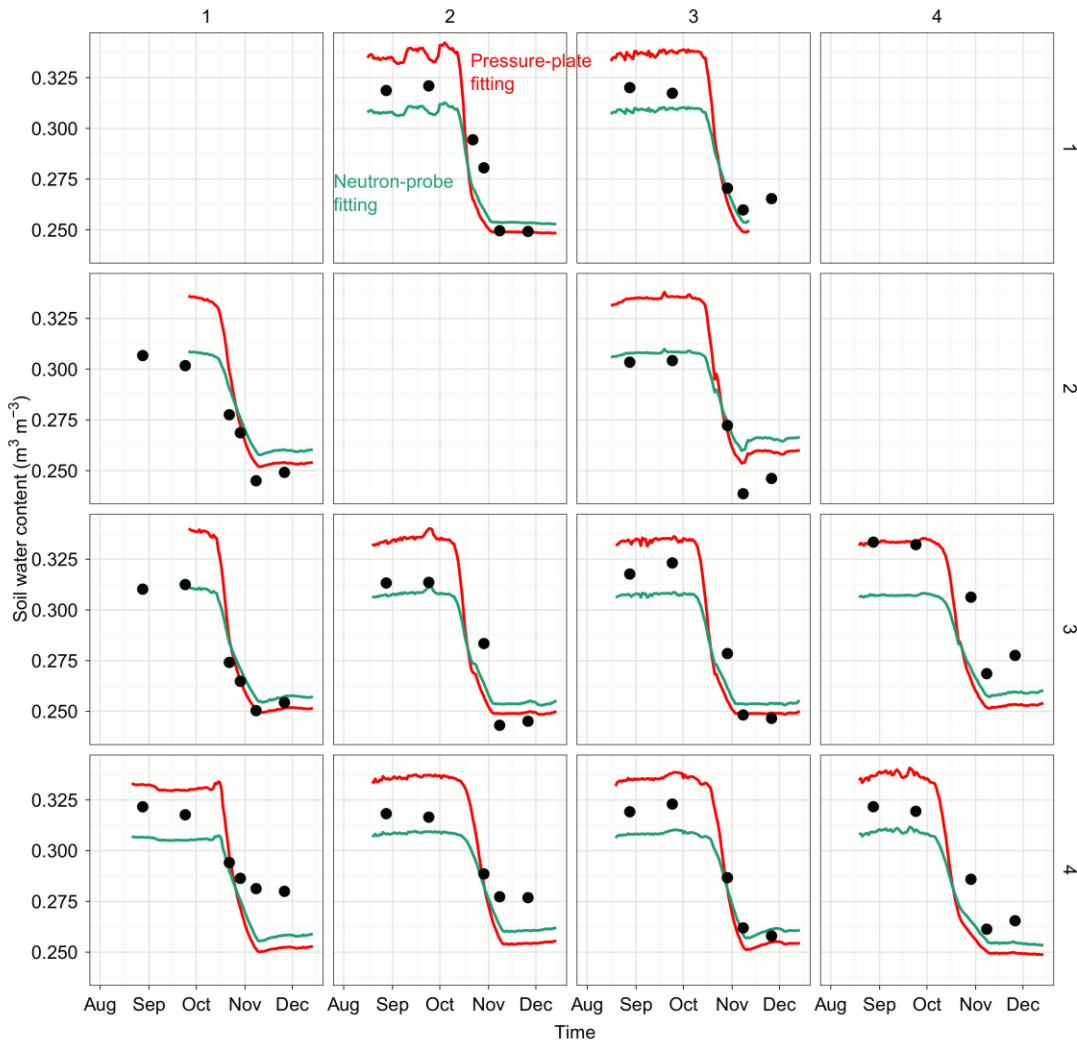


Figure B.4. Comparison of the soil water content estimated by gypsum blocks (lines) with the soil water content estimated with neutron probe (dots) in the soil layer corresponding to **80 cm** depth. The red line is the trajectory of soil water content estimated with gypsum blocks fitted to the water retention curve calibrated in the pressure plate. The green line is the trajectory estimated with the water retention curve estimated by fitting gypsum block suction to soil water content given by neutron probe. Each frame is a plot from experiment 4 (2013), where column numbers are 'columns' and row numbers are 'rows' of that experiment (see Figure 2.11 for a detailed map).

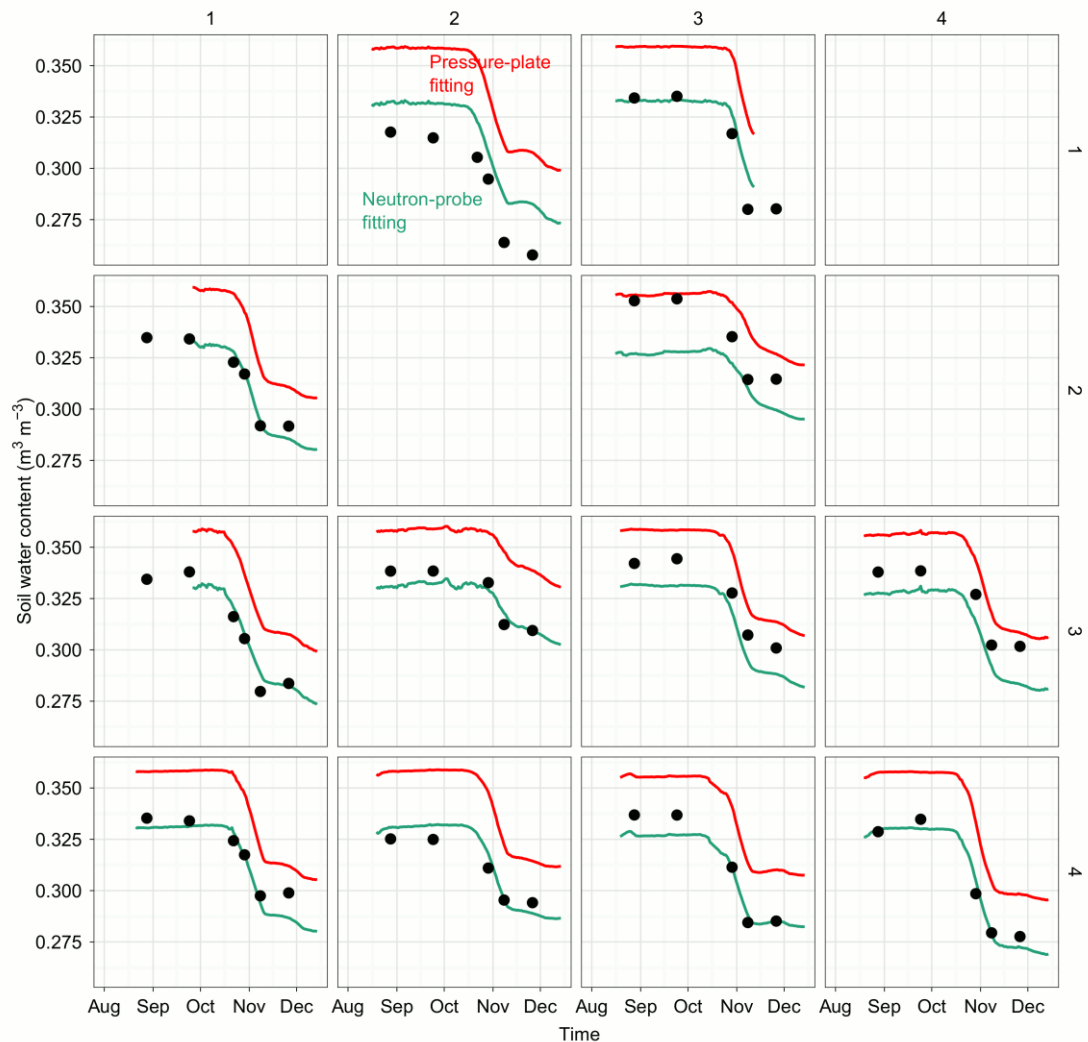


Figure B.5. Comparison of the soil water content estimated by gypsum blocks (lines) with the soil water content estimated with neutron probe (dots) in the soil layer corresponding to **100 cm** depth. The red line is the trajectory of soil water content estimated with gypsum blocks fitted to the water retention curve calibrated in the pressure plate. The green line is the trajectory estimated with the water retention curve estimated by fitting gypsum block suction to soil water content given by neutron probe. Each frame is a plot from experiment 4 (2013), where column numbers are 'columns' and row numbers are 'rows' of that experiment (see Figure 2.11 for a detailed map).

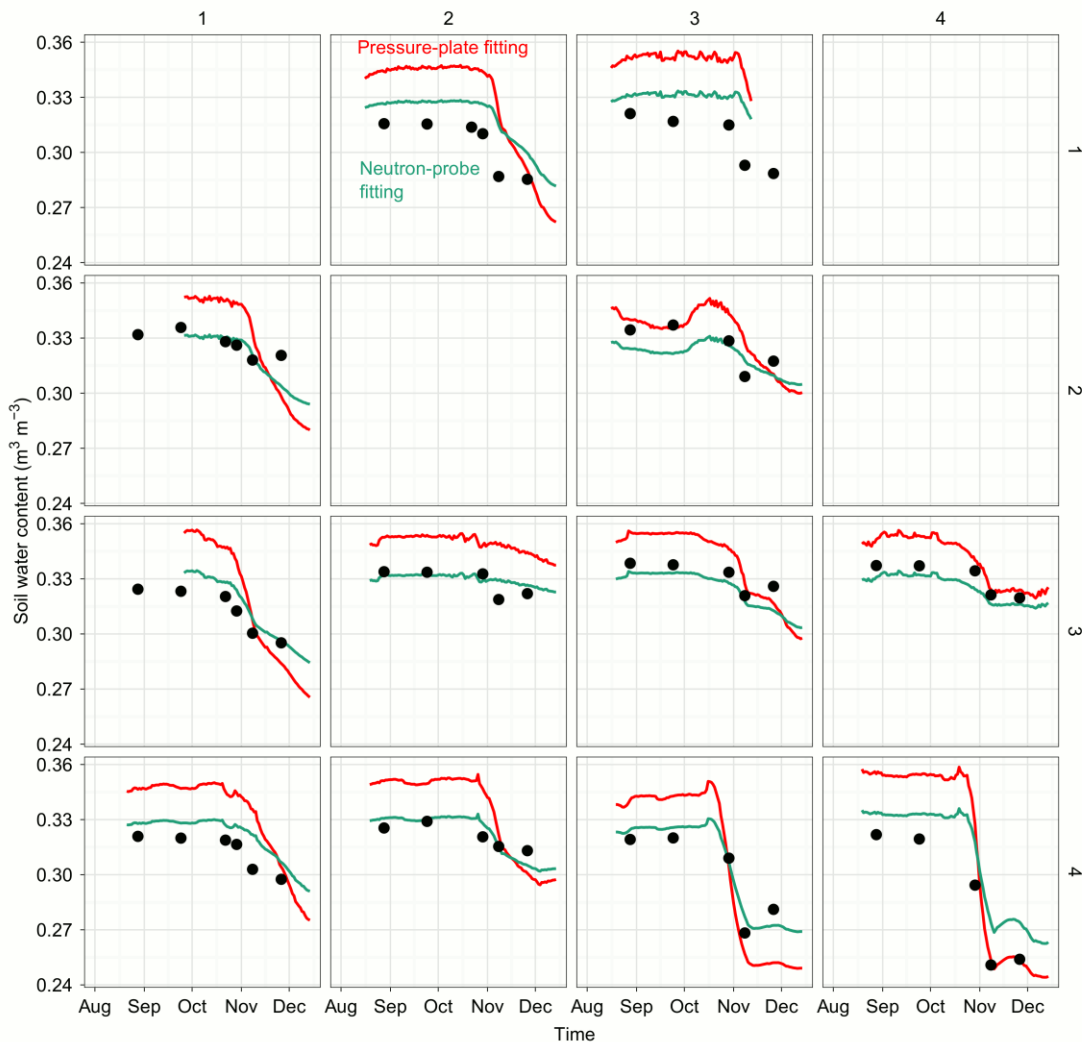


Figure B.6. Comparison of the soil water content estimated by gypsum blocks (lines) with the soil water content estimated with neutron probe (dots) in the soil layer corresponding to **120 cm** depth. The red line is the trajectory of soil water content estimated with gypsum blocks fitted to the water retention curve calibrated in the pressure plate. The green line is the trajectory estimated with the water retention curve estimated by fitting gypsum block suction to soil water content given by neutron probe. Each frame is a plot from experiment 4 (2013), where column numbers are 'columns' and row numbers are 'rows' of that experiment (see Figure 2.11 for a detailed map).

References

- Aitchison G, Butler P (1951) Gypsum block moisture meters as instruments for the measurement of tension in soil water. *Aust J Appl Sci* **2**, 257–266.
- Amani I, Fischer RA, Reynolds MP (1996) Canopy temperature depression association with yield of irrigated spring wheat cultivars in a hot climate. *Journal of Agronomy and Crop Science* **176**, 119–129. doi:10.1111/j.1439-037X.1996.tb00454.x.
- Asseng S, Turner NC, Botwright T, Condon AG (2003) Evaluating the impact of a trait for increased specific leaf area on wheat yields using a crop simulation model. *Agronomy Journal* **95**, 10–19.
- Blum A (2009) Effective use of water (EUW) and not water-use efficiency (WUE) is the target of crop yield improvement under drought stress. *Field Crops Research* **112**, 119–123. doi:10.1016/j.fcr.2009.03.009.
- Borrás L, Slafer GA, Otegui ME (2004) Seed dry weight response to source–sink manipulations in wheat, maize and soybean: a quantitative reappraisal. *Field Crops Research* **86**, 131–146.
- Borrell AK, Hammer GL, Douglas ACL (2000) Does maintaining green leaf area in sorghum improve yield under drought? I. leaf growth and senescence. *Crop Science* **40**, 1026–1037. doi:10.2135/cropsci2000.4041026x.
- Botwright Acuña TL, Condon AG, Rebetzke GJ, Richards RA (2002) Field evaluation of early vigour for genetic improvement of grain yield in wheat. *Crop and Pasture Science* **53**, 1137–1145.
- Botwright Acuña TL, Pasuquin E, Wade LJ (2007) Genotypic differences in root penetration ability of wheat through thin wax layers in contrasting water regimes and in the field. *Plant and Soil* **301**, 135–149. doi:10.1007/s11104-007-9428-9.
- Botwright Acuña TL, Wade LJ (2005) Root penetration ability of wheat through thin wax-layers under drought and well-watered conditions. *Australian Journal of Agricultural Research* **56**, 1235–1244.
- Botwright Acuña TL, Wade LJ (2012) Genotype × environment interactions for root depth of wheat. *Field Crops Research* **137**, 117–125. doi:10.1016/j.fcr.2012.08.004.
- Bouyoucos GJ, Mick AH (1940) An electrical resistance method for the continuous measurement of soil moisture under field conditions. *Technical Bulletin Michigan Agricultural Experiment Station* **172**, 38 pp.
- Butler D (2009) ‘asreml: asreml() fits the linear mixed model.’ www.vsni.co.uk.

-
- Campos H, Cooper M, Habben JE, Edmeades GO, Schussler JR (2004) Improving drought tolerance in maize: a view from industry. *Field Crops Research* **90**, 19–34. doi:10.1016/j.fcr.2004.07.003.
- Cárcova J, Maddonni GA, Ghera CM (1998) Crop water stress index of three maize hybrids grown in soils with different quality. *Field Crops Research* **55**, 165–174. doi:10.1016/S0378-4290(97)00076-2.
- Chandler PM, Harding CA (2013) ‘Overgrowth’ mutants in barley and wheat: new alleles and phenotypes of the ‘Green Revolution’ *Della* gene. *Journal of Experimental Botany* **64**, 1603–1613. doi:10.1093/jxb/ert022.
- Chandler PM, Marion-Poll A, Ellis M, Gubler F (2002) Mutants at the slender1 locus of barley cv himalaya. molecular and physiological characterization. *Plant Physiology* **129**, 181–190. doi:10.1104/pp.010917.
- Chenu K, Dehifard R, Chapman SC (2013) Large-scale characterization of drought pattern: a continent-wide modelling approach applied to the Australian wheatbelt – spatial and temporal trends. *New Phytologist* **198**, 801–820. doi:10.1111/nph.12192.
- Choudhury BJ, Reginato RJ, Idso SB (1986) An analysis of infrared temperature observations over wheat and calculation of latent heat flux. *Agricultural and Forest Meteorology* **37**, 75–88. doi:10.1016/0168-1923(86)90029-8.
- Christopher JT, Manschadi AM, Hammer GL, Borrell AK (2008) Developmental and physiological traits associated with high yield and stay-green phenotype in wheat. *Australian Journal of Agricultural Research* **59**, 354–364.
- Condon AG, Richards RA, Rebetzke GJ, Farquhar GD (2002) Improving intrinsic water-use efficiency and crop yield. *Crop Science* **42**, 122. doi:10.2135/cropsci2002.0122.
- Cowan IR (1965) Transport of water in the soil-plant-atmosphere system. *Journal of Applied Ecology* **2**, 221–239. doi:10.2307/2401706.
- Dardanelli JL, Bachmeier OA, Sereno R, Gil R (1997) Rooting depth and soil water extraction patterns of different crops in a silty loam Haplustoll. *Field Crops Research* **54**, 29–38. doi:10.1016/S0378-4290(97)00017-8.
- Dardanelli JL, Ritchie JT, Calmon M, Andriani JM, Collino DJ (2004) An empirical model for root water uptake. *Field Crops Research* **87**, 59–71. doi:10.1016/j.fcr.2003.09.008.
- De Wit C, Penning de Vries F (1983) Crop growth models without hormones. *Netherlands journal of agricultural science* **31**, 313–323.

-
- Deery DM (2008) Water uptake by a single plant: Analysis using experimentation and modeling. Charles Sturt University.
- Deery DM, Passioura JB, Condon JR, Katupitiya A (2012) Uptake of water from a Kandosol subsoil: I. Determination of soil water diffusivity. *Plant and Soil* **368**, 483–492. doi:10.1007/s11104-012-1525-8.
- Delhaize E, Ryan PR, Hebb DM, Yamamoto Y, Sasaki T, Matsumoto H (2004) Engineering high-level aluminum tolerance in barley with the ALMT1 gene. *Proceedings of the National Academy of Sciences of the United States of America* **101**, 15249–15254. doi:10.1073/pnas.0406258101.
- Denison RF (2012) ‘Darwinian agriculture: how understanding evolution can improve agriculture.’ (Princeton University Press)
- Denison RF (2015) Evolutionary tradeoffs as opportunities to improve yield potential. *Field Crops Research* **182**, 3–8. doi:10.1016/j.fcr.2015.04.004.
- Depuydt S (2014) Arguments for and against self and non-self root recognition in plants. *Functional Plant Ecology* **5**, 614. doi:10.3389/fpls.2014.00614.
- Donald CM (1968) The breeding of crop ideotypes. *Euphytica* **17**, 385–403. doi:10.1007/BF00056241.
- Drew MC, Saker LR (1980) Assessment of a rapid method, using soil cores, for estimating the amount and distribution of crop roots in the field. *Plant and Soil* **55**, 297–305. doi:10.1007/BF02181809.
- Duggan BL, Richards RA, van Herwaarden AF (2005) Agronomic evaluation of a tiller inhibition gene (tin) in wheat. II. Growth and partitioning of assimilate. *Australian Journal of Agricultural Research* **56**, 179–186.
- Dunin FX, Barrs HD, Meyer WS, Trevitt ACF (1991) Foliage temperature and latent heat flux of irrigated wheat. *Agricultural and Forest Meteorology* **55**, 133–147. doi:10.1016/0168-1923(91)90027-N.
- Elzhov TV, Mullen KM, Spiess A-N, Bolker B (2013) ‘minpack.lm: R interface to the Levenberg-Marquardt nonlinear least-squares algorithm found in MINPACK, plus support for bounds.’ <http://CRAN.R-project.org/package=minpack.lm>
- Evelt S, Heng L, Moutonnet P, Nguyen M (2008) Field estimation of soil water content: A practical guide to methods, instrumentation, and sensor technology. *IAEA: Vienna*.
- Falik O, Reides P, Gersani M, Novoplansky A (2003) Self/non-self discrimination in roots. *Journal of Ecology* **91**, 525–531. doi:10.1046/j.1365-2745.2003.00795.x.

-
- Fischer RA (1985) Number of kernels in wheat crops and the influence of solar radiation and temperature. *The Journal of Agricultural Science* **105**, 447–461. doi:10.1017/S0021859600056495.
- French R, Schultz J (1984) Water use efficiency of wheat in a Mediterranean-type environment. I. The relation between yield, water use and climate. *Australian Journal of Agricultural Research* **35**, 743–764.
- van Genuchten MT (1980) A closed-form equation for predicting the hydraulic conductivity of unsaturated soils. *Soil science society of America journal* **44**, 892–898.
- van Genuchten MT, Leij F, Yates S, others (1991) ‘The RETC code for quantifying the hydraulic functions of unsaturated soils.’ (Robert S. Kerr Environmental Research Laboratory)
- Gersani M, Brown JS, O’Brien EE, Maina GM, Abramsky Z (2001) Tragedy of the commons as a result of root competition. *Journal of Ecology* **89**, 660–669. doi:10.1046/j.0022-0477.2001.00609.x.
- Ghezzehei T, Bogie N, Albalasmeh A (2015) Plant roots can actively regulate hydraulic redistribution by modifying the hydraulic properties of the rhizosphere using exudates. In ‘Geophys. Res. Abstr.’,
- Giunta F, Motzo R, Deidda M (1993) Effect of drought on yield and yield components of durum wheat and triticale in a Mediterranean environment. *Field Crops Research* **33**, 399–409. doi:10.1016/0378-4290(93)90161-F.
- Gomez-Macpherson H, Richards RA (1995) Effect of sowing time on yield and agronomic characteristics of wheat in south-eastern Australia. *Australian Journal of Agricultural Research* **46**, 1381–1399.
- Gornall J, Betts R, Burke E, Clark R, Camp J, Willett K, Wiltshire A (2010) Implications of climate change for agricultural productivity in the early twenty-first century. *Philosophical Transactions of the Royal Society of London B: Biological Sciences* **365**, 2973–2989. doi:10.1098/rstb.2010.0158.
- Greenhouse SW, Geisser S (1959) On methods in the analysis of profile data. *Psychometrika* **24**, 95–112. doi:10.1007/BF02289823.
- Gruntman M, Novoplansky A (2004) Physiologically mediated self/non-self discrimination in roots. *Proceedings of the National Academy of Sciences of the United States of America* **101**, 3863–3867. doi:10.1073/pnas.0306604101.
- Hammer GL, Dong Z, McLean G, Doherty A, Messina C, Schussler J, Zinselmeier C, Paszkiewicz S, Cooper M (2009) Can changes in canopy and/or root system architecture explain historical maize yield trends in the US corn belt? *Crop Science* **49**, 299. doi:10.2135/cropsci2008.03.0152.

-
- Hammer GL, Sinclair TR, Chapman SC, Oosterom E van (2004) On systems thinking, systems biology, and the in silico plant. *Plant Physiology* **134**, 909–911. doi:10.1104/pp.103.034827.
- Hendriks PW, Kirkegaard JA, Lilley JM, Gregory PJ, Rebetzke GJ (2015) A tillering inhibition gene influences root–shoot carbon partitioning and pattern of water use to improve wheat productivity in rainfed environments. *Journal of Experimental Botany* **erv457**. doi:10.1093/jxb/erv457.
- Idso SB (1982) Non-water-stressed baselines: A key to measuring and interpreting plant water stress. *Agricultural Meteorology* **27**, 59–70. doi:10.1016/0002-1571(82)90020-6.
- Idso SB, Jackson RD, Pinter Jr. PJ, Reginato RJ, Hatfield JL (1981) Normalizing the stress-degree-day parameter for environmental variability. *Agricultural Meteorology* **24**, 45–55. doi:10.1016/0002-1571(81)90032-7.
- Isbell RF (1993) ‘A Classification System for Australian Soils.’ (CSIRO Division of Soils)
- Johnston WH (2000) Calibration of gypsum blocks and data loggers and their evaluation for monitoring soil water status. *Australian Journal of Experimental Agriculture* **40**, 1131–1136.
- Jordan W, Miller F (1980) Genetic variability in sorghum root systems: implications for drought tolerance. *Adaptation of Plants to Water and High Temperature Stress* (NC Turner and PJ Kramer, Editors) 383–399.
- Keating BA, Meinke H, Probert ME, Huth NI, Hills IG (2001) ‘Nwheat: documentation and performance of a wheat module for APSIM. Tropical Agronomy Memorandum.’ (CSIRO Division of Tropical Agriculture)
- Kebrom TH, Richards RA (2013) Physiological perspectives of reduced tillering and stunting in the tiller inhibition (tin) mutant of wheat. *Functional Plant Biology* **40**, 977–985.
- Kemanian AR, Stöckle CO, Huggins DR (2005) Transpiration-use efficiency of barley. *Agricultural and Forest Meteorology* **130**, 1–11. doi:10.1016/j.agrformet.2005.01.003.
- Kirkegaard JA, Hunt JR (2010) Increasing productivity by matching farming system management and genotype in water-limited environments. *Journal of Experimental Botany* **erq245**. doi:10.1093/jxb/erq245.
- Kirkegaard JA, Lilley JM (2007) Root penetration rate -- a benchmark to identify soil and plant limitations to rooting depth in wheat. *Australian Journal of Experimental Agriculture* **47**, 590–602.

-
- Kirkegaard JA, Lilley JM, Howe GN, Graham JM (2007) Impact of subsoil water use on wheat yield. *Australian Journal of Agricultural Research* **58**, 303–315.
- Klepper B, Belford RK, Rickman RW (1984) Root and Shoot Development in Winter Wheat1. *Agronomy Journal* **76**, 117.
doi:10.2134/agronj1984.00021962007600010029x.
- Köppen WP (1918) Klassifikation der klimate nach temperatur, niederschlag und jahreslauf. *Petterm Geogr Mitt* **64**, 193–203, 243–248.
- Liao M, Palta JA, Fillery IRP (2006) Root characteristics of vigorous wheat improve early nitrogen uptake. *Australian Journal of Agricultural Research* **57**, 1097–1107.
- Lilley JM, Kirkegaard JA (2011) Benefits of increased soil exploration by wheat roots. *Field Crops Research* **122**, 118–130. doi:10.1016/j.fcr.2011.03.010.
- Lopes MS, Reynolds MP (2010) Partitioning of assimilates to deeper roots is associated with cooler canopies and increased yield under drought in wheat. *Functional Plant Biology* **37**, 147–156.
- Ludlow M, Muchow R (1990) A critical evaluation of traits for improving crop yields in water-limited environments. *Advances in agronomy* **43**, 107–153.
- Lynch JP (1995) Root architecture and plant productivity. *Plant Physiology* **109**, 7–13.
- Lynch JP (2013) Steep, cheap and deep: an ideotype to optimize water and N acquisition by maize root systems. *Annals of Botany* **112**, 347–357.
doi:10.1093/aob/mcs293.
- Manschadi AM, Christopher J, deVoil P, Hammer GL (2006) The role of root architectural traits in adaptation of wheat to water-limited environments. *Functional Plant Biology* **33**, 823–837.
- Manschadi AM, Hammer GL, Christopher JT, deVoil P (2008) Genotypic variation in seedling root architectural traits and implications for drought adaptation in wheat (*Triticum aestivum* L.). *Plant and Soil* **303**, 115–129.
doi:10.1007/s11104-007-9492-1.
- Miralles DJ, Slafer GA, Lynch V (1997) Rooting patterns in near-isogenic lines of spring wheat for dwarfism. *Plant and Soil* **197**, 79–86.
doi:10.1023/A:1004207407979.
- Mitchell JH, Chapman SC, Rebetzke GJ, Bonnett DG, Fukai S (2012) Evaluation of a reduced-tillering (tin) gene in wheat lines grown across different production environments. *Crop and Pasture Science* **63**, 128–141.

-
- Murphy SR, Lodge GM (2004) Surface soil water dynamics in pastures in northern New South Wales. 1. Use of electrical resistance sensors. *Australian Journal of Experimental Agriculture* **44**, 273–281.
- Northcote KH (1971) A factual key for the recognition of Australian soils.
- Olivares-Villegas JJ, Reynolds MP, McDonald GK (2007) Drought-adaptive attributes in the Seri/Babax hexaploid wheat population. *Functional Plant Biology* **34**, 189–203.
- Palta JA, Chen X, Milroy SP, Rebetzke GJ, Dreccer MF, Watt M (2011) Large root systems: are they useful in adapting wheat to dry environments? *Functional Plant Biology* **38**, 347–354.
- Palta JA, Watt M (2009) Chapter 13 - Vigorous crop root systems: form and function for improving the capture of water and nutrients. 'Crop Physiol.' (Eds VO Sadras, D Calderini) pp. 309–325. (Academic Press: San Diego)
<http://www.sciencedirect.com/science/article/pii/B978012374431900013X>.
- Pask AJD, Reynolds MP (2013) Breeding for Yield Potential has Increased Deep Soil Water Extraction Capacity in Irrigated Wheat. *Crop Science* **53**, 2090.
doi:10.2135/cropsci2013.01.0011.
- Passioura JB (1976) Physiology of grain yield in wheat growing on stored water. *Functional Plant Biology* **3**, 559–565.
- Passioura JB (1977) Grain yield, harvest index, and water use of wheat. *Journal of the Australian Institute of Agricultural Science*.
- Passioura JB (1983) Roots and drought resistance. *Agricultural Water Management* **7**, 265–280. doi:10.1016/0378-3774(83)90089-6.
- Passioura JB (2007) The drought environment: physical, biological and agricultural perspectives. *Journal of Experimental Botany* **58**, 113–117.
doi:10.1093/jxb/erl212.
- Paydar Z, Cresswell H (1996) Water retention in Australian soils. 2.* Prediction using particle size, bulk density, and other properties. *Soil Research* **34**, 679–693.
- Pinto RS, Reynolds MP (2015) Common genetic basis for canopy temperature depression under heat and drought stress associated with optimized root distribution in bread wheat. *Theoretical and Applied Genetics* **128**, 575–585.
doi:10.1007/s00122-015-2453-9.
- R Core Team (2014) 'R: A Language and Environment for Statistical Computing.' (R Foundation for Statistical Computing: Vienna, Austria) <http://www.R-project.org/>.

-
- Ray DK, Mueller ND, West PC, Foley JA (2013) Yield trends are insufficient to double global crop production by 2050. *PLoS ONE* **8**, e66428. doi:10.1371/journal.pone.0066428.
- Rebetzke GJ, Botwright TL, Moore CS, Richards RA, Condon AG (2004) Genotypic variation in specific leaf area for genetic improvement of early vigour in wheat. *Field Crops Research* **88**, 179–189. doi:10.1016/j.fcr.2004.01.007.
- Rebetzke GJ, Rattey AR, Farquhar GD, Richards RA, Condon A (Tony) G (2012) Genomic regions for canopy temperature and their genetic association with stomatal conductance and grain yield in wheat. *Functional Plant Biology* **40**, 14–33.
- Rebetzke GJ, Richards RA (1999) Genetic improvement of early vigour in wheat. *Australian Journal of Agricultural Research* **50**, 291–302.
- Reynolds M, Dreccer F, Trethowan R (2007) Drought-adaptive traits derived from wheat wild relatives and landraces. *Journal of Experimental Botany* **58**, 177–186. doi:10.1093/jxb/erl250.
- Richards RA (1991) Crop improvement for temperate Australia: Future opportunities. *Field Crops Research* **26**, 141–169. doi:10.1016/0378-4290(91)90033-R.
- Richards RA (1992) The effect of dwarfing genes in spring wheat in dry environments. II. Growth, water use and water-use efficiency. *Australian Journal of Agricultural Research* **43**, 529–539.
- Richards RA, Passioura JB (1989) A breeding program to reduce the diameter of the major xylem vessel in the seminal roots of wheat and its effect on grain yield in rain-fed environments. *Australian Journal of Agricultural Research* **40**, 943–950.
- Richards RA, Watt M, Rebetzke GJ (2006) Physiological traits and cereal germplasm for sustainable agricultural systems. *Euphytica* **154**, 409–425. doi:10.1007/s10681-006-9286-1.
- Sadras VO (2007) Evolutionary aspects of the trade-off between seed size and number in crops. *Field Crops Research* **100**, 125–138. doi:10.1016/j.fcr.2006.07.004.
- Sadras VO, Connor DJ (1991) Physiological basis of the response of harvest index to the fraction of water transpired after anthesis: A simple model to estimate harvest index for determinate species. *Field Crops Research* **26**, 227–239. doi:10.1016/0378-4290(91)90001-C.
- Sadras VO, Lawson C (2013) Nitrogen and water-use efficiency of Australian wheat varieties released between 1958 and 2007. *European Journal of Agronomy* **46**, 34–41. doi:10.1016/j.eja.2012.11.008.

-
- Sadras VO, Milroy SP (1996) Soil-water thresholds for the responses of leaf expansion and gas exchange: A review. *Field Crops Research* **47**, 253–266. doi:10.1016/0378-4290(96)00014-7.
- Semchenko M, Saar S, Lepik A (2014) Plant root exudates mediate neighbour recognition and trigger complex behavioural changes. *New Phytologist* **204**, 631–637. doi:10.1111/nph.12930.
- Siddique K, Tennant D, Perry M, Belford R (1990) Water use and water use efficiency of old and modern wheat cultivars in a Mediterranean-type environment. *Australian Journal of Agricultural Research* **41**, 431–447.
- Sinclair TR, Hammer GL, van Oosterom EJ (2005) Potential yield and water-use efficiency benefits in sorghum from limited maximum transpiration rate. *Functional Plant Biology* **32**, 945–952.
- Sirault XR (2007) Leaf rolling in wheat. Australian National University.
- Sleeman JR (1979) The Soils of the Ginninderra Experiment Station, ACT. CSIRO, 41.
- Smucker A, McBurney S, Srivastava A (1982) Quantitative separation of roots from compacted soil profiles by the hydropneumatic elutriation system. *Agronomy Journal* **74**, 500–503.
- Soil Survey Staff (1999) ‘Soil taxonomy: a basic system of soil classification for making and interpreting soil surveys.’ (US Department of Agriculture, Soil Conservation Service)
- Stace HC, Hubble GD, Brewer R, Northcote KH, Sleeman JR, Mulcahy MJ, Hallsworth EG (1968) A handbook of Australian soils. <https://trid.trb.org/view.aspx?id=1199558>.
- Stirzaker RJ, Passioura JB (1996) The water relations of the root–soil interface. *Plant, Cell & Environment* **19**, 201–208. doi:10.1111/j.1365-3040.1996.tb00241.x.
- Tennant D (1976) Root growth of wheat. I. Early patterns of multiplication and extension of wheat roots including effects of levels of nitrogen, phosphorus and potassium. *Crop and Pasture Science* **27**, 183–196.
- Trachsel S, Kaeppler SM, Brown KM, Lynch JP (2013) Maize root growth angles become steeper under low N conditions. *Field Crops Research* **140**, 18–31. doi:10.1016/j.fcr.2012.09.010.
- Wasson AP, Rebetzke GJ, Kirkegaard JA, Christopher J, Richards RA, Watt M (2014) Soil coring at multiple field environments can directly quantify variation in deep root traits to select wheat genotypes for breeding. *Journal of Experimental Botany*. doi:10.1093/jxb/eru250.

-
- Wasson AP, Richards RA, Chatrath R, Misra SC, Prasad SVS, Rebetzke GJ, Kirkegaard JA, Christopher J, Watt M (2012) Traits and selection strategies to improve root systems and water uptake in water-limited wheat crops. *Journal of Experimental Botany* **63**, 3485–3498. doi:10.1093/jxb/ers111.
- Watt M, Kirkegaard JA, Rebetzke GJ (2005) A wheat genotype developed for rapid leaf growth copes well with the physical and biological constraints of unploughed soil. *Functional Plant Biology* **32**, 695–706.
- Watt M, Magee LJ, McCully ME (2008) Types, structure and potential for axial water flow in the deepest roots of field-grown cereals. *New Phytologist* **178**, 135–146. doi:10.1111/j.1469-8137.2007.02358.x.
- Watt M, Moosavi S, Cunningham SC, Kirkegaard JA, Rebetzke GJ, Richards RA (2013) A rapid, controlled-environment seedling root screen for wheat correlates well with rooting depths at vegetative, but not reproductive, stages at two field sites. *Annals of Botany* **112**, 447–455. doi:10.1093/aob/mct122.
- Wesseling J, van Wijk WR, Fireman M, van't Woudt BD, Hagan RM (1957) 'Land drainage in relation to soils and crops in drainage of agricultural lands.' (American Society of Agronomy)
<https://dl.sciencesocieties.org/publications/books/abstracts/agronomymonogra/drainageofagric/461>.
- White RG, Kirkegaard JA (2010) The distribution and abundance of wheat roots in a dense, structured subsoil – implications for water uptake. *Plant, Cell & Environment* **33**, 133–148. doi:10.1111/j.1365-3040.2009.02059.x.
- Wikipedia (2014) Köppen climate classification --- Wikipedia, The Free Encyclopedia. http://en.wikipedia.org/w/index.php?title=K%C3%B6ppen_climate_classification&oldid=606957479.
- Wilson PB, Rebetzke GJ, Condon AG (2015) Pyramiding greater early vigour and integrated transpiration efficiency in bread wheat; trade-offs and benefits. *Field Crops Research* **183**, 102–110. doi:10.1016/j.fcr.2015.07.002.
- Wojciechowski T, Gooding M, Ramsay L, Gregory P (2009) The effects of dwarfing genes on seedling root growth of wheat. *Journal of Experimental Botany* **erp107**.
- Zadoks JC, Chang TT, Konzak CF (1974) A decimal code for the growth stages of cereals. *Weed Research* **14**, 415–421. doi:10.1111/j.1365-3180.1974.tb01084.x.
- Zhang D-Y, Sun G-J, Jiang X-H (1999) Donald's ideotype and growth redundancy: a game theoretical analysis. *Field Crops Research* **61**, 179–187. doi:10.1016/S0378-4290(98)00156-7.
- Zotarelli L, Dukes MD, Romero CC, Migliaccio KW, Morgan KT (2010) Step by step calculation of the Penman-Monteith Evapotranspiration (FAO-56 Method).

